Advanced Therapeutic Strategies for Diabetic Foot Ulcers

Lead Guest Editor: Yun-Feng Yang
Guest Editors: Adriana C. Panayi, Huachao Shen, and Yong Xu

Advanced Therapeutic Strategies for Diabetic Foot Ulcers

Advanced Therapeutic Strategies for Diabetic Foot Ulcers

Lead Guest Editor: Yun-Feng Yang
Guest Editors: Adriana C. Panayi, Huachao Shen, and Yong Xu

Contents

Research Article

Type 2 Diabetic Mellitus Inhibits Skin Renewal through Inhibiting WNT-Dependent Lgr5+ Hair Follicle Stem Cell Activation in C57BL/6 Mice

Minghui Wang [1], **Shangsheng Yao,**[1] **Dehua He,**[1] **Mulan Qahar,**[1] **Jinqing He,**[1] **Meifang Yin,**[1]
Jun Wu [1,2] **and Guang Yang** [1]

[1]*Department of Burn and Plastic Surgery, Shenzhen Institute of Translational Medicine, Shenzhen Second People's Hospital, The First Affiliated Hospital of Shenzhen University Health Science Center, Shenzhen 518035, China*
[2]*Human Histology & Embryology Section, Department of Surgery, Dentistry, Pediatrics & Gynecology, University of Verona Medical School, Verona 37134, Italy*

Correspondence should be addressed to Jun Wu; junwupro@126.com and Guang Yang; yakoaka@foxmail.com

Background. Hair follicles are important accessory organs of the skin, and it is important for skin renewal and performs variety of important functions. Diabetes can cause several dermatoses; however, its effect on hair follicles is unclear. The purpose of this study was to investigate the effect of type II diabetes (T2DM) on the hair follicles of mice. *Methods*. Seven-week-old male C57BL/6 littermate mice were divided into two groups. The treatment group was injected with streptozotocin (STZ) to induce T2DM, and the control group was parallelly injected with the same dose of buffer. Seven days after injection, the back is depilated to observe the hair follicle regeneration. Hair follicle regeneration was observed by naked eyes and HE staining. The proliferation of the skin cells was observed by PCNA and K14 staining. The altered genes were screened by RNA sequencing and verified by qRT-PCR. In addition, Lgr5 + GFP/mTmG transgenic mice were used to observe the effect of T2DM on Lgr5 hair follicle stem cells (HFSC). And the expression of WNT4 and WNT8A were measured by Western Blot. *Results*. T2DM inhibited hair follicle regeneration. Compared to control mice, T2DM mice had smaller hair follicles, reduced skin thickness, and less expression of PCNA and K14. RNA sequencing showed that the two groups had significant differences in cell cycle and proliferation-related pathways. Compared with the control mice, the mRNA expression of Lgr4, Lgr5, Wnt4, and Wnt8a was decreased in the T2DM group. Moreover, T2DM inhibited the activation of Lgr5 HFSC and the expression of WNT4 and WNT8A. *Conclusions*. T2DM inhibited hair follicle regeneration and skin cells proliferation by inhibiting WNT-dependent Lgr5 HFSC activation. This may be an important reason for the reduction of skin renewal ability and the formation of chronic wounds caused by diabetes. It is important for the treatment of chronic diabetic wounds and the development of tissue engineering.

1. Introduction

Diabetes affects more than 340 million people worldwide, and about one-third of patients are accompanied by skin disorders [1, 2]. Hyperglycemia causes damage to a wide range of skin cell populations, including endothelial cells, keratinocytes, fibroblasts, and neurons. Diabetic ulcers are one of the common complications of diabetes, and about 20% of patients are affected by diabetic ulcers [3]. Diabetic ulcer is difficult to heal and is usually accompanied by infection, which causes a significant economic burden to the patients [4]. The most common diabetic ulcer is diabetic foot, and about 6% of diabetic patients have different degrees of foot infection and ulcers [5]. Between 0.03% and 1.5% of patients require amputation because of long-term ulcers [6]. At present, the most useful methods to prevent foot

complications are foot care and screening [7]. Until now, there is no effective medication or method for the treatment of diabetic ulcers.

The skin is the first line of defense against external aggressions. The keratinocytes on the skin surface form a natural barrier, which can prevent the invasion of various microorganisms and physical and chemical substances. There are various stem cell populations in the skin, and they maintain the skin's stability to resist the external environment by continuously proliferating new cells to replace the aging skin cells [8]. When the cell proliferation capacity decreases, the skin renewal rate will decrease. Undoubtedly, when the cell proliferation rate cannot follow the skin renewal requirements, it will increase the ulcers probability and decrease wound healing. Previous studies have confirmed that diabetes can cause a variety of skin complications [1, 9]. In vivo studies have shown that hyperglycemia can cause epidermal dysfunction, accelerate skin aging, inhibit the proliferation and differentiation of keratinocytes, and increase skin cell apoptosis [10–12]. In vitro studies also proved that high-glucose environment can inhibit the differentiation and function of human immortal keratinocyte line (HaCaT), inhibit the viability of fibroblasts, and reduce the migration of keratinocytes [1, 13–15]. These studies have provided sufficient evidence for diabetes to reduce skin renewal capacity. The classical opinion believes that diabetic ulcers are usually caused by neuropathy, insufficient blood supply, and infection [3]. However, the concept that the formation of diabetic ulcers is associated with reduced skin renewal capacity has not been widely accepted. Stronger evidence is needed to support this view.

Hair follicle is a complex micro-organ in the dermis. When the skin is injured, the epidermal stem cells in the hair follicle are activated and migrated to the wound site and then differentiated into epidermal cells, which contributes to the reepithelialization of the wound [16, 17]. Mice with defective hair follicle development showed a significant delay in reepithelialization [18, 19]. Hair follicles are one of the deepest components in the skin. The activation of hair follicle stem cells (HFSCs) helps to repair non-full-thickness skin injury, allowing missing skin to regenerate from hair follicles. Leucine-rich repeat-containing G protein-coupled receptor (Lgr5) is one of the biomarkers of HFSCs [20, 21]. The activation of Lgr5/Wnt/β-catenin signaling pathway is the key to hair follicle regeneration. Lgr5 depletion inhibits hair follicle regeneration [22]. This phenomenon is reversible due to the transdifferentiation between stem cells [22]. In addition, the activation of HFSCs determines the hair follicle cycle. The hair follicle cycle includes anagen, catagen, and telogen [23, 24]. The anagen (active growth phase) is the period when the hair follicles grow most vigorously. At the same time, activated melanocytes secrete melanin to defend against light radiation. During the catagen (transition phase), follicle matrix cells stop proliferating and melanocytes stop secreting melanin. The size of the hair follicle begins to decrease. During the telogen (resting phase), the hair follicle shrinks further, and the hair begins to fall out. When the body needs it, the hair follicles retransition from the telogen to the anagen. Based on our experience, the hair

follicles of C57BL/6 mice transit from the anagen to the telogen when they are 6-8 weeks old. Hair regrowth could be observed 10-14 days after the back is depilated, and the skin turns from white to bluish-black, which means that the HFSCs start to proliferate. After 21 days, the new hair will be the same length as the original hair.

Recently, hair follicle transplantation is considered a promising method for the treatment of diabetic ulcer. Traditional hair follicle transplantation collects hair follicles from the occipital region and transplants them to the bald area. The transplanted hair follicles will regenerate new hair within a few months [25]. Recent clinical studies show that autologous hair follicle transplantation can promote wound healing, especially diabetic ulcers [26–28]. For example, hair follicle transplantation can promote the diabetic leg ulcers healing and vascular regeneration [29]. Transplantation of epidermal sheets derived from hair follicles can accelerate chronic wound healing in patients with diabetes and chronic venous insufficiency of the lower extremities [30, 31]. Compared with abdominal skin without hair follicles, head skin with hair follicles accelerates the diabetic ulcer healing [32]. In addition, hair follicle transplantation can promote the wound healing of autosomal recessive dystrophic epidermolysis bullosa [33]. These studies not only prove the importance of hair follicles in maintaining skin regeneration, but also prove that hair follicles have great application potential as a tissue engineering biomaterial.

Diabetes affects skin regeneration, but the effect of diabetes on hair follicles is controversial. Only a few studies have put forward the idea that diabetes is associated with hair loss, but there is a lack of experimental proof [34–36]. We hypothesize that diabetes reduces the skin renewal capacity by inhibiting the hair follicles regeneration. Therefore, to observe the effect of diabetes on the hair follicles, we used streptozotocin (STZ) to induce type II diabetes (T2DM) in mice and observed the hair follicles regeneration on the back of the mice and explored the underlying mechanisms.

2. Materials and Methods

2.1. Ethical. The study related to animal use has been complied with all the relevant national regulations and institutional policies for the care and use of animals and has been approved by the Animal Care and Use Committee of Shenzhen Second People's Hospital.

2.2. Animals. Male C57BL/6 mice were purchased from Charles River (Beijing, China). Lgr5 + GFP/mTmG mice, which show green fluorescence in LGR5 protein and red fluorescence in the cell membrane, were gifts from Prof. Wang Xusheng of Sun Yat-sen University (Guangzhou, China). Animals were housed at the animal center of the Shenzhen Institute of Translational Medicine, under constant temperature (22-26°C) and half-day light/dark cycle schedule with free access to food (1025; HFK, Beijing, China) and water. Mice were anaesthetized using isoflurane (970-00026-00; RWD, Shenzhen, China).

After fasting for 16 hours, 20 mice were injected with STZ (120 mg/kg, dissolved in 0.028 mol/L citric acid and

0.022 mol/L sodium citrate buffer with pH 4.4) to induce T2DM [37]. Blood glucose levels were checked during the 2nd and 7th day after the injection. Mice with blood glucose ≥16.7 mmol/L were included in the experiment. On the 7th day of the experiment, hair on the back was removed with Veet® hair removal cream and then continued to observe the hair regrowth and hair follicle cycle transition.

2.3. Histology. At execution, mice were perfused with PBS. Skin samples were fixed in 4% paraformaldehyde (PFA) overnight and sent to Servicebio (Wuhan, China) for paraffin fixation services. Five μm slides were stained using a hematoxylin-eosin (H&E) kit (Servicebio, Wuhan, China). Pictures were taken under a microscope scanning system (SQS-40P, Shengqiang, Shenzhen, China).

2.4. Immunohistochemistry. For PCNA staining, the slides were incubated at 65°C for 2 h and dewaxed with xylene (15 min, 15 min), alcohols (100% 5 min, 100% 3 min, 95% 3 min, 80% 3 min), and water (5 min, 5 min). Slides were soaked in a pH 6.0 citrate solution at 95°C for 12 min and naturally cooled for 30 minutes. Next, the slides were incubated with endogenous peroxidase blocker (Kit-7310 reagent 1, Maixin, Fuzhou, China) for 15 min at 37°C, nonspecific staining blocker (Kit-7310 reagent 2, Maixin, Fuzhou, China) for 60 min, anti-PCNA antibody (A0264, ABclonal, Wuhan, China) overnight at 4°C, biotin-labeled goat anti-mouse/rabbit IgG polymer (Kit-7310 reagent 3, Maixin, Fuzhou, China) for 30 min at 37°C, and streptavidin-peroxidase (Kit-7310 reagent 4) for 15 min at 37°C. Diaminobenzidine (DAB, DAB-1031, Maixin, Fuzhou, China) staining is used for the brown color and hematoxylin staining for the background. Seal the slides with neutral gum.

2.5. Immunofluorescence. To assess cell proliferation, we used the immunohistochemistry kit (Kit-7310, Maixin, Fuzhou, China). Briefly, slides were incubated with 3% H_2O_2 for 30 min at 37°C, nonspecific staining blocker for 60 min, anti-K14 antibody (10143-1-AP, Proteintech, Wuhan, China) overnight at 4°C, HRP secondary antibody (ab150165, Abcam, Cambridge, UK) for 60 min 37°C, and DAPI (G1235-4, Servicebio, Wuhan, China). Pictures were taken under a microscope (Revolve FL, Discover echo, San Diego CA, USA).

2.6. RNA Sequencing. Samples were preserved in RNALater® at 4°C overnight. Then, samples were stored in dry ice and sent to the RNA-sequencing company (Nuomi, Suzhou, China). The data were processed by cluster heatmap, volcano map, Gene Ontology (GO), Reactome, and Kyoto Encyclopedia of Genes and Genomes (KEGG) enrichment analysis through the company technicians.

2.7. qRT-PCR. RNA samples were returned from the company after sequencing and transcribed to complementary DNA (cDNA) by synthesis kit (K1622, Thermo, Waltham MA, USA). Quantitative real-time PCR (qRT-PCR) kit was purchased from Bimake (B21203, Bimake, Shanghai, China). All the steps were performed according to the manufacturer's instructions. The qRT-PCR analysis was performed on an ABI-Q3 apparatus (ABI, Foster, USA) with normalization to Gapdh as the reference gene. Details were described as before [38, 39]. Primers sequences: Lgr4, forward 5′-CCCG ACTTCGCATTCACCAA-3′, reverse 5′-CCTGAGGAAAT TCATCCAAGTT-3′; Lgr5, forward 5′- CCTACTCGAAG ACTTACCCAGT-3′, reverse 5′-GCATTGGGGTGAATGA TAGCA-3′; Wnt4, forward 5′- AGACGTGCGAGAAACT CAAAG-3′, reverse 5′- GGAACTGGTATTGGCACTCCT-3′; Wng8a, forward 5′-GGGAACGGTGGAATTGTCCTG -3′, reverse 5′-GCAGAGCGGATGGCATGAA -3′; Gapdh, forward 5′-AGGTCGGTGTGAACGGATTTG -3′, reverse 5′-GGGGTCGTTGATGGCAACA -3′.

2.8. Western Blot. Details have been previously described [40]. Proteins were detected by anti-WNT4 and anti-WNT8A (GB112192, GB112250, Servicebio, Wuhan, China) rabbit polyclonal antibodies. Anti-β-TUBULIN mouse monoclonal antibody was obtained from Servicebio (GB13017-2).

2.9. Statistics. Data are reported as mean ± standard deviation (SD). Group size assayed in each experiment is indicated in the figure legends. Group mean differences were analyzed by Student's t-test using GraphPad Prism 6 (San Diego, USA). A $P < 0.05$ was considered statistically significant.

3. Results

3.1. T2DM Inhibits Hair Regrowth and Reduces Skin Thickness. Mice were depilated on day 7 after successful induction of T2DM. As expected, on the 10th day after depilation, there was a significant difference in hair regrowth between the two groups. Compared to control group, T2DM inhibited hair regrowth (Figures 1(a) and 1(b)). To further confirm the inhibitory effect of T2DM on hair follicles, we observed skin tissue sections. The H&E staining showed that T2DM not only inhibited the hair follicles regeneration, but also reduced the skin thickness (Figures 1(c) and 1(d)). It means that T2DM may delay the hair follicles cycle transition and inhibit skin cells proliferation. Apart from this, we did not observe any changes in other skin structures and organs.

3.2. T2DM Inhibits the PCNA Expression and K14 Proliferation. To study whether T2DM inhibited the hair follicles regeneration and skin cells proliferation, we observed the expression of PCNA and K14, which are important biomarkers of cell proliferation. T2DM inhibited the expression of PCNA in hair follicles and epidermis (Figures 2(a) and 2(b)). Also, T2DM reduced the fluorescence intensity of K14 (Figures 2(c) and 2(d)). This shows that T2DM can inhibit hair follicles regeneration and skin cells proliferation.

3.3. T2DM Inhibits HFSCs Activation and Cell Cycle-Related Pathways. To explore the underlying mechanism of T2DM inhibited skin cells proliferation and hair follicles regeneration, we analyzed the differences in mRNA expression between the two groups. The results showed that there were significant differences in mRNA expression between the two groups (Figures 3(a) and 3(b)). Moreover, the bioinformatics

(a)

S = Significant

A = Alteration

N = No change

(b)

Figure 1: Continued.

(c)
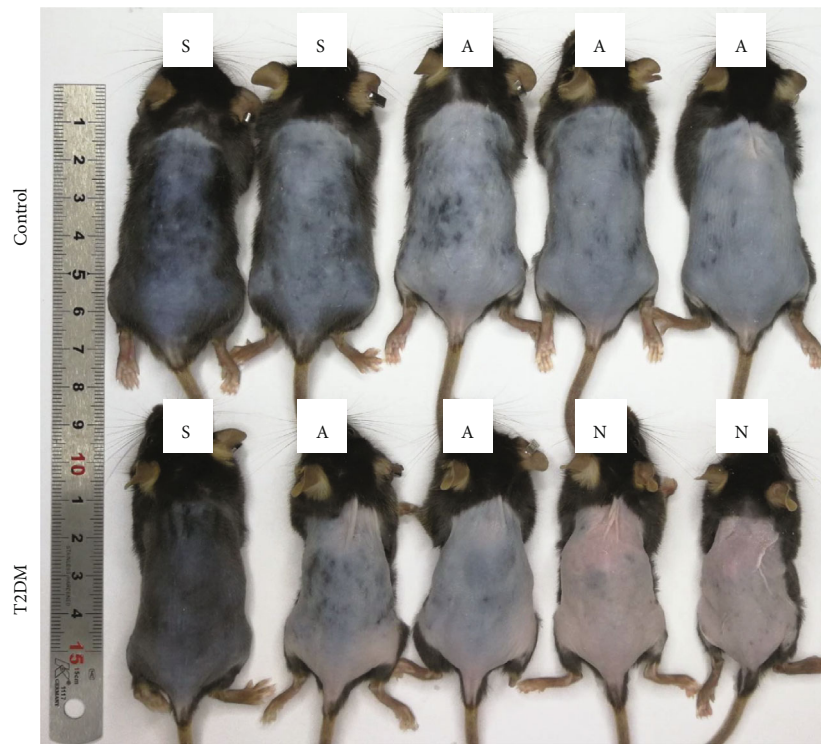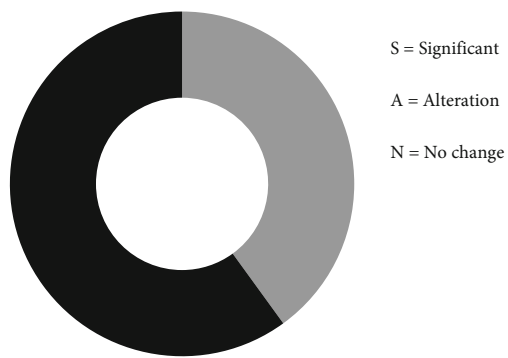
(d)
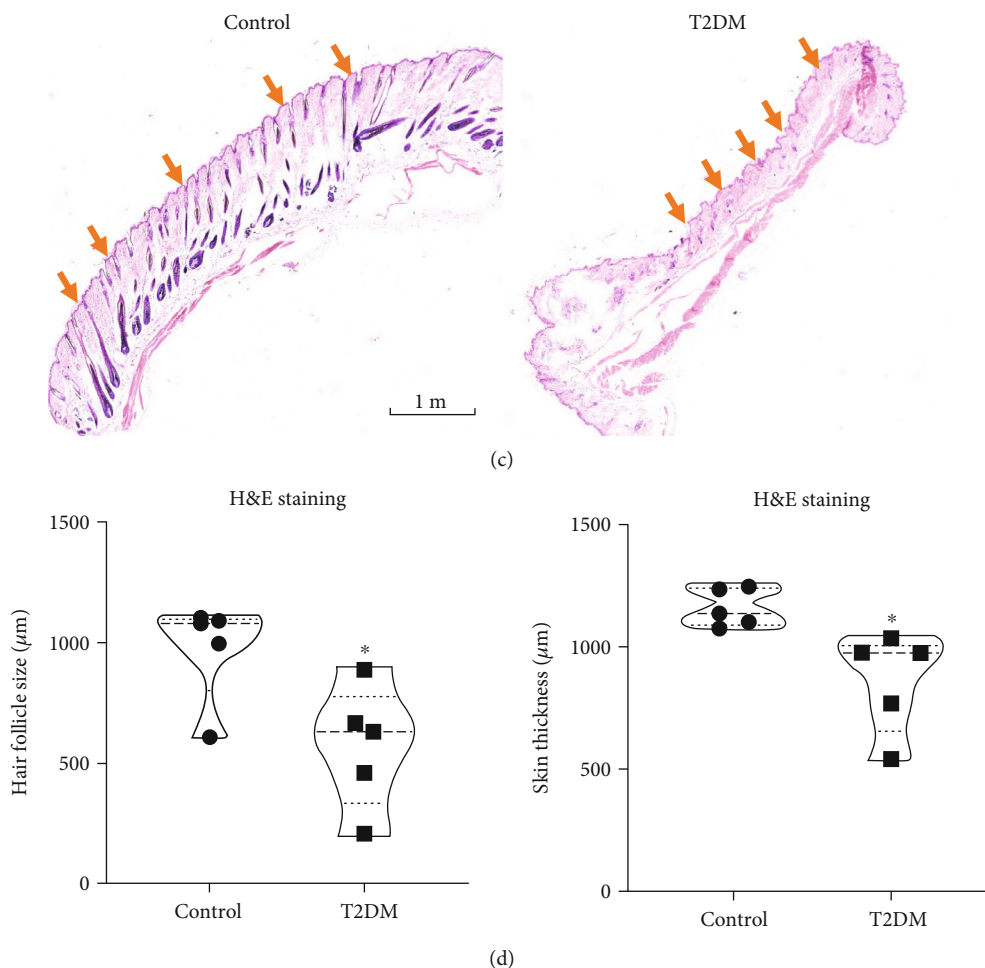
FIGURE 1: T2DM inhibits hair cycling and reduces skin thickness. (a) Representative photo of hair regrowth on the back of mice. S: significant; A: alteration; N: no change. (b) 40% and 60% of control mice show significant hair regrowth and hair follicle alteration, respectively. 20% and 40% of T2DM mice show significant hair regrowth and hair follicle alteration, respectively. The other 40% of mice have no change. (c) Representative photos of hair follicles. Orange arrows direct the hair follicles. (d) T2DM significantly decreased hair follicle size (control 975 ± 210 vs. T2DM 568.8 ± 254.3 μm, $P = 0.0249$, $n = 5$) and skin thickness (control 1159 ± 77.69 vs. T2DM 859.8 ± 204.4 μm, $P = 0.0155$, $n = 5$). $*P < 0.05$.

analysis of GO, Reactome, and KEGG showed significant differences in the expression of genes related to cell cycle, proliferation, and division (Figures 3(e), 3(f), and 3(g)). Compared with the control group, T2DM significantly inhibited the expression of *Lgr4*, *Lgr5*, *Wnt4*, and *Wnt8a* genes, which are related to the activation of HFSCs (Figure 3(c)). The results of qRT-PCR are consistent with the results of RNA sequencing (Figure 3(d)). These results suggest that T2DM inhibits the proliferation of skin cell populations by inhibiting the cell cycle. And it is closely related to LGR5/WNT pathway-dependent HFSCs activation.

3.4. T2DM Inhibits Lgr5+ Hair Follicle Stem Cells Activation and WNT Expression. To identify whether T2DM inhibited WNT-dependent Lgr5 hair follicle stem cell activation, we used Lgr5 + GFP/mTmG mice. Compared with the control mice, the green fluorescence of the T2DM mice was significantly reduced as shown in Figure 4(a). Similarly, T2DM suppressed the expression of WNT4 protein (Figure 4(b)). However, the level of WNT8A protein was not significantly

different between the two groups, which may be related to the lower group size and lower protein expression level (Figure 4(c)).

4. Discussion

The cause of diabetic ulcers has been attributed to neuropathy, insufficient blood supply, and infection [3]. Here, it is the first time shown that T2DM inhibits the skin renewal capacity by inhibiting the WNT-dependent Lgr5 hair follicle stem cells activation. In addition, T2DM directly inhibits cutaneous cells proliferation, including K14 and HFSCs, by inhibiting the cell cycling. This may be a new mechanism for the formation of diabetic ulcers. This study not only explains why T2DM affects skin regeneration, but also gives a new way for the development of treatments for diabetic ulcers in the future.

There is no doubt that high glucose affects cells activity and physiological functions. For example, high glucose can inhibit the differentiation of neural stem cells [41] and also

250 μm

25 μm

250 μm

25 μm

(a)

PCNA in HFSC
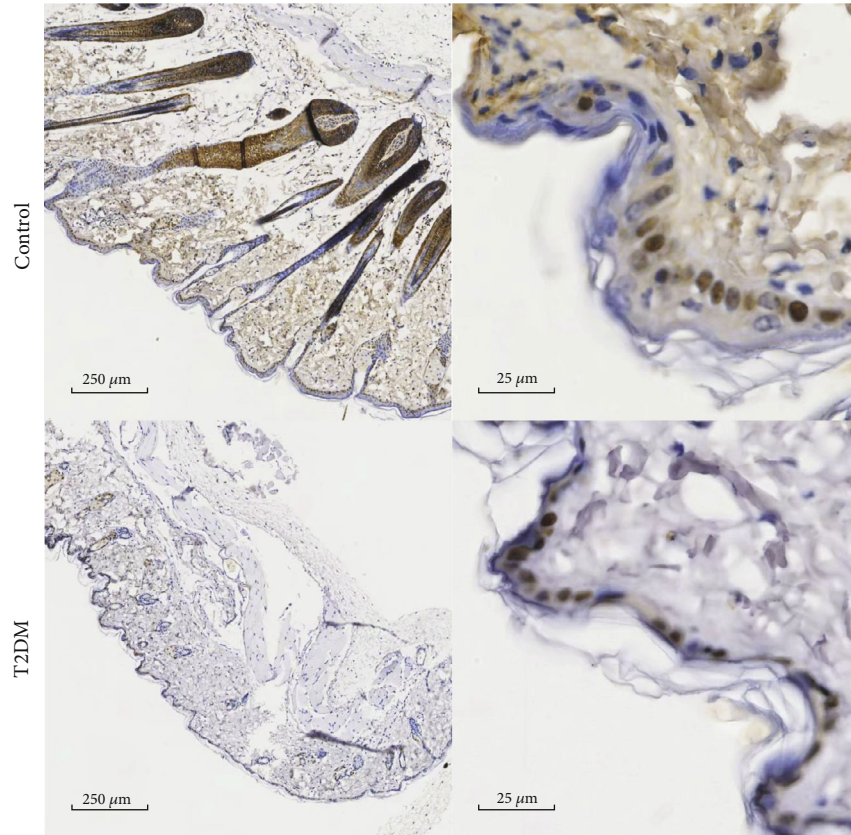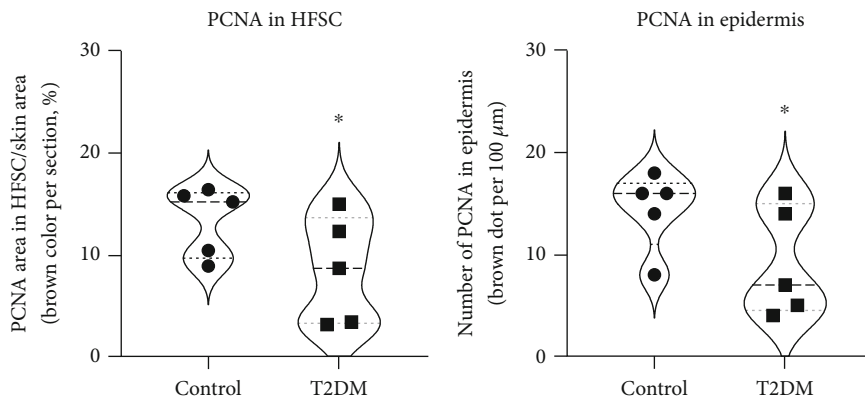
PCNA in epidermis

(b)

FIGURE 2: Continued.

(c)

(d)
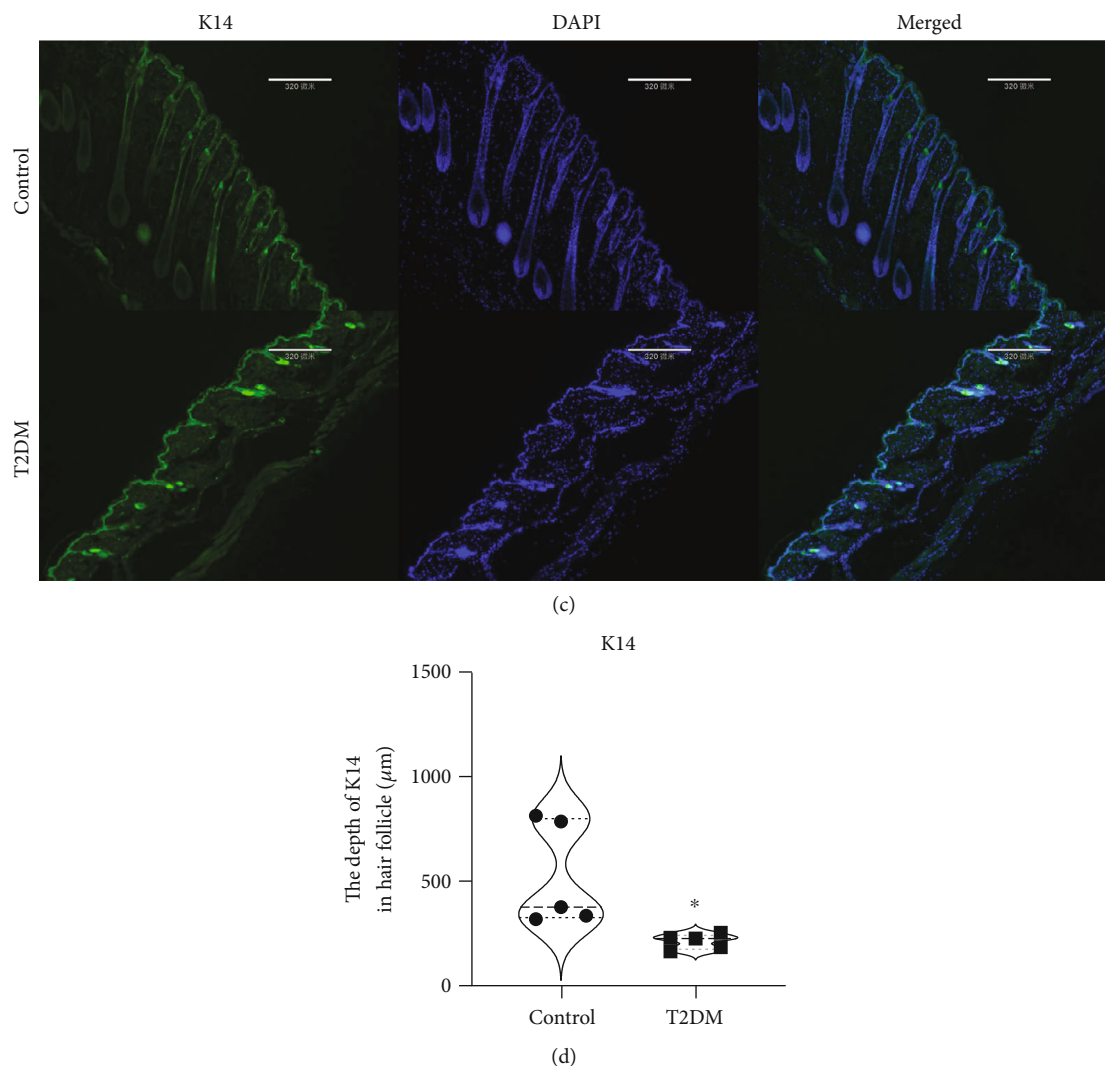
FIGURE 2: T2DM inhibits skin cells proliferation. (a) Representative photos of PCNA in the skin. (b) T2DM decreased the PCNA expression in hair follicles (control 13.31 ± 3.428 vs. T2DM 8.462 ± 5.272, brown area %, $P = 0.0204$, $n = 5$) and epidermis (control 14.4 ± 3.387 vs. T2DM 9.2 ± 5.45, brown dot per $100\,\mu m$, $P = 0.0387$, $n = 5$). (c) Representative photos of K14 and DAPI staining in skin. (d) T2DM reduced the depth of K14 in hair follicles (control 525.8 ± 250.5 vs. T2DM 212.2 ± 36.23, μm, $P = 0.0353$, $n = 5$). $*P < 0.05$.

lead to the death of cardiac stem cells [42]. In this study, T2DM inhibited the activation of Lgr5 HFSC, the proliferation of K14, and the production of PCNA, which means that T2DM reduced the renewal capacity of the skin. The following RNA sequencing results further proved our hypothesis that the T2DM inhibited cell cycling. Because HFSCs can differentiate into a variety of skin cells, we believe that T2DM inhibits the skin renewal capacity by inhibiting the Lgr5 HFSCs activation.

Hair follicles are distributed in most areas of the body, but there are differences in distribution and morphology [43]. In humans, most of the hair on the body surface is small and colorless, while the hair on the head is longer and denser. The hair follicles in the same area may also have significant characteristics differences in different districts, such as the top of the head and the headrest area. Compared with the hair follicles on the top of the head, the hair follicles of the headrest have stronger environmental adaptability and can resist androgenetic alopecia [44]. Therefore, the hair follicles in the headrest area are also considered as premium donor sites for hair follicle transplantation [45]. Similarly, it is considered that the skin from the head is more suitable to be a donor site for skin grafting. It can be explained that the headrest contains high-quality hair follicles, which increases the success rate of skin grafting. In contrast, hair follicles from nonpremium donor sites may have reduced proliferation and differentiation capacity due to environmental interference. As far as we know, Balb/c background nude mice have no hair in most areas of their bodies, but a small amount of hair growth can be observed on the head and beard. This study focused the effect of T2DM on hair follicles from the back of mice. As expected, these hair follicles are sensitive to diabetes. This can explain why diabetic patients have reduced skin renewal capacity and are more likely to form chronic wounds. Nevertheless, diabetic ulcers rarely occur on the head, and hair loss is not yet considered a
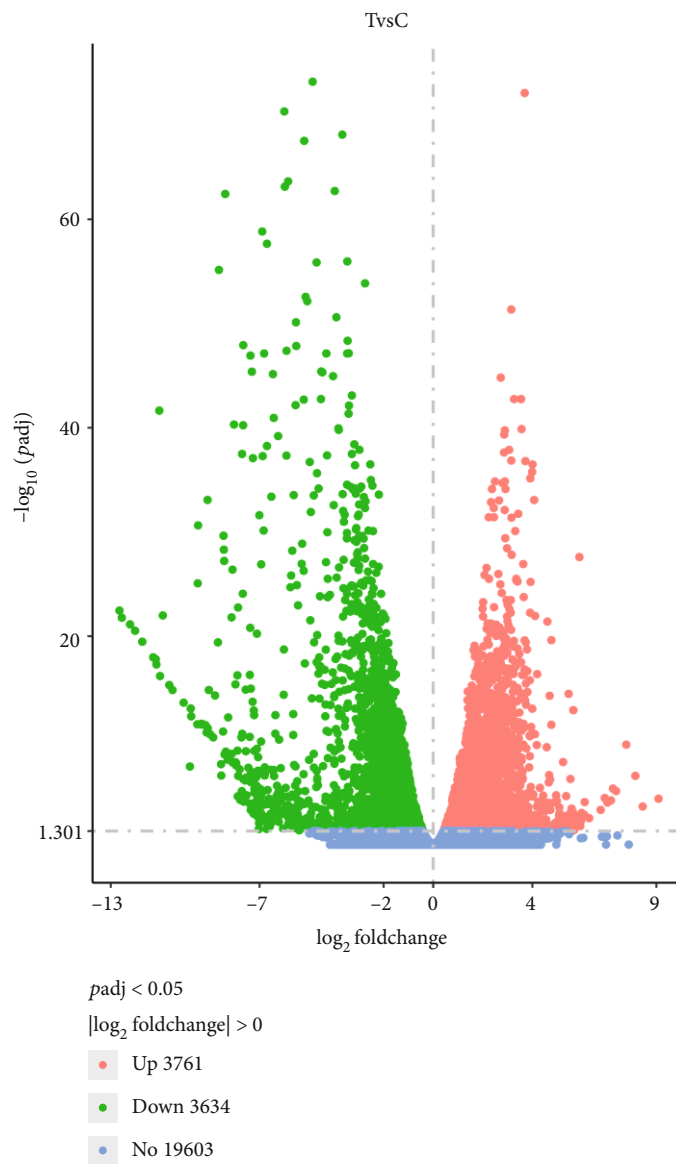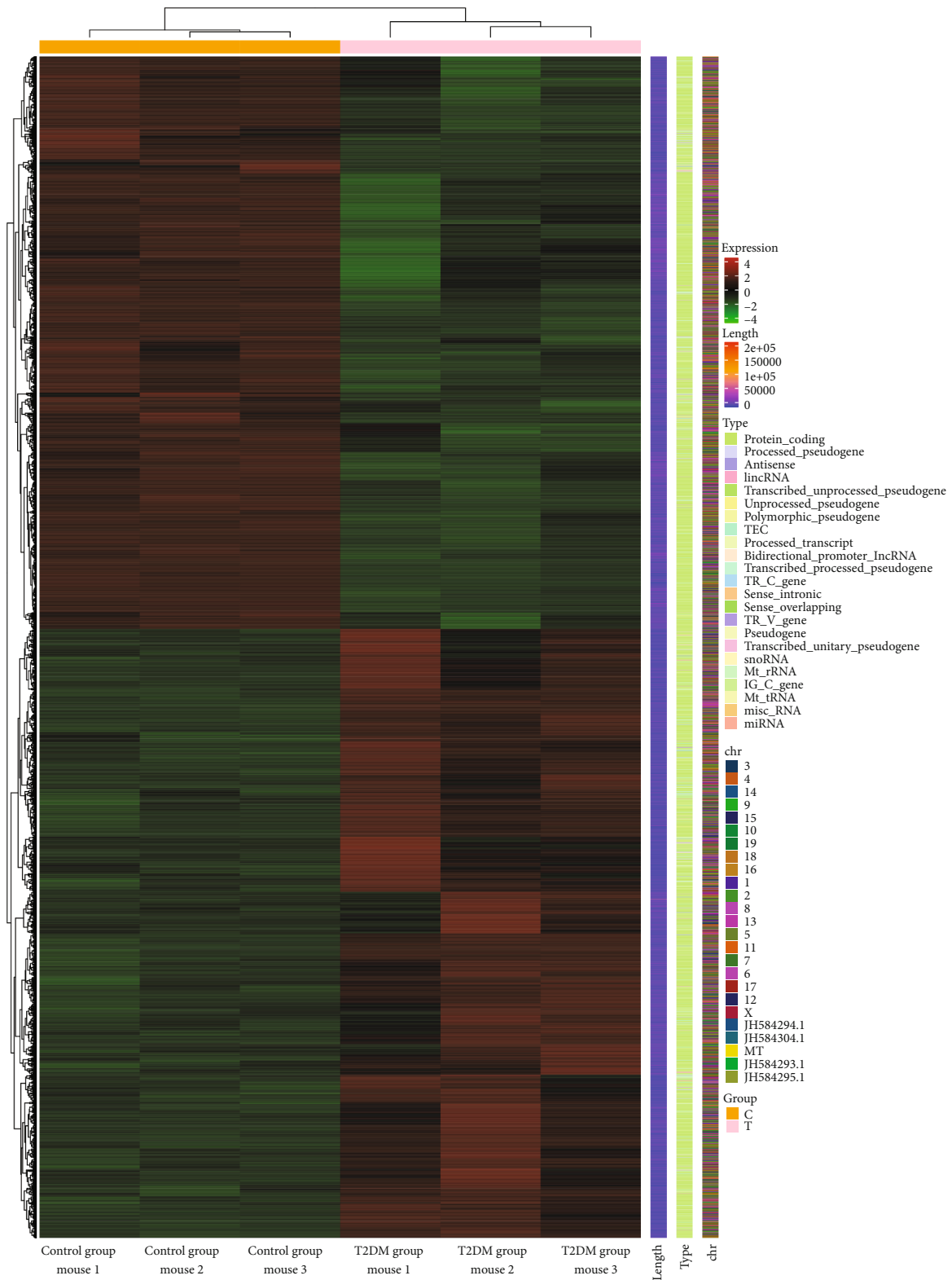
FIGURE 3: Continued.

(b)

FIGURE 3: Continued.

(c)

(d)

(e)
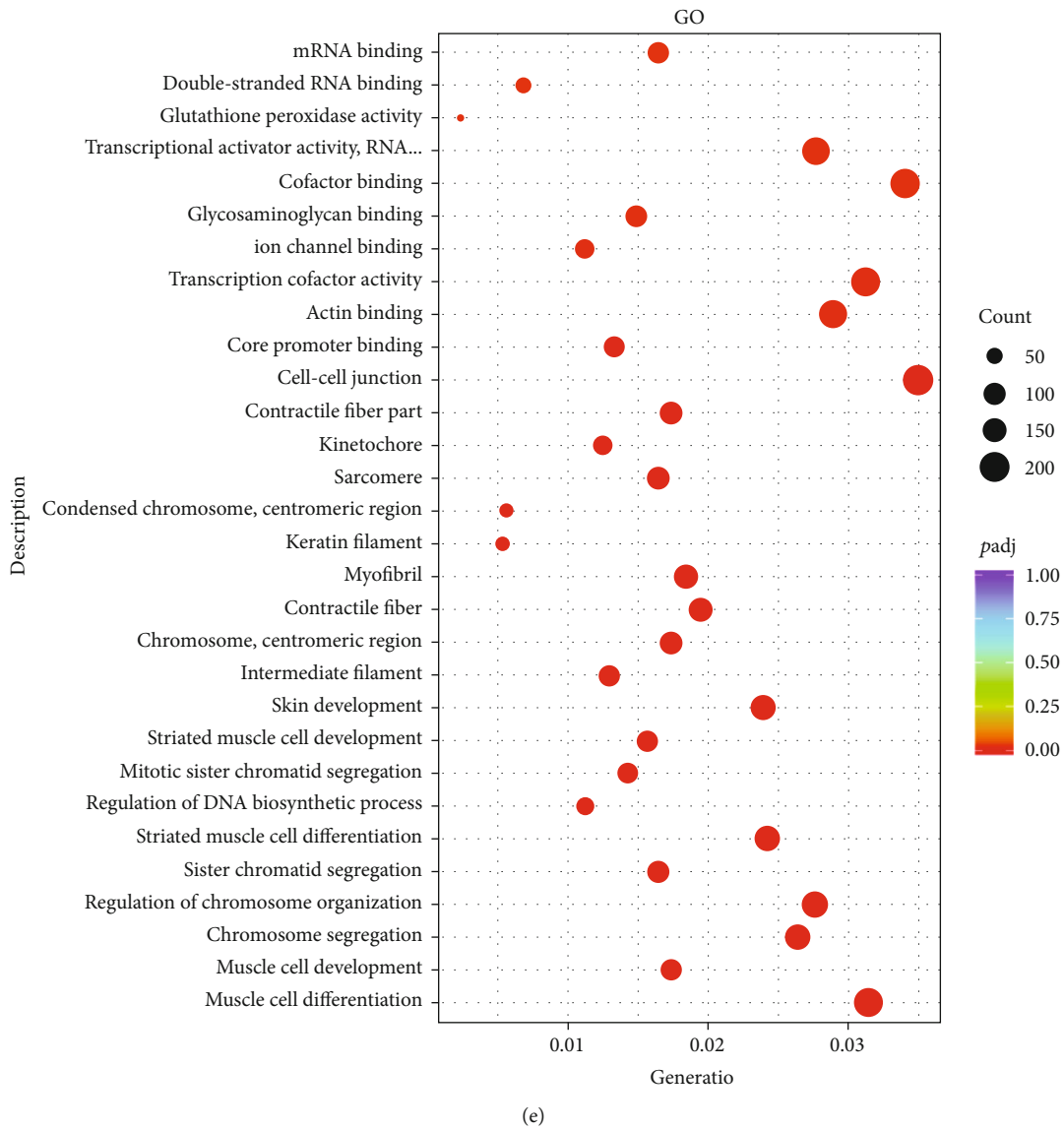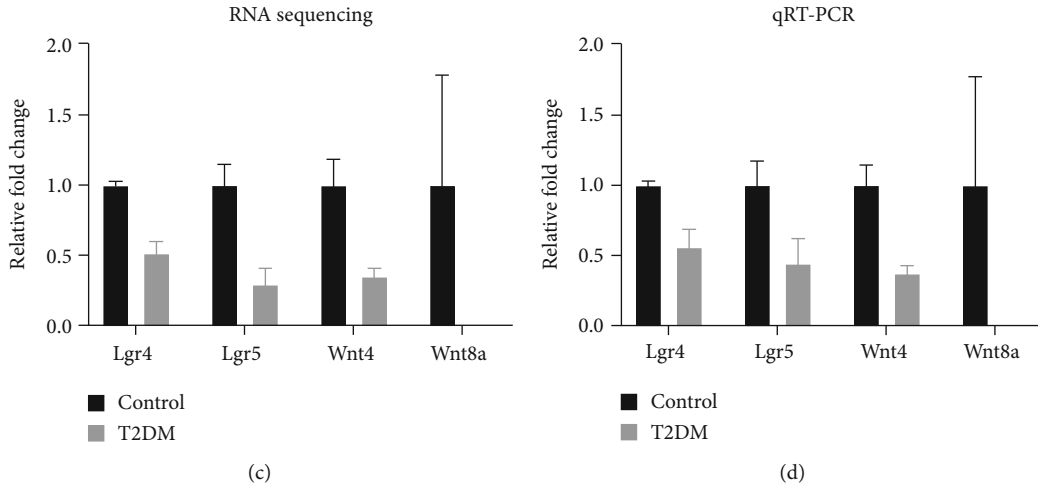
Figure 3: Continued.
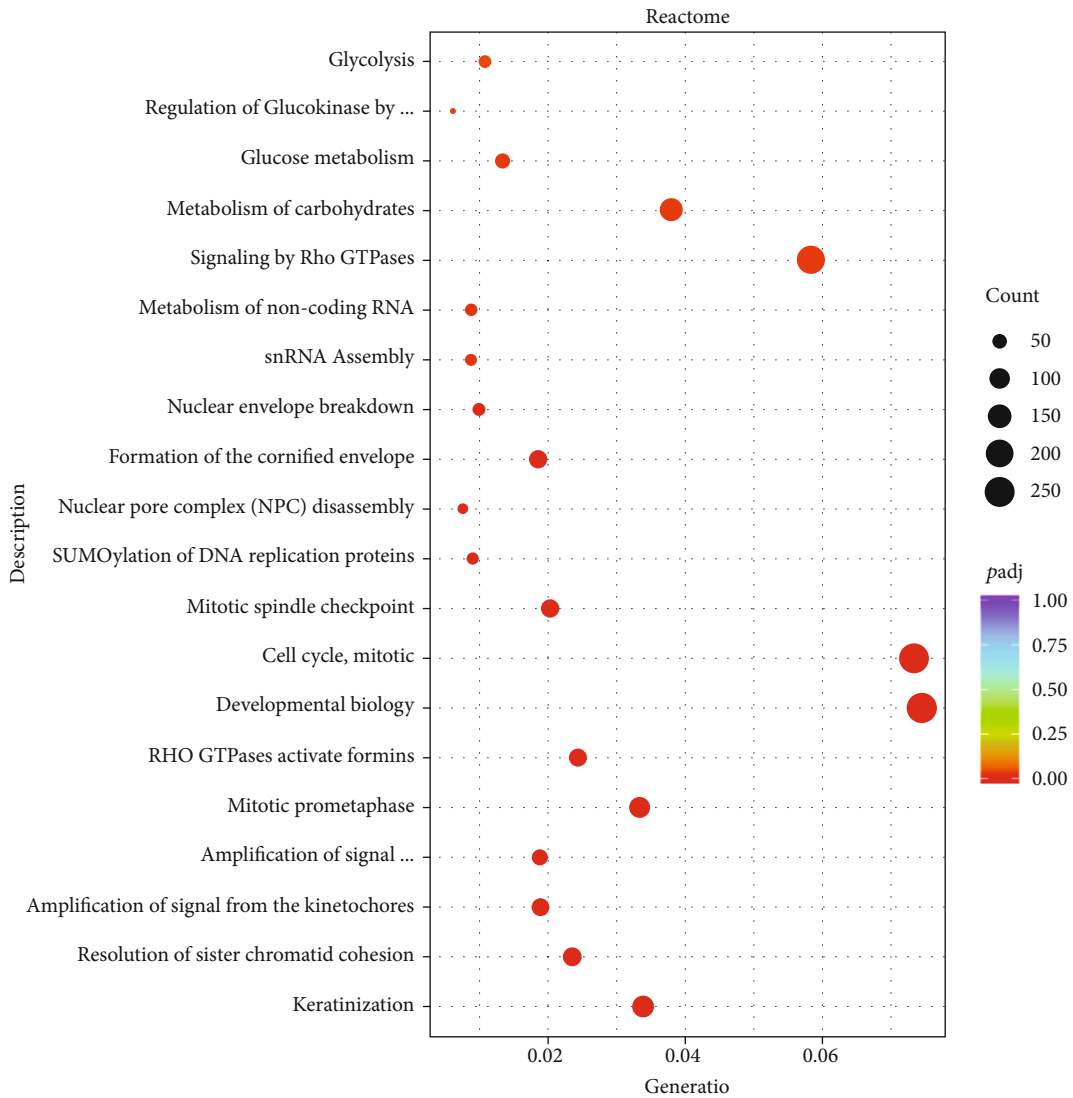
(f)

Figure 3: Continued.

(g)
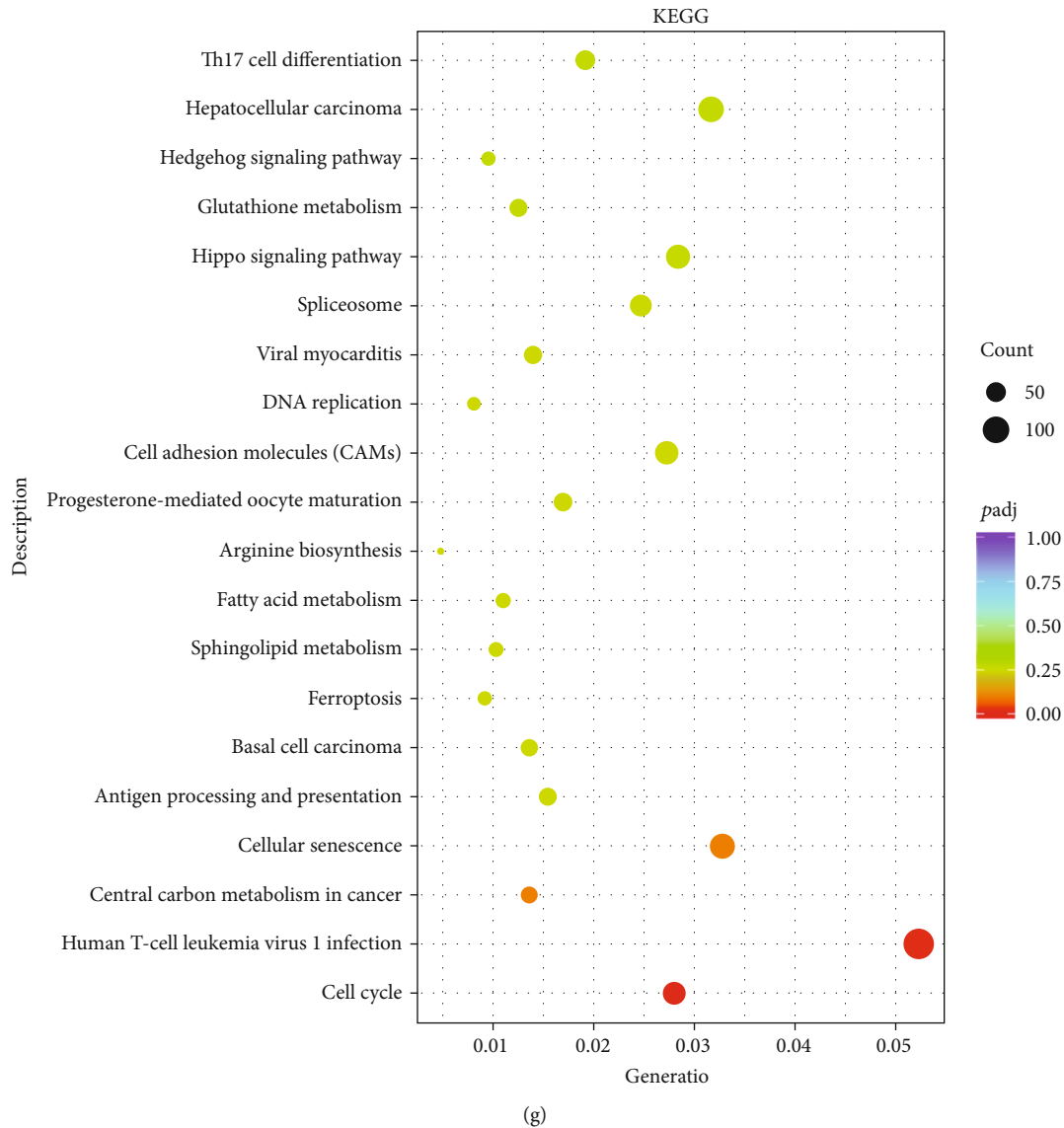
Figure 3: RNA sequencing results. (a) Volcano map. (b) The mRNA expression levels between samples. (c, d) Lgr4, Lgr5, Wnt4, and Wnt8a expression levels in RNA sequencing and qRT-PCR, respectively. (e, f, g) GO, Reactome, and KEGG bioinformatic analysis results.

symptom of diabetes. Unfortunately, the effect of diabetes on hair follicles of the head and the limbs in mice has not been studied yet. This is also an important area to research upon in the future.

In addition, the demand for glucose of hair follicles from different regions is inconsistent. Generally, the growth of hair follicles on the head has a higher energy requirement, which is related to the metabolism of glucose and glucose derivatives [46, 47]. Moreover, the glucose sensitivity of stem cells activation and differentiation are inconsistent [48, 49]. For example, muscle stem cells have different requirements for glucose during proliferation, resting, and differentiation [50]. However, we have not found any research on the relationship between hyperglycemia and trunk hair follicles. At least, our research supports the result that trunk hair follicles are sensitive to hyperglycemia.

Skin grafting is the golden standard for the treatment of large-area burns and full-thickness wounds [51–53]. The

success rate is related to problems, such as poor grafts, infections, and donor site morbidity [52, 54]. For diabetic patients, skin grafting may also cause new wounds, which may have complications and difficult to heal. For patients with skin defects and burns that exceed 50%-60% of the total body surface, autologous skin grafting is impractical due to insufficient donor sites [53, 55]. Although autologous skin grafting is the first choice, in some cases, artificial skin is also a good choice. Besides, hair follicle transplantation can provide a source of autologous keratinocytes for wound healing. Hair follicles can be obtained quickly and will not cause large wounds. Therefore, hair follicle transplantation has great potential in the treatment of diabetic ulcers. In addition to this, hair follicles can be proliferated through the hair follicle recombination technology in vitro, and it can be used in the treatment of patients with severe burns or diabetes. It does not only reduce the need for donation area, but also reduces the risk of infection. Recently, bioprinting

(a)

(b)

(c)
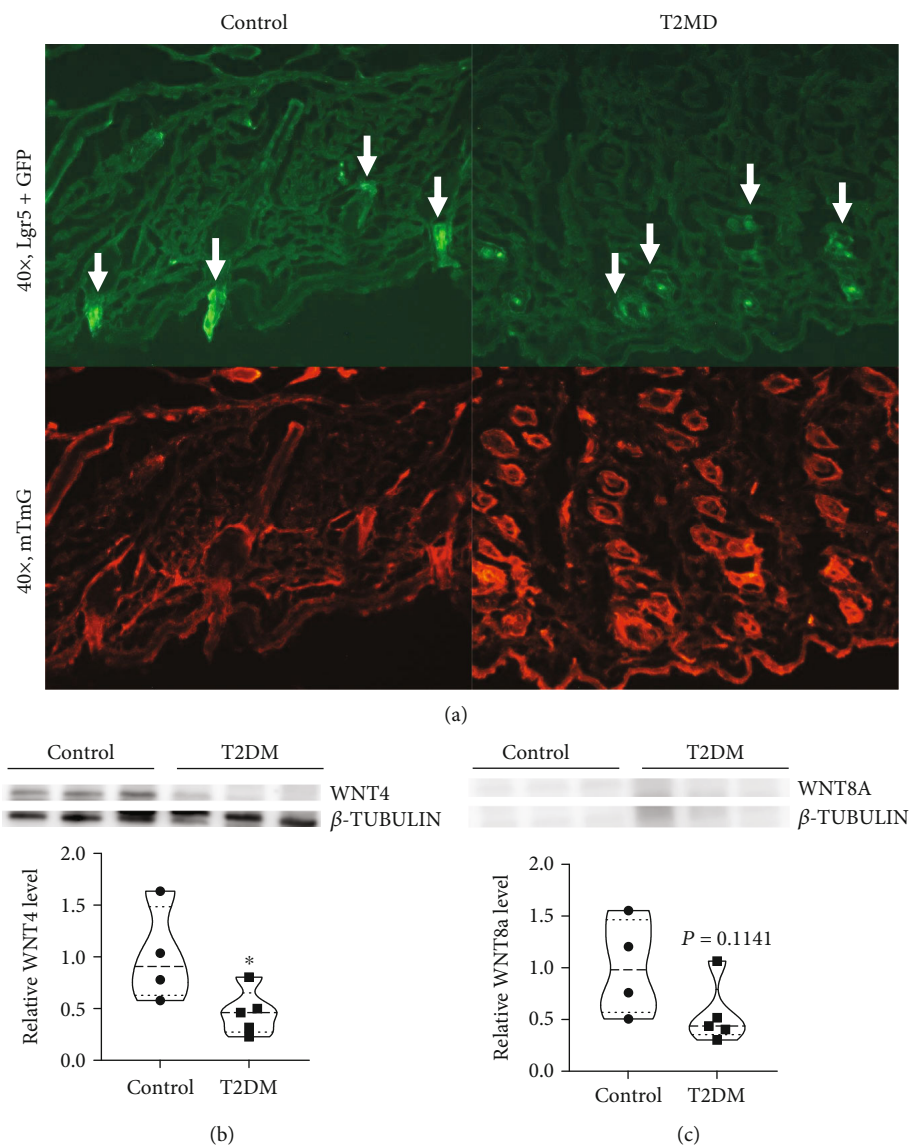
FIGURE 4: T2DM inhibits Lgr5+ hair follicle stem cells activation and WNT expression. (a) Representative photos of skin sections from Lgr5 + GFP/mTmG mice. (b, c) WNT4 (control 1 ± 0.4579 vs. T2DM 0.4562 ± 0.2201, $P = 0.05$, $n = 4 - 5$) and WNT8A (control 1 ± 0.4648 vs. T2DM 0.5404 ± 0.3002, $P = 0.1141$, $n = 4 - 5$) protein levels in skin. $*P < 0.05$.

technology has provided a good choice for wound repair. It does not only print 3-dimensional bionic skin, but also create a stable structure. Although there are more and more biomaterials that combine stem cells with bioprinting, there is no biomaterial containing hair follicles and HFSCs [53]. The development of biomaterials containing HFSCs or hair follicle structure has potential application prospects and clinical value.

We were interested to publish this study as soon as possible; therefore, this study has some limitations. First, the group size is small, and we will increase the group size to confirm the accuracy and universality of the research. Second, we used male mice, and we are planning to use female mice as well in our future study. Third, hair follicles in mice are different from those in humans. It is not sure whether the phenomenon that diabetes inhibits hair follicle regeneration also exists in humans. And it is uncertain alopecia is

related to diabetes; therefore, further research is needed. Fourth, our research period is short. We only observed hair follicle and skin changes within 3 weeks after T2DM induction. We did not observe changes in other skin structures during this study period. Diabetes is known to cause chronic organ injury. Longer study periods are required if the long-term effects of T2DM on the skin are to be observed. Lastly, our research only explains the phenomenon and mechanism of T2DM inhibiting the regeneration of hair follicles on the back of mice, and the rest of the site is still unclear. We are planning to add more data in the future.

5. Conclusions

In summary, T2DM inhibits skin self-renewal by inhibiting WNT-dependent Lgr5 HFSCs activation. It may be a key factor in the formation of diabetic chronic wounds. This

study not only provides a new explanation for the formation of diabetic chronic wounds, but also provides a new theoretical basis for hair follicle transplantation. Finding a mechanism that can resist the HFSCs inhibitory effects of diabetes may lead to the development of new drugs.

Data Availability

The data used to support the findings of this study are available from the corresponding author upon request.

Conflicts of Interest

The authors do not have any conflicts of interest to declare.

Authors' Contributions

Minghui Wang and Shangsheng Yao contributed equally to this work.

Acknowledgments

References

[1] A. L. Lima, T. Illing, S. Schliemann, and P. Elsner, "Cutaneous manifestations of diabetes mellitus: a review," *American Journal of Clinical Dermatology*, vol. 18, no. 4, pp. 541–553, 2017.

[2] "World Health Organization: Facts and Figures about Diabetes," 2014, http://www.who.int/mediacentre/factsheets/fs312/en/.

[3] S. Patel, S. Srivastava, M. R. Singh, and D. Singh, "Mechanistic insight into diabetic wounds: pathogenesis, molecular targets and treatment strategies to pace wound healing," *Biomedicine & Pharmacotherapy*, vol. 112, article 108615, 2019.

[4] W. Jeffcoate and K. Bakker, "World diabetes day: footing the bill," *Lancet*, vol. 365, no. 9470, p. 1527, 2005.

[5] P. Zhang, J. Lu, Y. Jing, S. Tang, D. Zhu, and Y. Bi, "Global epidemiology of diabetic foot ulceration: a systematic review and meta-analysis," *Annals of Medicine*, vol. 49, no. 2, pp. 106–116, 2017.

[6] P. A. Lazzarini, S. E. Hurn, M. E. Fernando et al., "Prevalence of foot disease and risk factors in general inpatient populations: a systematic review and meta-analysis," *BMJ Open*, vol. 5, no. 11, article e008544, 2015.

[7] S. C. Mishra, K. C. Chhatbar, A. Kashikar, and A. Mehndiratta, "Diabetic foot," *BMJ*, vol. 359, article j5064, 2017.

[8] K. A. U. Gonzales and E. Fuchs, "Skin and its regenerative powers: an alliance between stem cells and their niche," *Developmental Cell*, vol. 43, no. 4, pp. 387–401, 2017.

[9] A. L. Mendes, H. A. Miot, and V. J. Haddad, "Diabetes mellitus and the skin," *Anais Brasileiros de Dermatologia*, vol. 92, no. 1, pp. 8–20, 2017.

[10] J. Okano, H. Kojima, M. Katagi et al., "Hyperglycemia induces skin barrier dysfunctions with impairment of epidermal integrity in non-wounded skin of type 1 diabetic mice," *PLoS One*, vol. 11, no. 11, article e0166215, 2016.

[11] H. Y. Park, J. H. Kim, M. Jung et al., "A long-standing hyperglycaemic condition impairs skin barrier by accelerating skin ageing process," *Experimental Dermatology*, vol. 20, no. 12, pp. 969–974, 2011.

[12] S. Sakai, Y. Endo, N. Ozawa et al., "Characteristics of the epidermis and stratum corneum of hairless mice with experimentally induced diabetes mellitus," *The Journal of Investigative Dermatology*, vol. 120, no. 1, pp. 79–85, 2003.

[13] J. Zhang, P. Yang, D. Liu et al., "C-myc upregulated by high glucose inhibits hacat differentiation by s100a6 transcriptional activation," *Frontiers in Endocrinology*, vol. 12, article 676403, 2021.

[14] D. Wang, Y. Jiang, Z. Li et al., "The effect of candida albicans on the expression levels of toll-like receptor 2 and interleukin-8 in hacat cells under high- and low-glucose conditions," *Indian Journal of Dermatology*, vol. 63, no. 3, pp. 201–207, 2018.

[15] C. Zhang, B. Ponugoti, C. Tian et al., "Foxo1 differentially regulates both normal and diabetic wound healing," *The Journal of Cell Biology*, vol. 209, no. 2, pp. 289–303, 2015.

[16] Y. Amoh and R. M. Hoffman, "Hair follicle-associated-pluripotent (hap) stem cells," *Cell Cycle*, vol. 16, no. 22, pp. 2169–2175, 2017.

[17] E. Fuchs, "Scratching the surface of skin development," *Nature*, vol. 445, no. 7130, pp. 834–842, 2007.

[18] A. K. Langton, S. E. Herrick, and D. J. Headon, "An extended epidermal response heals cutaneous wounds in the absence of a hair follicle stem cell contribution," *The Journal of Investigative Dermatology*, vol. 128, no. 5, pp. 1311–1318, 2008.

[19] A. N. Vagnozzi, J. F. Reiter, and S. Y. Wong, "Hair follicle and interfollicular epidermal stem cells make varying contributions to wound regeneration," *Cell Cycle*, vol. 14, no. 21, pp. 3408–3417, 2015.

[20] N. Barker, J. H. van Es, J. Kuipers et al., "Identification of stem cells in small intestine and colon by marker gene Lgr5," *Nature*, vol. 449, no. 7165, pp. 1003–1007, 2007.

[21] V. Jaks, N. Barker, M. Kasper et al., "Lgr5 marks cycling, yet long-lived, hair follicle stem cells," *Nature Genetics*, vol. 40, no. 11, pp. 1291–1299, 2008.

[22] J. D. Hoeck, B. Biehs, A. V. Kurtova et al., "Stem cell plasticity enables hair regeneration following Lgr5+ cell loss," *Nature Cell Biology*, vol. 19, no. 6, pp. 666–676, 2017.

[23] J. W. Oh, J. Kloepper, E. A. Langan et al., "A guide to studying human hair follicle cycling in vivo," *The Journal of Investigative Dermatology*, vol. 136, no. 1, pp. 34–44, 2016.

[24] T. M. Brown and K. Krishnamurthy, "Histology, hair and follicle," in *Statpearls*, StatPearls Publishing Copyright, Treasure Island (FL), 2022.

[25] P. T. Rose, "Advances in hair restoration," *Dermatologic Clinics*, vol. 36, no. 1, pp. 57–62, 2018.

[26] F. Jimenez, E. Poblet, and A. Izeta, "Reflections on how wound healing-promoting effects of the hair follicle can be translated into clinical practice," *Experimental Dermatology*, vol. 24, no. 2, pp. 91–94, 2015.

[27] K. Nuutila, "Hair follicle transplantation for wound repair," *Advances in Wound Care*, vol. 10, no. 3, pp. 153–163, 2021.

[28] M. L. Martínez Martínez, E. E. Travesedo, and F. J. Acosta, "Hair-follicle transplant into chronic ulcers: a new graft concept," *Actas Dermo-Sifiliográficas (English Edition)*, vol. 108, pp. 524–531, 2017.

[29] F. Jimenez, C. Garde, E. Poblet et al., "A pilot clinical study of hair grafting in chronic leg ulcers," *Wound Repair and Regeneration*, vol. 20, no. 6, pp. 806–814, 2012.

[30] R. Renner, W. Harth, and J. C. Simon, "Transplantation of chronic wounds with epidermal sheets derived from autologous hair follicles–the leipzig experience," *International Wound Journal*, vol. 6, no. 3, pp. 226–232, 2009.

[31] A. Limat, L. E. French, L. Blal, J. H. Saurat, T. Hunziker, and D. Salomon, "Organotypic cultures of autologous hair follicle keratinocytes for the treatment of recurrent leg ulcers," *Journal of the American Academy of Dermatology*, vol. 48, no. 2, pp. 207–214, 2003.

[32] M. L. Martínez, E. Escario, E. Poblet et al., "Hair follicle-containing punch grafts accelerate chronic ulcer healing: a randomized controlled trial," *Journal of the American Academy of Dermatology*, vol. 75, no. 5, pp. 1007–1014, 2016.

[33] T. W. Wong, C. C. Yang, C. K. Hsu, C. H. Liu, and J. Yu-Yun Lee, "Transplantation of autologous single hair units heals chronic wounds in autosomal recessive dystrophic epidermolysis bullosa: a proof-of-concept study," *Journal of Tissue Viability*, vol. 30, no. 1, pp. 36–41, 2021.

[34] P. F. Coogan, T. N. Bethea, Y. C. Cozier et al., "Association of type 2 diabetes with central-scalp hair loss in a large cohort study of african american women," *International Journal of Women's Dermatology*, vol. 5, no. 4, pp. 261–266, 2019.

[35] E. Cakir, "Is prediabetes risk factor for hair loss?," *Medical Hypotheses*, vol. 79, no. 6, p. 879, 2012.

[36] J. J. Miranda, A. Taype-Rondan, J. C. Tapia, M. G. Gastanadui-Gonzalez, and R. Roman-Carpio, "Hair follicle characteristics as early marker of type 2 diabetes," *Medical Hypotheses*, vol. 95, pp. 39–44, 2016.

[37] J. Yang, P. Zhao, D. Wan et al., "Antidiabetic effect of methanolic extract from Berberis julianae Schneid. via activation of amp-activated protein kinase in type 2 diabetic mice," *Evidence-based Complementary and Alternative Medicine*, vol. 2014, Article ID 106206, 12 pages, 2014.

[38] M. Zhu, M. Zhu, X. Wu et al., "Porcine acellular dermal matrix increases fat survival rate after fat grafting in nude mice," *Aesthetic Plastic Surgery*, vol. 45, no. 5, pp. 2426–2436, 2021.

[39] F. Meng, J. Qiu, H. Chen et al., "Dietary supplementation with n-3 polyunsaturated fatty acid-enriched fish oil promotes wound healing after ultraviolet b-induced sunburn in mice," *Food Science & Nutrition*, vol. 9, no. 7, pp. 3693–3700, 2021.

[40] A. Hammer, G. Yang, J. Friedrich et al., "Role of the receptor mas in macrophage-mediated inflammation in vivo," *Proceedings of the National Academy of Sciences of the United States of America*, vol. 113, no. 49, pp. 14109–14114, 2016.

[41] X. Chen, W. B. Shen, P. Yang, D. Dong, W. Sun, and P. Yang, "High glucose inhibits neural stem cell differentiation through oxidative stress and endoplasmic reticulum stress," *Stem Cells and Development*, vol. 27, no. 11, pp. 745–755, 2018.

[42] S. K. Yadav, T. N. Kambis, S. Kar, S. Y. Park, and P. K. Mishra, "Mmp9 mediates acute hyperglycemia-induced human cardiac stem cell death by upregulating apoptosis and pyroptosis in vitro," *Cell Death & Disease*, vol. 11, no. 3, p. 186, 2020.

[43] B. Buffoli, F. Rinaldi, M. Labanca et al., "The human hair: from anatomy to physiology," *International Journal of Dermatology*, vol. 53, no. 3, pp. 331–341, 2014.

[44] H. A. Chen, J. Y. Pan, C. H. Chiang, A. H. Jhang, and W. T. Ho, "New idea for hair transplantation to preserve more donor hair follicles," *Medical Hypotheses*, vol. 128, pp. 83–85, 2019.

[45] G. E. Seery, "Hair transplantation: management of donor area," *Dermatologic Surgery*, vol. 28, pp. 136–142, 2002.

[46] M. Choi, Y. M. Choi, S. Y. Choi et al., "Glucose metabolism regulates expression of hair-inductive genes of dermal papilla spheres via histone acetylation," *Scientific Reports*, vol. 10, no. 1, p. 4887, 2020.

[47] P. Vingler, B. Gautier, M. Dalko et al., "6-o glucose linoleate supports in vitro human hair growth and lipid synthesis," *International Journal of Cosmetic Science*, vol. 29, no. 2, pp. 85–95, 2007.

[48] A. Flores, J. Schell, A. S. Krall et al., "Lactate dehydrogenase activity drives hair follicle stem cell activation," *Nature Cell Biology*, vol. 19, no. 9, pp. 1017–1026, 2017.

[49] C. Sun, J. Shang, Y. Yao et al., "O-glcnacylation: a bridge between glucose and cell differentiation," *Journal of Cellular and Molecular Medicine*, vol. 20, no. 5, pp. 769–781, 2016.

[50] N. Yucel, Y. X. Wang, T. Mai et al., "Glucose metabolism drives histone acetylation landscape transitions that dictate muscle stem cell function," *Cell Reports*, vol. 27, no. 13, pp. 3939–3955.e6, 2019, e6.

[51] D. G. Greenhalgh, "Management of burns," *The New England Journal of Medicine*, vol. 380, no. 24, pp. 2349–2359, 2019.

[52] M. Singh, K. Nuutila, K. C. Collins, and A. Huang, "Evolution of skin grafting for treatment of burns: Reverdin pinch grafting to tanner mesh grafting and beyond," *Burns*, vol. 43, no. 6, pp. 1149–1154, 2017.

[53] P. He, J. Zhao, J. Zhang et al., "Bioprinting of skin constructs for wound healing," *Burns Trauma*, vol. 6, p. 5, 2018.

[54] S. B. Archer, A. Henke, D. G. Greenhalgh, and G. D. Warden, "The use of sheet autografts to cover extensive burns in patients," *The Journal of Burn Care & Rehabilitation*, vol. 19, no. 1, pp. 33–38, 1998.

[55] S. B. Mahjour, F. Ghaffarpasand, and H. Wang, "Hair follicle regeneration in skin grafts: current concepts and future perspectives," *Tissue Engineering. Part B, Reviews*, vol. 18, no. 1, pp. 15–23, 2012.

Hindawi

Research Article

Factors Influencing the Risk of Major Amputation in Patients with Diabetic Foot Ulcers Treated by Autologous Cell Therapy

J. Husakova [ID],[1,2] **R. Bem** [ID],[1] **V. Fejfarova** [ID],[1,2,3] **A. Jirkovska** [ID],[1] **V. Woskova,**[1] **R. Jarosikova,**[1,2] **V. Lovasova** [ID],[2,4] **E. B. Jude** [ID],[5] **and M. Dubsky** [ID][1,2]

[1]*Diabetes Centre, Institute for Clinical and Experimental Medicine, Prague, Czech Republic*
[2]*First Faculty of Medicine, Charles University, Prague, Czech Republic*
[3]*Second Faculty of Medicine, Charles Unviersity, Prague, Czech Republic*
[4]*Transplant Surgery Department, Institute for Clinical and Experimental Medicine, Prague, Czech Republic*
[5]*Diabetes Center, Tameside and Glossop Integrated Care NHS Foundation Trust and University of Manchester, Lancashire, UK*

Correspondence should be addressed to M. Dubsky; mids@ikem.cz

Introduction. Autologous cell therapy (ACT) is one of the last options for limb salvage in patients with chronic limb-threatening ischemia (CLTI) and diabetic foot ulcers (DFU). However, some patients may still undergo a major amputation even after ACT, but the risk factors for this are not known. Therefore, the aim of our study was to assess the risk factors for major amputation in patients with CLTI and DFU during a 2-year follow-up after ACT. *Methods*. One hundred and thirteen patients after ACT were included in our study and divided into two groups: Group 1 with major amputation (AMP; $n = 37$) and Group 2 without amputation (nAMP, $n = 76$). The risk factors for major amputation were evaluated before ACT and included factors relating to the patient, the DFU, and the cell product. *Results*. The AMP group had significantly higher C-reactive protein (CRP) levels compared to the nAMP group (22.7 vs. 10.7 mg/L, $p = 0.024$). In stepwise logistic regression, independent predictors for major amputation were mutation of the gene for methylenetetrahydrofolate reductase (MTHFR) with heterozygote and homozygote polymorphism 1298 (OR 4.33 [95% CI 1.05-17.6]), smoking (OR 3.83 [95% CI 1.18-12.5]), and CRP > 10 mg/L (OR 2.76 [95% CI 0.93-8.21]). Lower transcutaneous oxygen pressure (TcPO$_2$) values were observed in AMP patients compared to the nAMP group at one month (24.5 vs. 33.2, $p = 0.012$) and at 3 months (31.1 vs. 40.9, $p = 0.009$) after ACT. *Conclusion*. Our study showed that the risk for major amputation after ACT in patients with CLTI and DFU is increased by the presence of MTHFR heterozygote and homozygote gene mutations, smoking, and higher CRP at baseline. Lower TcPO$_2$ at one and 3 months after ACT may also have a predictive value. Therefore, it is necessary to stop smoking before ACT, treat any infection, and, above all, consider antiaggregation or anticoagulant treatment after the procedure.

1. Introduction

Diabetic foot ulcers (DFU) represent a late complication of diabetes and result in delayed healing and often to minor or major amputation and are associated with higher morbidity and mortality [1–3]. A meta-analysis of 16 studies reported that the 5-year mortality rate after major amputation in patients with diabetes and PAD was 62.2% [4].

The main factor leading to amputation is delayed wound healing in patients with diabetes. Poor healing of DFU is influenced by hyperglycaemia, chronic inflammation, micro- and macrovascular dysfunction, and neuropathy [5, 6]. Other factors for impaired healing are immunological abnormalities such as disruption of macrophage function, altered function of keratinocytes and fibroblasts, and decreased stem cell homing [2, 7, 8].

One of the most important factors that influence ulcer healing is tissue perfusion. Chronic limb-threatening ischemia (CLTI) represents the end stage of peripheral arterial disease with high mortality and morbidity, increased rates of major amputation, and decreased quality of life [9]. PAD affects almost 20% of older Americans (above 60 years). The risk factors were hyperlipidemia, hypertension, diabetes, chronic kidney disease, and smoking. Firnhaber and Powell described the risk of PAD to be ten times higher in patients with at least three of these factors [10]. Levels of circulating omentin-1 have been proved to be associated with the severity of PAD [11].

Cigarette smoking is a major risk factor for cardiovascular disease, stroke, and mainly PAD [12]. Tobacco use also has a strong correlation with CLTI [13, 14].

One of the factors influencing tissue perfusion is hemocoagulation disorders [15, 16]. Acquired abnormalities of the coagulation cascade and inherited thrombophilia in patients with diabetes can be a predictive factor for thrombosis [17]. Methylenetetrahydrofolate reductase (MTHFR) with polymorphism A1298C (MTHFR A1298C) may be associated with high levels of homocysteine and increases the risk of cardiovascular disease [18].

Another factor that contributes to impaired wound healing and reduced tissue oxygenation is infection. Acute inflammatory marker C-reactive protein (CRP) helps to diagnose infection at an early stage [19]. The presence of raised CRP and reduced lower limb perfusion significantly decreased wound healing in diabetic patients with CLTI [20]. CRP and increased proinflammatory cytokines interleukin 6 correlated with worse outcomes after endovascular procedure in patients with diabetes and PAD [21].

To reduce amputations in patients with CLTI and DFU, additional methods are needed to improve tissue oxygenation. Autologous cell therapy (ACT) represents an important therapeutic role in CLTI in whom revascularization is not an option (no-option CLTI, NO-CLTI) [22]. The goal of ACT is to promote the growth of collateral vessels through neovascularization and arteriogenesis. Nowadays, it is reserved only for NO-CLTI because in accordance with international guidelines, we should always prefer standard revascularization procedures if possible and to reserve cell therapy only for patients in clinical trials [9]. The cost of this procedure is usually comparable to that of PTA with stenting. ACT may reduce amputation rate, rest pain, and tissue loss and lead to a decrease in mortality and an increase in amputation-free survival [23]. At our centre, we have extensive experience in the use of ACT in management of CLTI and DFU [24]. Although we have shown that this treatment reduces the risk of amputation, we cannot prevent this complication in some patients. Therefore, we decided to analyse the factors that may increase the risk of amputation even after ACT.

The aim of our study was to assess the factors that increase the risk of major amputation in patients with CLTI and DFU during a 2-year follow-up after ACT.

2. Methods

One hundred and thirteen patients with diabetes type 1 or 2, CLTI, and chronic foot ulcer that were not suitable for standard revascularization and treated in our foot centre during the last 13 years were included in the study and treated with ACT. For the purposes of this study, patients were divided into two groups (Group 1 ($n = 37$) with major amputation (AMP) and Group 2 ($n = 76$) without amputation (nAMP)) and followed up for 2 years after ACT. Demographic and baseline characteristics of both groups are shown in Table 1.

Exclusion criteria for ACT were as follows: deep infection in the foot, limb edema, untreated advanced diabetic retinopathy requiring laser therapy or retinopathy with high risk of retinal bleeding, severe hematological disease and deep vein thrombosis, myocardial infarction or stroke in the last 6 months, neoplastic process of any organ, and life expectancy less than 6 months.

The CLTI was evaluated by angiography, ultrasound, computed tomography, or magnetic resonance angiography of the lower limb and by transcutaneous oxygen pressure ($TcPO_2$) of less than 30 mm Hg at baseline (measured by Radiometer TCM400, Radiometer Medical ApS, Brønshøj, Denmark). Patients with CLTI and DFU were consented for ACT after discussion with interventional radiologists, vascular surgeons, and foot care specialists.

All factors that might potentially increase risk for amputation were assessed at baseline and before ACT and were divided into three groups: first group was patient-related factors such as patient's age, body mass index, smoking history, diabetes duration and diabetes control, and laboratory results such as CRP, number of leucocytes, renal function, serum lipids, coagulation parameters (levels of protein S, protein C, fibrinogen, and homocysteine), and thrombophilic mutations (factor V Leiden, prothrombin mutation MTHFR C677T and A1298C). The second group included ulcer characteristics (size and depth, presence of infection, edema, and limb perfusion, presence of ischemia and gangrene, and value of $TcPO_2$). The third group of factors was related to the cell product that included cells' viability, number of leukocytes, and CD34+ cells (Table 1).

Foot ulcers were classified by WIfI score assessing the size of the wound, presence of infection and/or ischemia, and by other classification systems focused on foot ulcers, ischemia, and infection (PEDIS, TEXAS, and Wagner; Table 2). The presence of local inflammation was confirmed if any of the following were present: purulence, erythema, tenderness, warmth, or induration with limitation to the skin and tissue [25].

We have described the ACT method in detail in our previous publication [24]. Briefly, the ACT was obtained from bone marrow from the iliac crest using a Jamshidi needle under local or general anesthesia. The separation of mononuclear fraction was performed either by Harvest Smart PReP2 (Harvest Technologies Corporation, Plymouth, MA, USA) or by succinyl gelatin (Gelofusine; B. Braun, Melsungen, Germany) which accelerated erythrocyte sedimentation.

The final suspension, a volume of 40-60 mL, was injected intramuscularly in the ischemic lower limb in a series of 40–50 punctures injecting 1 mL at each site and keeping 1-2 cm distance between them on both sides of the gastrocnemius muscle, deep into the soleus muscle and into the dorsal and plantar muscles and also into the edges of the wound.

Table 1: Baseline characteristics of patients.

	Amputation (AMP) ($n = 37$)	Without amputation (nAMP) ($n = 76$)	p
Sex			
Male	30 (81%)	64 (84%)	
Female	7 (19%)	12 (16%)	
Age (years)	66 ± 13.7	67 ± 10.5	
Cholesterol (mmol/L)	4.0 ± 0.9	4.2 ± 1.1	NS
LDL cholesterol (mmol/L)	2.3 ± 0.74	2.4 ± 0.98	
Body mass index (kg/m^2)	27.8	26.7	
Malnutrition	8 (22%)	15 (20%)	
Diabetes mellitus			
Diabetes type 1	5 (14%)	19 (25%)	
Diabetes type 2	32 (86%)	57 (75%)	NS
HbA1c (mmol/mol)	57 ± 16.7	58.7 ± 13.5	
Duration of diabetes (years)	25.6 ± 13.2	24.9 ± 12.1	
CRP (mg/L)	22.7 ± 28	10.7 ± 12	$p = 0.024$
Comorbidities			
Chronic kidney disease (CKD)	2.43	2.63	
Modification of diet in renal disease study equation (MDRD)	0.74	0.95	NS
Chronic heart failure	26 (70%)	41 (54%)	
Smoking			
Smoker	5 (13%)	9 (12%)	
Ex-smoker	21 (57%)	22 (29%)	NS
Years of history of smoking	23 ± 20	18 ± 18	
Nonsmoker	11 (30%)	45 (59%)	
Treatment			
Acetylsalicylic acid	22 (59%)	34 (45%)	
Clexane	2 (5%)	6 (8%)	
Clopidogrel	5 (14%)	12 (16%)	
Rivaroxaban	0 (0%)	5 (7%)	NS
Dabigatran	2 (5%)	12 (16%)	
Warfarin	6 (16%)	7 (9%)	
Statins	25 (68%)	37 (49%)	
Vascular interventions			
Percutaneous transluminal angioplasty (PTA) (number of patients (%)/number of procedures)	35 (95%)/1.62	29 (38%)/1.74	NS
Bypass (number of patients (%)/number of procedures)	13 (35%)/0.59	25 (33%)/0.36	
Cultivation			
MRSA or ESBL infection	5 (14%)	7 (9%)	
Another ATB-resistant infection	6 (16%)	23 (30%)	NS
Osteomyelitis	6 (16%)	23 (30%)	
Osteomyelitis			
Osteomyelitis in X-ray	11 (29.7%)	33 (43.4%)	NS
Positive probe to bone test	6 (16%)	17 (22%)	

TABLE 1: Continued.

	Amputation (AMP) ($n = 37$)	Without amputation (nAMP) ($n = 76$)	p
Prothrombophilic factors			
MTHFR A1298C	22 (61%)	29 (38%)	
Homocysteine (μmol/L)	12.07	16.51	
MTHFR C677T	13 (35%)	31 (41%)	NS
Homocystein (μmol/L)	12.80	15.40	
Protein C (%)	105.9 ± 29.1	104 ± 29.6	
Protein S (%)	90.7 ± 31.8	98.8 ± 34.3	
Cell product			
Viability (%)	96.2	93.9	
Total CD34+ in product ($*10^6$)	12.6	13.9	NS
Total leucocytes in product ($*10^9$)	2.6	2.2	

TABLE 2: Classification systems of DFU at baseline and at all follow-up visits.

	AMP				nAMP			
	Baseline ($n = 37$)	1 M ($n = 35$)	3 M ($n = 29$)	6 M ($n = 14$)	Baseline ($n = 76$)	1 M ($n = 76$)	3 M ($n = 72$)	6 M ($n = 71$)
Wagner (mean)	3.43	3.40	3.14	2.93	2.87	2.79	1.78	1.06
Wagner 3 (%)	6 (16%)	8 (23%)	8 (28%)	3 (21%)	7 (9%)	9 (38%)	5 (7%)	4 (6%)
Wagner 4 (%)	24 (65%)	21 (60%)	11 (38%)	4 (29%)	33 (43%)	30 (12%)	12 (17%)	4 (6%)
PEDIS infection	1.54	1.91	2.07	2.00	0.68	0.58	0.22	0.08
WIfI (mean)								
Wound	1.81	1.91	2.00	1.93	1.93	1.84	1.74	0.86
Ischemia	2.95	2.49	2.31	1.93	2.97	2.20	1.74	1.48
Foot infection	0.57	0.91	1.07	1.00	0.64	0.47	0.19	0.07
TEXAS (%)								
TEXAS B only infection	0 (0%)	1 (3%)	5 (17%)	1 (7%)	0 (0%)	0 (0%)	2 (3%)	2 (3%)
TEXAS C only ischemia	28 (76%)	14 (40%)	3 (10%)	4 (29%)	49 (64%)	33 (43%)	26 (36%)	20 (28%)
TEXAS D infection and ischemia	9 (24%)	17 (49%)	16 (55%)	5 (36%)	27 (36%)	27 (36%)	4 (6%)	1 (1%)

Patients were followed up at intervals of 1, 3, and 6 months and after 1 and 2 years after therapy. At baseline and at each follow-up visit, TcPO$_2$ was measured. The effect of ACT was evaluated by ulcer healing and changes in TcPO$_2$ and compared to baseline values. All patients were checked up biweekly or monthly and received best local wound care with regard to their type of wound (iodium-based solutions for gangrene or wet healing dressings for chronic nonhealing ulcers); in some cases for deep wounds, a negative pressure wound therapy was used.

3. Statistical Analysis

Statistical analysis was done using BMDP Statistical Software Inc. 8.1 (Medcalc, Ostend, Belgium) and Medcalc version 17.8.6. We used the χ^2 test, stepwise logistic regression, and calculated univariate odds ratios (ORs), with 95% confidence intervals (CIs). The figures were performed by GraphPad Prism 7.0.4 (GraphPad Software, La Jolla, CA, USA).

4. Results

Of the 113 patients included in the study, 37 underwent major amputation and 76 did not have an amputation during the 2-year follow-up. There was no difference in patients' characteristics between the amputated and nonamputated groups at baseline (Table 1). The time to major amputation in the AMP group is shown in Figure 1. The classifications of DFU at baseline and up to 6 months in both groups are shown in Table 2.

In a stepwise logistic regression, the independent predictors for amputation after ACT were MTHFR A1298C mutation, previous or present smoking history, CRP > 10 mg/L at baseline, and a decrease in TcPO$_2$ 1 month after ACT (Table 3). The most important predictor for major amputation (OR 4.33 [95% CI 1.05-17.6]) was MTHFR mutation with homo- and heterozygous polymorphism A1298C. Our results also confirmed tobacco use as a significant risk factor of major amputation almost 4 times in smokers compared to ex-smokers (OR 3.83 [95% CI 1.18-12.5]). CRP represented a risk factor with levels higher than
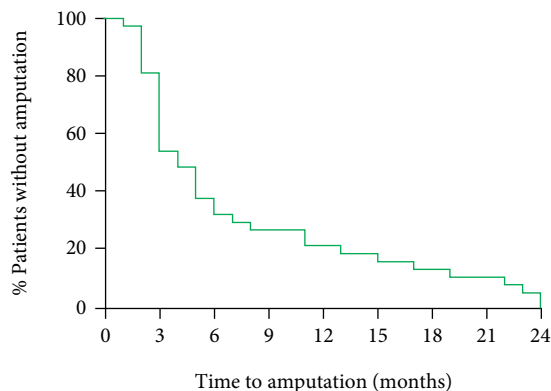
FIGURE 1: Time to amputation in the AMP group ($n = 37$).

TABLE 3: Independent predictors for major amputation.

Factor	OR	95% CI
MTHFR A1298C	4.33	1.05-17.6
Smoking	3.83	1.18-12.5
CRP > 10 mg/L	2.76	0.93-8.21
$TcPO_2$ at 1 month	0.959	0.926-0.993

FIGURE 2: Baseline CRP in the nAMP and AMP groups.

FIGURE 3: $TcPO_2$ in the AMP and nAMP groups up to 6 months after ACT. ∗∗ represents a significant difference between the AMP and nAMP groups in 1 month and 3 months.

scores (AMP 3.8 vs. nAMP 3.7, NS) and SINBAD scores (AMP 4.1 vs. nAMP 4.1) were not different between the AMP and nAMP groups at baseline (Table 1).

5. Discussion

This is the first study to report on amputation after ACT. We have shown that the main major amputation risk factors in patients with DFU and CLTI treated by ACT were MTHFR A1928C mutation, smoking, elevated CRP, and decrease in $TcPO_2$. Many of these factors have been associated with amputations in other studies, but have not been evaluated after ACT [26–28].

In our study, the incidence of major amputations over the 2 years after ACT was 32.7%; however, majority of the patients underwent an amputation in the first 6 months (Figure 1). The incidence of major amputation in patients with diabetes and CLTI in the literature is very high (23-72%) [9, 29]. Kalbaugh et al. observed in a retrospective population-based analysis incidence of major amputation in 72% of patients with CLTI and predominantly in diabetic patients in 61% within 16 years [29].

Risk factors for amputation have been studied previously. The risk of major amputation was, for example, higher in men, people with neuropathy, foot ulcers with higher Wagner score, patients with worse diabetes control, with higher leucocytes, thrombocytes, C-reactive protein, and decrease in HDL-cholesterol, albumin, C-peptide, uric acid, and ankle-brachial index below 0.8 [26–28]. Prior minor amputation increased the risk of subsequent major amputation ten times and almost twentyfold increased risk of minor reamputation [27].

In our study, in contrast to previous studies, we demonstrated the predictive value of $TcPO_2$ measured at 1 month after ACT for major amputation. $TcPO_2$ is a commonly used

10 mg/L (OR 2.76 [95% CI 0.93-8.21]). CRP levels in the AMP group were higher in comparison with those of the nAMP group (22.7 vs. 10.7 mg/L, $p = 0.024$; Figure 2).

Lower $TcPO_2$ values were observed in AMP patients compared to the nAMP group at one month (24.5 vs. 33.2, $p = 0.012$) and at 3 months (31.1 vs. 40.9, $p = 0.009$) after ACT (Figure 3). The results also showed that a decrease in $TcPO_2$ by 1 mm Hg increased the risk of major amputation by 4% (OR 0.959; 95% CI 0.926-0.993).

We observed the presence of multiresistant bacteria in the wound swabs (methicillin-resistant Staphylococcus aureus, Proteus sp., Klebsiella sp.) in both groups without a significant difference between them (Table 1). The WIfI

indicator of the effect of ACT on improving tissue perfusion [30]. We believe that our study could contribute to more usage of TcPO$_2$ to assess the effect of ACT in upcoming studies, because TcPO$_2$ directly evaluates microcirculation (and therefore can assess the formation of new collaterals) and usually is more definitive and less variable than the laser Doppler flowmetry. The increased value of TcPO$_2$ may indicate the revascularization effect of cell therapy and improvement in limb perfusion. We assume that both values are important—rate of TcPO$_2$ increase and the absolute value of TcPO$_2$—at the end of the follow-up period, but we do not suppose that there is an absolute TcPO$_2$ threshold that could predict the major amputation after ACT because amputation could be influenced by other factors such as osteomyelitis, cellulitis, or unbearable pain.

Another factor that is not usually listed among the risks for major amputation is inherited thrombophilia. An association of thrombophilic mutations with other pathological conditions has been published. For example, an association of the polymorphism MTHFR A1298C was strongly associated with the presence of end-stage renal disease [18]. MTHFR A1298C is found in 7 to 12% of North American, European, and Australian populations [31]. In our study, we observed substantially higher prevalence of this mutation (38% in nAMP group and 61% in AMP group). Gemmati et al. demonstrated the interaction between MTHFR homozygotes and the prevalence of and also the increased risk for both arterial and venous thromboses [32]. Lupi-Herrera et al. observed a higher risk of arterial and venous thromboembolic disease and described an increase in massive and submassive pulmonary embolism and acute myocardial ischemia in patients with MTHFR A1298C ($p = 0.017$) and increased homocysteine levels [33]. In our study, we did not show a clear association of major amputations with higher homocysteine levels, although there is a pathogenetic link between the MTHFR mutation and homocysteine [31]. Homocysteine is an intermediate amino acid containing a sulfhydryl group that comes from the methylation of methionine. The accumulation of homocysteine leads to pathologies such as rheumatoid arthritis, cancer, and vascular occlusive disease, and it is used also as a coronary artery disease risk factor [33, 34]. Hyperhomocysteinemia in association with accelerated atherosclerosis is an independent risk factor for cardiovascular, cerebrovascular, and peripheral artery disease. Homocysteine induces endothelial dysfunction and vascular inflammation [35].

Another important predictor of major amputation in our study was tobacco use. Smoking increased the risk of major amputation in patients after ACT almost four times (OR 3.83). The risk of PAD increases after 30 years of smoking, with cardiovascular disease after 20 years, and intense smoking of more than 20 cigarettes daily increased the probability of subclinical PAD in comparison with lower intensity use [36, 37]. In patients who stop smoking, the risk would return to the level of nonsmokers after 10 years of smoking cessation [36]. Kianoush et al. observed an 8-fold increased risk of PAD, with ankle-brachial index less than 1.0, and also an increase in aortoiliac calcium by almost tenfold in smokers [37].

Another independent predictor for major amputation after ACT was CRP above 10 mg/L. Chronic inflammation with elevated CRP has been shown to be associated with PAD [9]. In studies evaluating DFU and osteomyelitis in people with diabetes, it was observed that CRP above 35 mg/L had a sensitivity of 80% and specificity of 89% for the presence of diabetic foot infection [38]. A higher CRP level in patients with CLTI has been associated not only with increased risk of major amputation but was also with higher mortality and poorer prognosis [39].

Our study showed no significant differences between groups in LDL cholesterol, but in both groups the values of LDL-c were above the recommended levels. All included patients met the criteria of high risk of proatherosclerotic changes and cardiovascular disease, but at baseline, it did not meet the recommended levels of 1.8 mmol/L of LDL cholesterol (AMP 2.25 ± 0.74 vs. nAMP 2.4 ± 0.98) [40].

The DFU classification was without significant differences between the AMP and nAMP groups because patients included in our study had advanced diabetic complications such as neuropathy and CLTI and most of them were classified in the higher grades of WIfI and other classification systems. Their chronic ulcers were either deep and colonised with bacteria or gangrenous that worsened the prognosis of the wound (Table 1).

Therefore, we feel that the findings from our study could help with selection of the patients for ACT. To maximize the success of ACT, we should instruct patients to stop smoking and increase their adherence with DFU treatment and to aggressively treat infection before the ACT procedure. Test of MTHFR gene prior to ACT could possibly prevent later thrombotic complications after the procedure by early indication of antithrombotic treatment. On the other hand, this test is very expensive and the prothrombotic status is also dependent on the levels of homocysteine [31].

6. Study Limitations

All patients who included in the study had severe PAD with no revascularization possibilities and as mentioned were NO-CLTI patients. ACT was performed as the last treatment option before considering limb amputation. The results of the study may be affected by the lower number of patients in the groups. The indication for amputation was made on the basis of a group decision of experts and the patient's opinion; however, a more subjective bias cannot be excluded. The nature of the study meant that a control group could not be included. Some of the baseline data could not be influenced such as smoking history, long-term glycaemic control, or LDL cholesterol levels.

7. Conclusion

The results of our study showed that the risk of major amputation in patients with diabetes after ACT with no-option CLTI is increased by inherited thrombophilia—MTHFR A1298C gene mutations, smoking, and higher CRP levels before ACT treatment. The decrease in TcPO$_2$ 1 month after ACT may also have a predictive value for major amputation.

Therefore, for these patients, it is necessary to stop smoking and before ACT treat any diabetic foot infection. After ACT, it is advisable to monitor the level of $TcPO_2$ and, above all, consider adequate antiaggregation or anticoagulant treatment after the procedure mainly in patients with thrombophilic mutations.

Data Availability

The data will be uploaded together with the manuscript. The data used to support the findings of this study are included within the supplementary information file in the folder Supplementary_Information_files_KB_all_amputation_JoDR_SI.

Disclosure

We declare that the results presented in this paper have not been published previously in whole or part, except in an abstract format. The paper was presented in the Diabetic Foot Study Group 2021.

Conflicts of Interest

No potential conflicts of interest relevant to this article were reported.

Acknowledgments

References

[1] L. Dalla Paola, P. Cimaglia, A. Carone et al., "Limb salvage in diabetic patients with no-option critical limb ischemia: outcomes of a specialized center experience," *Diabetic Foot & Ankle*, vol. 10, no. 1, p. 1696012, 2019.

[2] J. Gorecka, V. Kostiuk, A. Fereydooni et al., "The potential and limitations of induced pluripotent stem cells to achieve wound healing," *Stem Cell Research & Therapy*, vol. 10, no. 1, p. 87, 2019.

[3] J. C. Thorud, B. Plemmons, C. J. Buckley, N. Shibuya, and D. C. Jupiter, "Mortality after nontraumatic major amputation among patients with diabetes and peripheral vascular disease: a systematic review," *The Journal of Foot and Ankle Surgery*, vol. 55, no. 3, pp. 591–599, 2016.

[4] J. R. Stern, C. K. Wong, M. Yerovinkina et al., "A meta-analysis of long-term mortality and associated risk factors following lower extremity amputation," *Annals of Vascular Surgery*, vol. 42, pp. 322–327, 2017.

[5] D. Baltzis, I. Eleftheriadou, and A. Veves, "Pathogenesis and treatment of impaired wound healing in diabetes mellitus: new insights," *Advances in Therapy*, vol. 31, no. 8, pp. 817–836, 2014.

[6] F. Biscetti, D. Pitocco, G. Straface et al., "Glycaemic variability affects ischaemia-induced angiogenesis in diabetic mice," *Clinical Science (London, England)*, vol. 121, no. 12, pp. 555–564, 2011.

[7] F. Biscetti, G. Straface, R. de Cristofaro et al., "High-mobility group box-1 protein promotes angiogenesis after peripheral ischemia in diabetic mice through a VEGF-dependent mechanism," *Diabetes*, vol. 59, no. 6, pp. 1496–1505, 2010.

[8] A. den Dekker, F. M. Davis, S. L. Kunkel, and K. A. Gallagher, "Targeting epigenetic mechanisms in diabetic wound healing," *Translational Research*, vol. 204, pp. 39–50, 2019.

[9] M. S. Conte, A. W. Bradbury, P. Kolh et al., "Global vascular guidelines on the management of chronic limb-threatening ischemia," *European Journal of Vascular and Endovascular Surgery*, vol. 58, no. 1, pp. S1–S109.e33, 2019.

[10] J. M. Firnhaber and C. S. Powell, "Lower extremity peripheral artery disease: diagnosis and treatment," *American Family Physician*, vol. 99, no. 6, pp. 362–369, 2019.

[11] F. Biscetti, E. Nardella, N. Bonadia et al., "Association between plasma omentin-1 levels in type 2 diabetic patients and peripheral artery disease," *Cardiovascular Diabetology*, vol. 18, no. 1, p. 74, 2019.

[12] V. Aboyans, M. A. Sevestre, I. Désormais, P. Lacroix, G. Fowkes, and M. H. Criqui, "Epidemiology of lower extremity artery disease," *Presse Médicale*, vol. 47, no. 1, pp. 38–46, 2018.

[13] A. Farber and R. T. Eberhardt, "The current state of critical limb ischemia," *JAMA Surgery*, vol. 151, no. 11, pp. 1070–1077, 2016.

[14] D. G. Kokkinidis, S. Giannopoulos, M. Haider et al., "Active smoking is associated with higher rates of incomplete wound healing after endovascular treatment of critical limb ischemia," *Vascular Medicine*, vol. 25, no. 5, pp. 427–435, 2020.

[15] F. Biscetti, C. F. Porreca, F. Bertucci et al., "TNFRSF11B gene polymorphisms increased risk of peripheral arterial occlusive disease and critical limb ischemia in patients with type 2 diabetes," *Acta Diabetologica*, vol. 51, no. 6, pp. 1025–1032, 2014.

[16] F. Biscetti, G. Straface, G. Bertoletti et al., "Identification of a potential proinflammatory genetic profile influencing carotid plaque vulnerability," *Journal of Vascular Surgery*, vol. 61, no. 2, pp. 374–381, 2015.

[17] M. Dubsky, A. Jirkovská, L. Pagáčová et al., "Impact of inherited prothrombotic disorders on the long-term clinical outcome of percutaneous transluminal angioplasty in patients with diabetes," *Journal Diabetes Research*, vol. 2015, article 369758, 5 pages, 2015.

[18] A. Poduri, D. Mukherjee, K. Sud, H. S. Kohli, V. Sakhuja, and M. Khullar, "MTHFR A1298C polymorphism is associated with cardiovascular risk in end stage renal disease in North Indians," *Molecular and Cellular Biochemistry*, vol. 308, no. 1-2, pp. 43–50, 2008.

[19] N. R. Sproston and J. J. Ashworth, "Role of C-reactive protein at sites of inflammation and infection," *Frontiers in Immunology*, vol. 9, p. 754, 2018.

[20] M. Fujii, H. Terashi, K. Yokono, and D. G. Armstrong, "The degree of blood supply and infection control needed to treat diabetic chronic limb-threatening ischemia with forefoot osteomyelitis," *Journal of the American Podiatric Medical Association*, vol. 111, no. 2, 2021.

[21] F. Biscetti, P. M. Ferraro, W. R. Hiatt et al., "Inflammatory cytokines associated with failure of lower-extremity endovascular revascularization (LER): a prospective study of a

population with diabetes," *Diabetes Care*, vol. 42, no. 10, pp. 1939–1945, 2019.

[22] B. Xie, H. Luo, Y. Zhang, Q. Wang, C. Zhou, and D. Xu, "Autologous stem cell therapy in critical limb ischemia: a meta-analysis of randomized controlled trials," *Stem Cells International*, vol. 2018, Article ID 7528464, 12 pages, 2018.

[23] E. Benoit, T. F. O'Donnell Jr., M. D. Iafrati et al., "The role of amputation as an outcome measure in cellular therapy for critical limb ischemia: implications for clinical trial design," *Journal of Translational Medicine*, vol. 9, no. 1, p. 165, 2011.

[24] M. Dubsky, A. Jirkovska, R. Bem, A. Nemcova, V. Fejfarova, and E. B. Jude, "Cell therapy of critical limb ischemia in diabetic patients - state of art," *Diabetes Research and Clinical Practice*, vol. 126, pp. 263–271, 2017.

[25] M. Monteiro-Soares, E. J. Boyko, W. Jeffcoate et al., "Diabetic foot ulcer classifications: a critical review," *Diabetes/Metabolism Research and Reviews*, vol. 36, article e3272, Suppl 1, 2020.

[26] Z. Guo, C. Yue, Q. Qian, H. He, and Z. Mo, "Factors associated with lower-extremity amputation in patients with diabetic foot ulcers in a Chinese tertiary care hospital," *International Wound Journal*, vol. 16, no. 6, pp. 1304–1313, 2019.

[27] J. K. Gurney, J. Stanley, S. York, D. Rosenbaum, and D. Sarfati, "Risk of lower limb amputation in a national prevalent cohort of patients with diabetes," *Diabetologia*, vol. 61, no. 3, pp. 626–635, 2018.

[28] A. Kurniawati, Y. D. Ismiarto, and I. L. Hsu, "Prognostic factors for lower extremity amputation in diabetic foot ulcer patients," *Journal of Acute Medicine*, vol. 9, no. 2, pp. 59–63, 2019.

[29] C. A. Kalbaugh, P. D. Strassle, N. J. Paul, K. L. McGinigle, M. R. Kibbe, and W. A. Marston, "Trends in surgical indications for major lower limb amputation in the USA from 2000 to 2016," *European Journal of Vascular and Endovascular Surgery*, vol. 60, no. 1, pp. 88–96, 2020.

[30] M. Maufus, M. A. Sevestre-Pietri, C. Sessa et al., "Critical limb ischaemia and the response to bone marrow-derived cell therapy according to tcPO$_2$ measurement," *VASA*, vol. 46, no. 1, pp. 23–28, 2017.

[31] S. Moll and E. A. Varga, "Homocysteine and MTHFR mutations," *Circulation*, vol. 132, no. 1, pp. e6–e9, 2015.

[32] D. Gemmati, M. L. Serino, C. Trivellato, S. Fiorini, and G. L. Scapoli, "C677T substitution in the methylenetetrahydrofolate reductase gene as a risk factor for venous thrombosis and arterial disease in selected patients," *Haematologica*, vol. 84, no. 9, pp. 824–828, 1999.

[33] E. Lupi-Herrera, M. E. Soto-López, A. D. J. Lugo-Dimas et al., "Polymorphisms C677T and A1298C of MTHFR gene: homocysteine levels and prothrombotic biomarkers in coronary and pulmonary thromboembolic disease," *Clinical and Applied Thrombosis/Hemostasis*, vol. 25, article 1076029618780344, 2019.

[34] A. U. Chai and J. Abrams, "Homocysteine: a new cardiac risk factor?," *Clinical Cardiology*, vol. 24, no. 1, pp. 80–84, 2001.

[35] Q. Yang and G. W. He, "Imbalance of homocysteine and H2S: significance, mechanisms, and therapeutic promise in vascular injury," *Oxidative Medicine and Cellular Longevity*, vol. 2019, Article ID 7629673, 11 pages, 2019.

[36] D. Clark 3rd, L. R. Cain, M. J. Blaha et al., "Cigarette smoking and subclinical peripheral arterial disease in blacks of the Jackson Heart Study," *Journal of the American Heart Association*, vol. 8, no. 3, article e010674, 2019.

[37] S. Kianoush, M. Y. Yakoob, M. al-Rifai et al., "Associations of cigarette smoking with subclinical inflammation and atherosclerosis: ELSA-Brasil (the Brazilian longitudinal study of adult health)," *Journal of the American Heart Association*, vol. 6, no. 6, 2017.

[38] N. A. Zakariah, M. Y. Bajuri, R. Hassan et al., "Is procalcitonin more superior to hs-CRP in the diagnosis of infection in diabetic foot ulcer?," *The Malaysian Journal of Pathology*, vol. 42, no. 1, pp. 77–84, 2020.

[39] J. Barani, J. Å. Nilsson, I. Mattiasson, B. Lindblad, and A. Gottsäter, "Inflammatory mediators are associated with 1-year mortality in critical limb ischemia," *Journal of Vascular Surgery*, vol. 42, no. 1, pp. 75–80, 2005.

[40] M. Pignone, "Management of elevated low density lipoprotein-cholesterol (LDL-C) in primary prevention of cardiovascular disease," 2021, https://www.uptodate.com/contents/management-of-elevated-low-density-lipoprotein-cholesterol-ldl-c-in-primary-prevention-of-cardiovascular-disease.

Research Article

Novel Genes Potentially Involved in Fibroblasts of Diabetic Wound

Weirong Zhu,[1] Qin Fang,[2] Zhao Liu,[1] and Qiming Chen [1]

[1]*Department of Hand and Foot Surgery, Huizhou Municipal Central Hospital, Huizhou 516001, China*
[2]*Department of Breast Surgery, Huizhou Municipal Central Hospital, Huizhou 516001, China*

Correspondence should be addressed to Qiming Chen; cqm1254@163.com

Fibroblasts are the essential cell type of skin, highly involved in the wound regeneration process. In this study, we sought to screen out the novel genes which act important roles in diabetic fibroblasts through bioinformatic methods. A total of 811 and 490 differentially expressed genes (DEGs) between diabetic and normal fibroblasts were screened out in GSE49566 and GSE78891, respectively. Furthermore, the Kyoto Encyclopedia of Genes and Genomes (KEGG) pathways involved in type 2 diabetes were retrieved from miRWalk. Consequently, the integrated bioinformatic analyses revealed the shared KEGG pathways between DEG-identified and diabetes-related pathways were functionally enriched in the MAPK signaling pathway, and the MAPKAPK3, HSPA2, TGFBR1, and p53 signaling pathways were involved. Finally, ETV4 and NPE2 were identified as the targeted transcript factors of MAPKAPK3, HSPA2, and TGFBR1. Our findings may throw novel sight in elucidating the molecular mechanisms of fibroblast pathologies in patients with diabetic wounds and targeting new factors to advance diabetic wound treatment in clinic.

1. Introduction

As the global population ages, the incidence of diabetes is rapidly increasing during recent decades [1]. Diabetic foot ulcers (DFUs) are one of the most common and serious complications of diabetes. It was reported that the incidence of DFUs was up to 4% in diabetes [2]. The mechanism of DFUs remains unclear, and many factors contributed to the delayed healing of it, throwing a significant burden on patients with diabetic wound [3]. Early diagnosis and intervention of diabetic wound are important for reversing the poor prognosis of DFUs [4]. Unfortunately, few distinctive diagnostic biomarkers have been reported and demonstrated in diabetic wound. Thus, it is of great necessity to screen out the novel diagnostic biomarkers involved in the development of diabetic wound.

Fibroblasts are the essential cell type of skin, highly involved in the wound regeneration process, and acted in wound healing by interacting with other cells including keratinocytes and endothelial cells [5]. Exosomal miR-20b-5p derived from the high-glucose impaired fibroblast proliferation and differentiation, and delayed diabetic wound healing, suggesting the crucial role of fibroblasts in diabetic wound healing [6]. Furthermore, accumulative evidences have demonstrated the important role of genetic and epigenetic regulation in diabetic wound healing [7, 8].

In this study, we sought to identify the DEG modulation in diabetic fibroblasts by using bioinformatic methods. These findings may provide useful insights into understanding the molecular mechanisms of fibroblast pathologies in patients with DFUs.

2. Materials and Methods

2.1. DEG Identification. Microarray data of datasets comparing diabetes and the healthy controls were screened out from

(a)

(b)
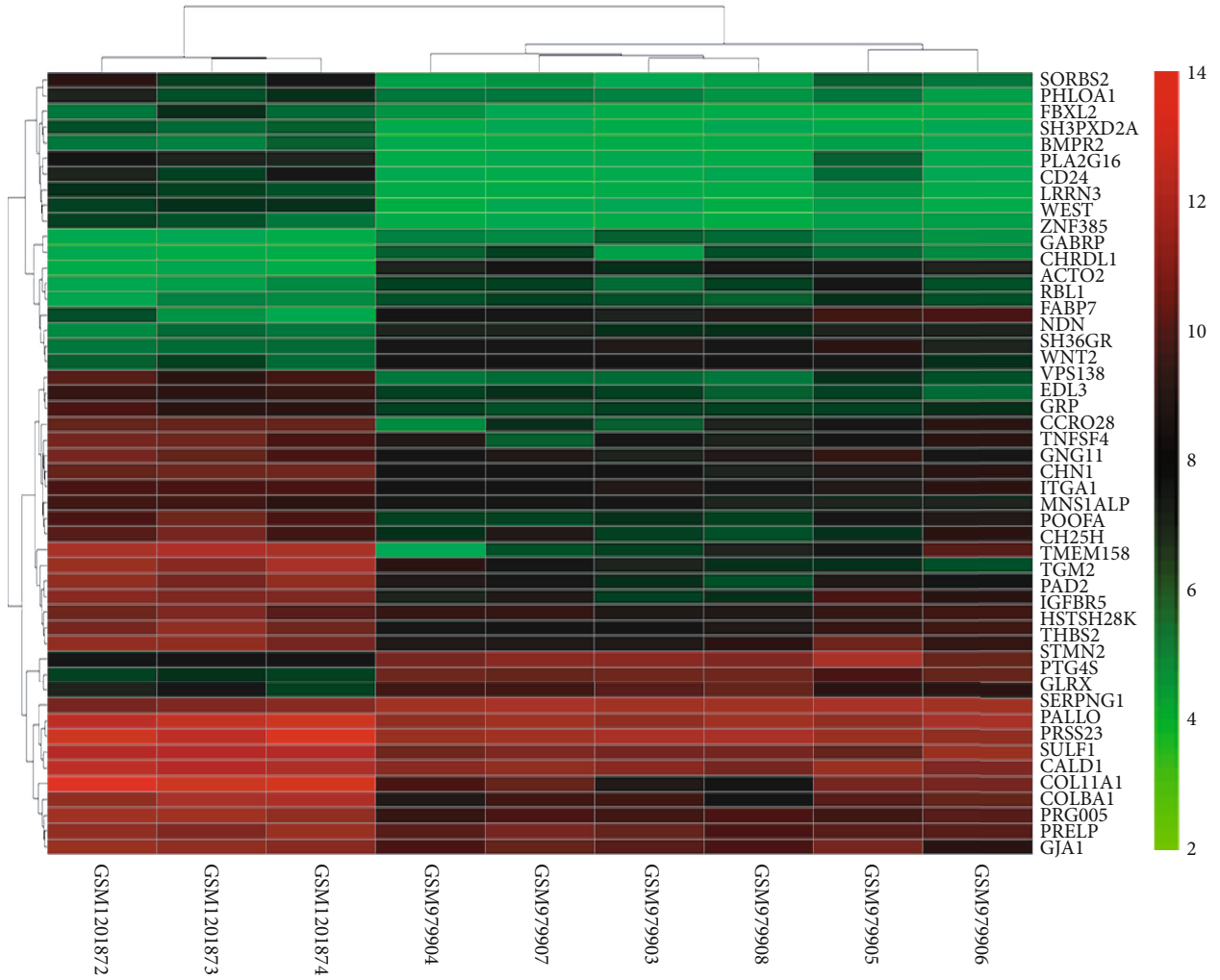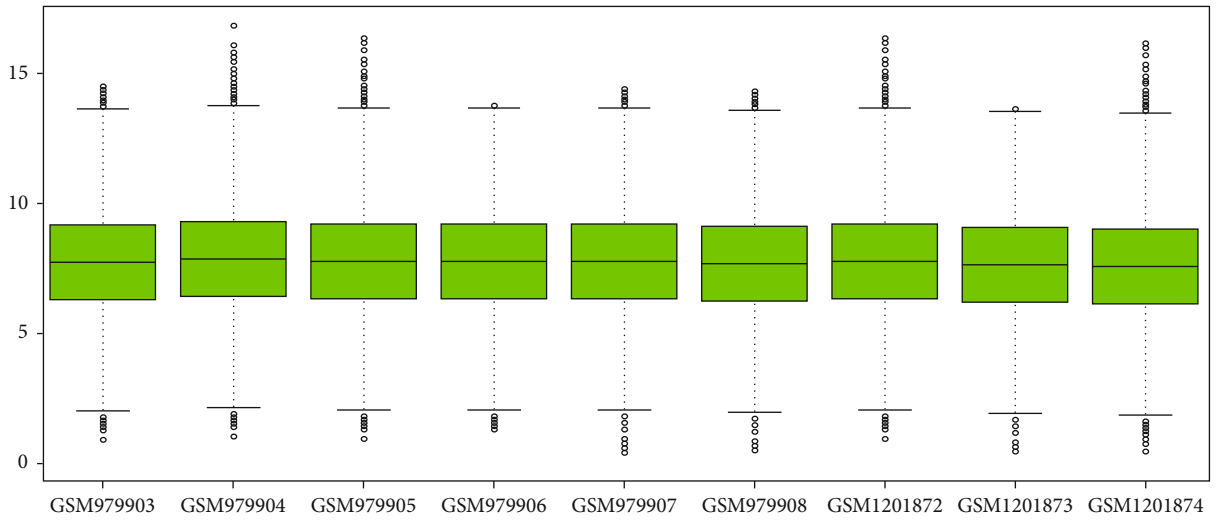
Figure 1: Continued.
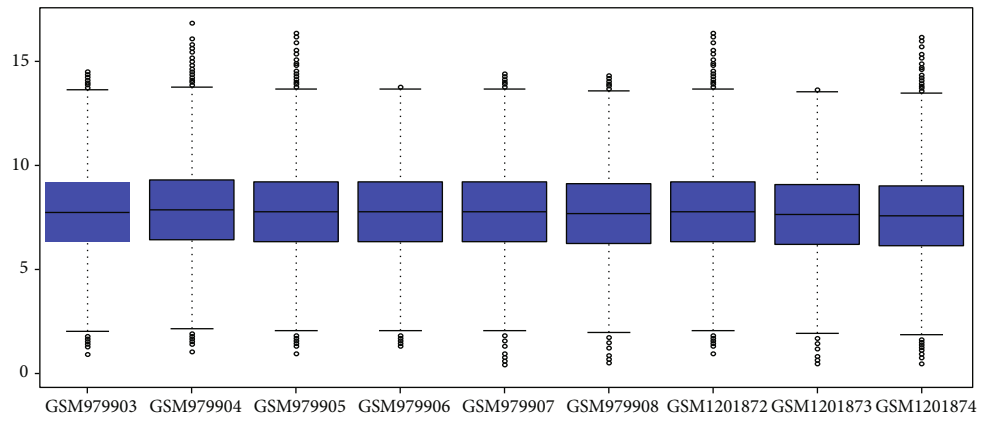
(c)
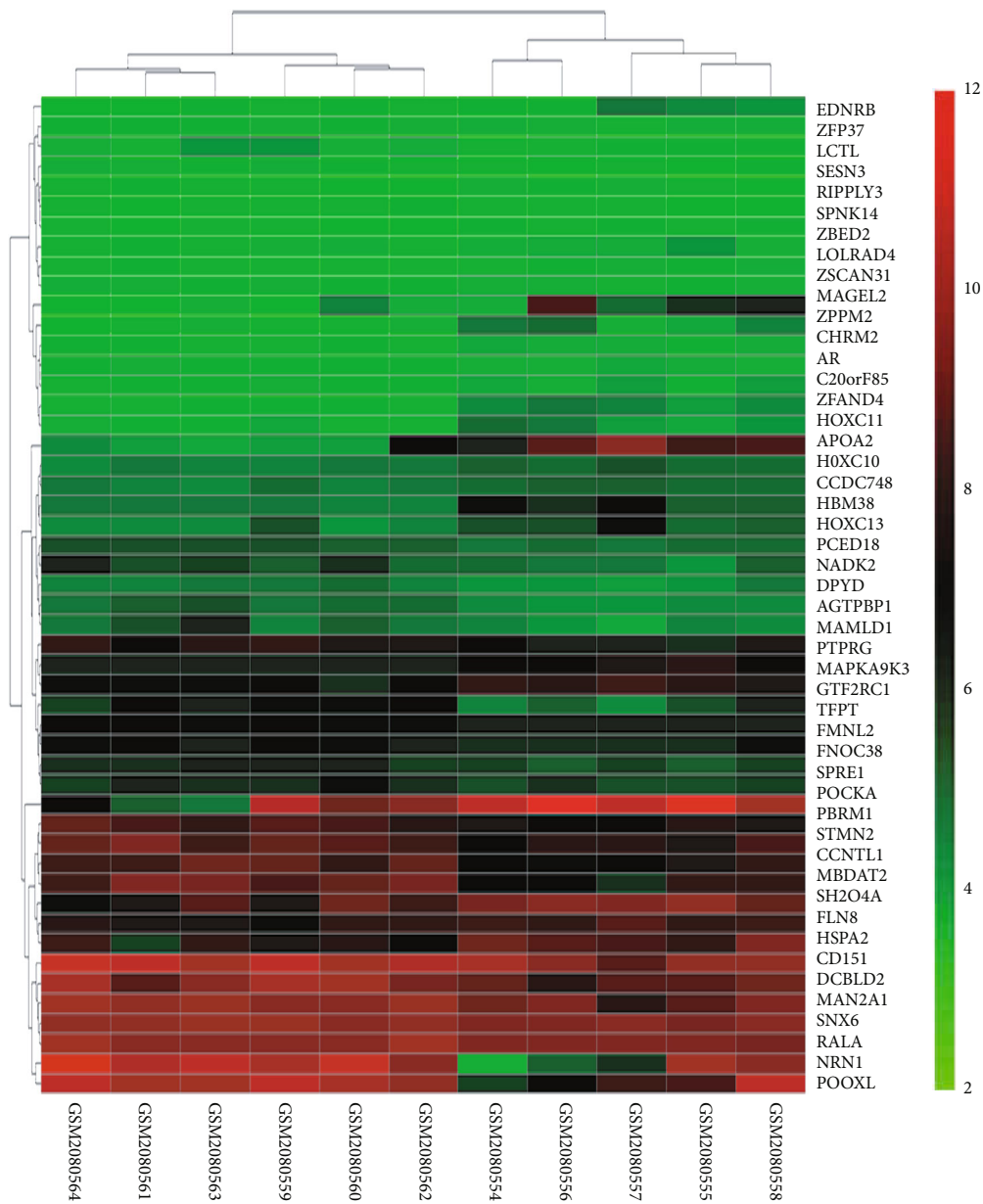
(d)

Figure 1: Continued.

(e)

(f)
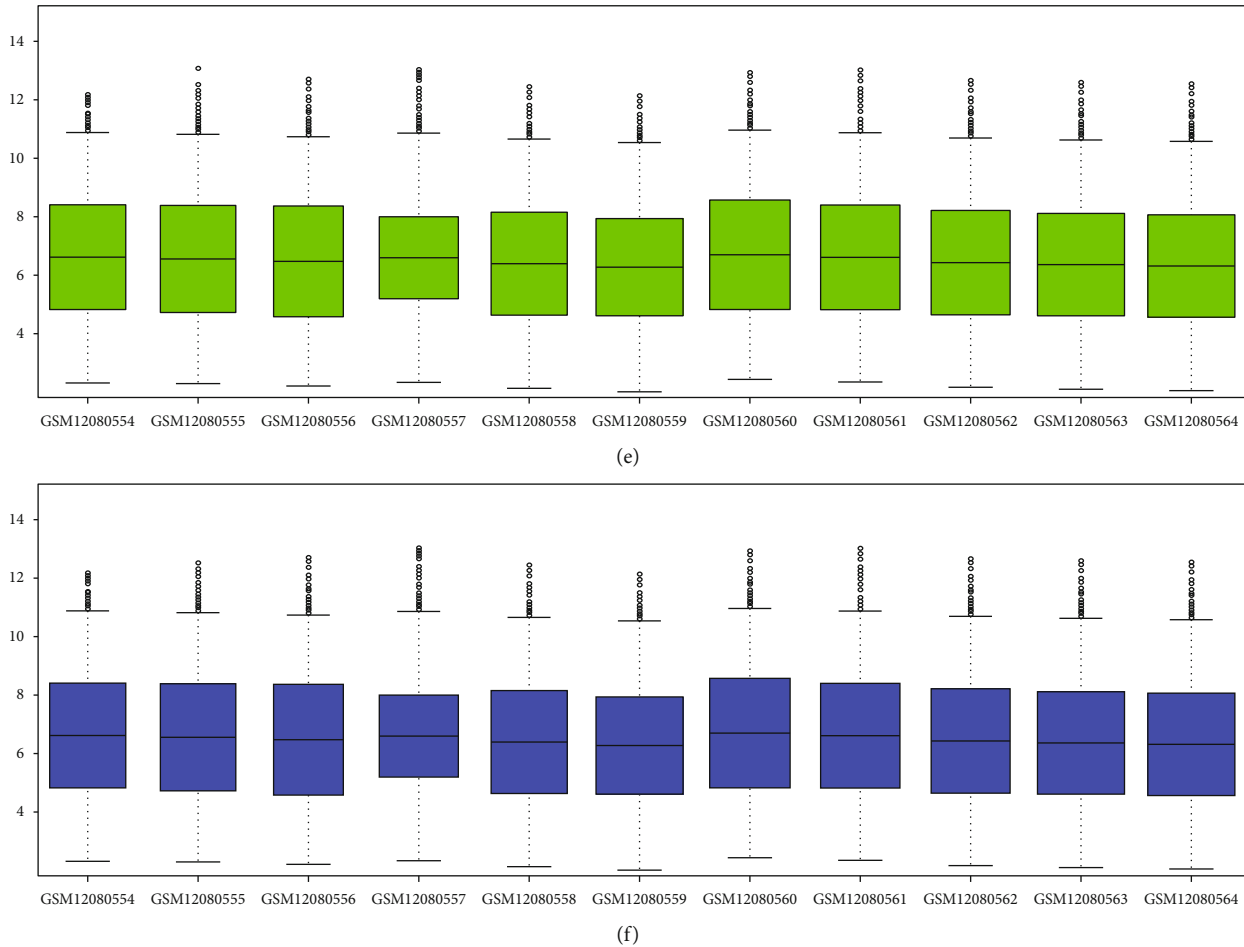
FIGURE 1: Heatmap of the DEGs between type 2 diabetes and normal people in GSE49566 and GSE78891: (a) heatmap clustering of the DEGs in GSE49566; (b) gene expression information of each sample before standardization in GSE49566; (c) gene expression information of each sample after standardization in GSE49566; (d) heatmap clustering of the DEGs in GSE78891; (e) gene expression information of each sample before standardization in GSE78891; (f) gene expression information of each sample after standardization in GSE78891.

the Gene Expression Omnibus database (GEO, http://www .ncbi.nlm.nih.gov/geo). DEGs were performed by Limma in R, and p values < 0.05 were considered as statistically significant. R package pheatmap was used to visualize Log2 mRNA gene expression. Using Circlize and ComplexHeatmap in R, common DEGs from different datasets were identified and visualized. The circular visualization of chromosomal information of common DEGs was achieved with circular visualization in R.

2.2. GO and KEGG Analyses. DAVID, an online bioinformatics tool, was used to perform GO and KEGG analyses. The top ten GO terms in biological process, molecular function, and cellular component and top five KEGG pathways were identified using the enrichment analysis. The result of enrichment analysis of hub genes was visualized with GOplot. DEGs were imported into Search Tool for the Retrieval of Interacting Genes (STRING) to construct the PPI network. Then, the TSV file of PPI network was imported into Cytoscape 3.7.2. The interactions between enriched KEGG pathways were calculated and visualized by Cytoscape 3.7.2.

2.3. Retrieval of KEGG Pathways Involved in Type 2 Diabetes and Calculation of Shared Pathways between Enriched Pathways and Type 2 Diabetes. miRWalk is an online bioinformatics atlas tool. In this study, the KEGG pathways involved in type 2 diabetes were retrieved from miRWalk. Then, the intersection of enriched KEGG pathways ($p \leq 0.05$) and type 2 diabetes-related KEGG pathways was obtained with Draw Venn Diagram (http://bioinformatics.psb.ugent.be/webtools/ Venn/). The top shared KEGG pathway with the smallest p value was selected. The enriched DEG-related part of the KEGG pathway was established with the PPT drawing tool.

2.4. Targeted Transcript Factor Prediction. http://amp.pharm .mssm.edu/Enrichr/, the online predicting tool, was used to predict targeted transcript factors of enriched DEGs in the shared KEGG pathway. The prediction result was visualized by Gephi.

3. Results

3.1. DEG Identification. Datasets of GSE49566 and GSE78891 were obtained from GEO, which are the genes from human

(a)

(b)
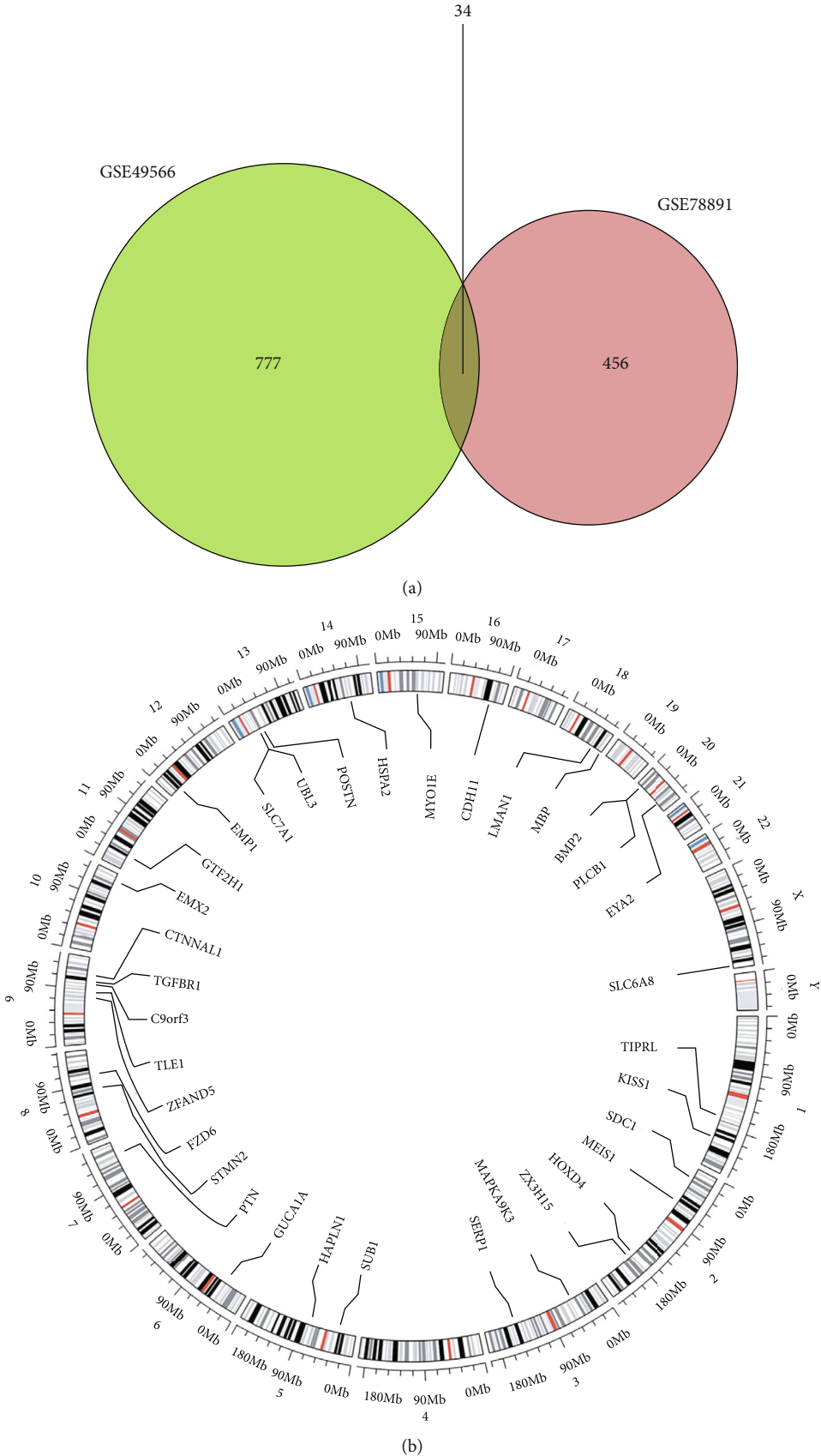
FIGURE 2: The information of common DEGs: (a) 34 common DEGs were identified between the two datasets; (b) the gene position information of the 34 common DEGs.

Table 1: Functional enrichment analysis of the DEGs. Top 10 terms were selected according to p value.

Term	Name	Count	p value	Genes
GO:0001501, BP	Skeletal system development	5	$2.3E-5$	POSTN, BMP2, CDH11, TGFBR1, HAPLN1
GO:0009986, CC	Cell surface	5	$3.7E-3$	BMP2, FZD6, PTN, HSPA2, TGFBR1
GO:0005515, MF	Protein binding	18	$6.1E-3$	EMX2, POSTN, TLE1, EYA2, FZD6, ZFAND5, STMN2, HSPA2, SLC7A1, TGFBR1, KISS1, LMAN1, BMP2, MEIS1, MAPKAPK3, TIPRL, MBP, PLCB1
GO:0048762, BP	Mesenchymal cell differentiation	2	$9.9E-3$	BMP2, TGFBR1
GO:0060389, BP	Pathway-restricted SMAD protein phosphorylation	2	$1.6E-2$	BMP2, TGFBR1
GO:0060317, BP	Cardiac epithelial to mesenchymal transition	2	$1.6E-2$	BMP2, TGFBR1
GO:0007507, BP	Heart development	3	$2.2E-2$	BMP2, PTN, TGFBR1
GO:0001701, BP	In utero embryonic development	3	$2.3E-2$	BMP2, ZFAND5, TGFBR1
GO:0006355, BP	Regulation of transcription, DNA-templated	6	$3.5E-2$	EMX2, MEIS1, BMP2, TLE1, EYA2, TGFBR1
GO:0048705, BP	Skeletal system morphogenesis	2	$3.9E-2$	ZFAND5, TGFBR1

BP: biological process; MF: molecular function; CC: cellular component.

Table 2: Pathway enrichment analysis of the DEGs. Top 5 KEGG pathways were selected according to p value.

Term	Name	Count	p value	Genes
hsa05200	Pathways in cancer	4	$8.4E-3$	BMP2, FZD6, PLCB1, TGFBR1
hsa04550	Signaling pathways regulating pluripotency of stem cells	3	$1.1E-2$	MEIS1, BMP2, FZD6
hsa04390	Hippo signaling pathway	3	$1.2E-2$	BMP2, FZD6, TGFBR1
hsa04010	MAPK signaling pathway	3	$3.3E-2$	MAPKAPK3, HSPA2, TGFBR1
hsa05217	Basal cell carcinoma	2	$6.1E-2$	BMP2, FZD6

KEGG: Kyoto Encyclopedia of Genes and Genomes.

skin fibroblasts (Figure 1). There were three type 2 diabetes samples and six normal in GSE49566. There were six type 2 diabetes samples and five normal in GSE78891. 446 upregulated and 365 downregulated DEGs were identified in GSE49566. 242 upregulated and 248 downregulated DEGs were identified in GSE78891. Totally, there were 34 common DEGs identified. They were STMN2, HAPLN1, PTN, POSTN, MAPKAPK3, CDH11, TLE1, ZFAND5, C9orf3, EMX2, TIPRL, MEIS1, FZD6, SLC6A8, SLC7A1, TGFBR1, EMP1, HSPA2, PLCB1, KISS1, HOXD4, EYA2, SERP1, UBL3, GTF2H1, MYO1E, LMAN1, BMP2, CTNNAL1, SDC1, GUCA1A, SUB1, ZC3H15, and MBP (Figure 2).

3.2. GO and KEGG Pathway Enrichment Analysis. GO analysis results showed that common DEGs were significantly enriched in skeletal system development, cell surface, protein binding, mesenchymal differentiation, pathway-restricted SMAD protein phosphorylation, cardiac epithelial to mesenchymal transi-

tion, heart development, in utero embryonic development, regulation of transcription, DNA-templated, and skeletal system morphogenesis (Table 1). KEGG pathway analysis showed that the common DEGs were significantly enriched in a pathway in cancer, signaling pathways regulating pluripotency of stem cells, Hippo signaling pathway, MAPK signaling pathways, and basal cell carcinoma pathway (Table 2). The information and interaction of the GO and KEGG terms are demonstrated in Figure 3.

3.3. Retrieval of KEGG Pathways Involved in Type 2 Diabetes and Calculation of Shared Pathways between Enriched Pathways and Type 2 Diabetes. The KEGG pathways linked with type 2 diabetes were obtained from miRWalk. They are listed in Table 3. Totally, there were 44 KEGG pathways involved in the development of type 2 diabetes. The common KEGG pathway between DEGs and type 2 diabetes with the highest p value was the MAPK signaling pathway. The part

(a)

Figure 3: Continued.

(b)
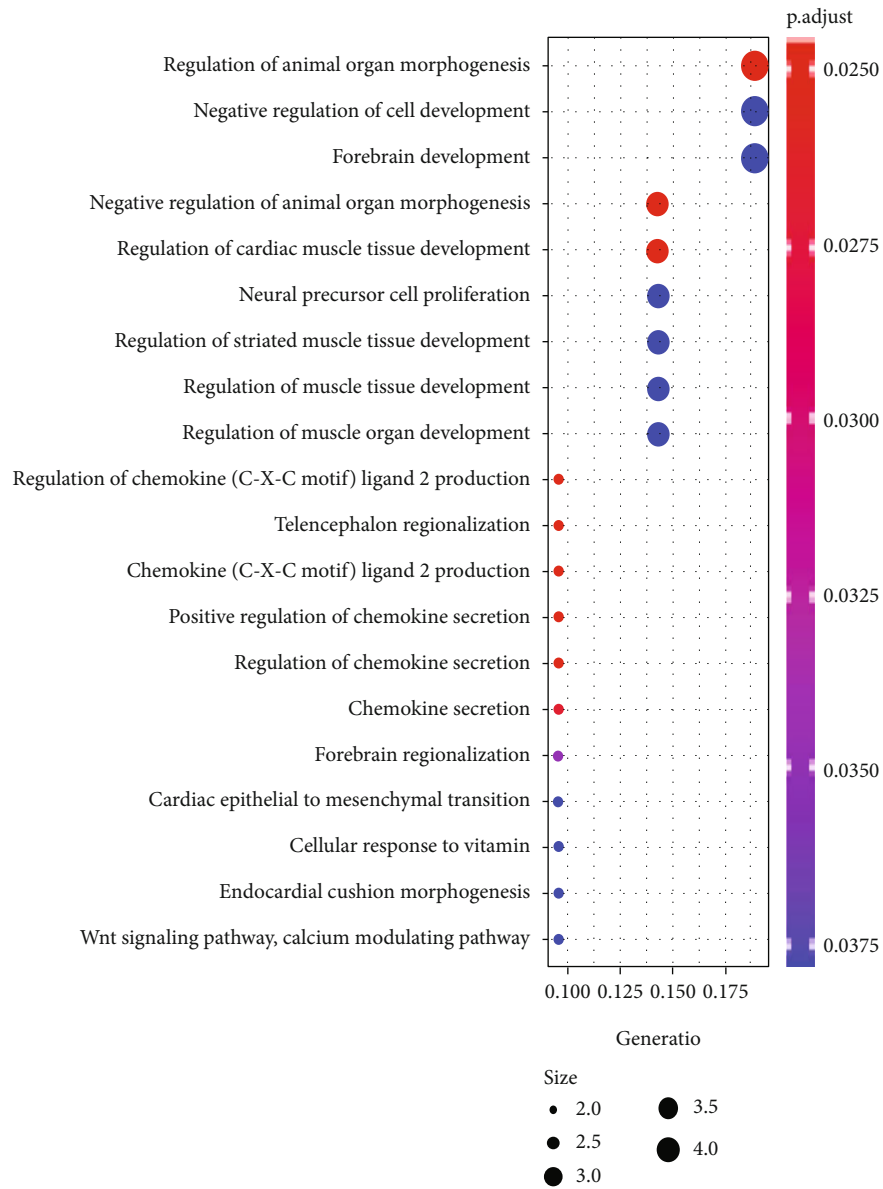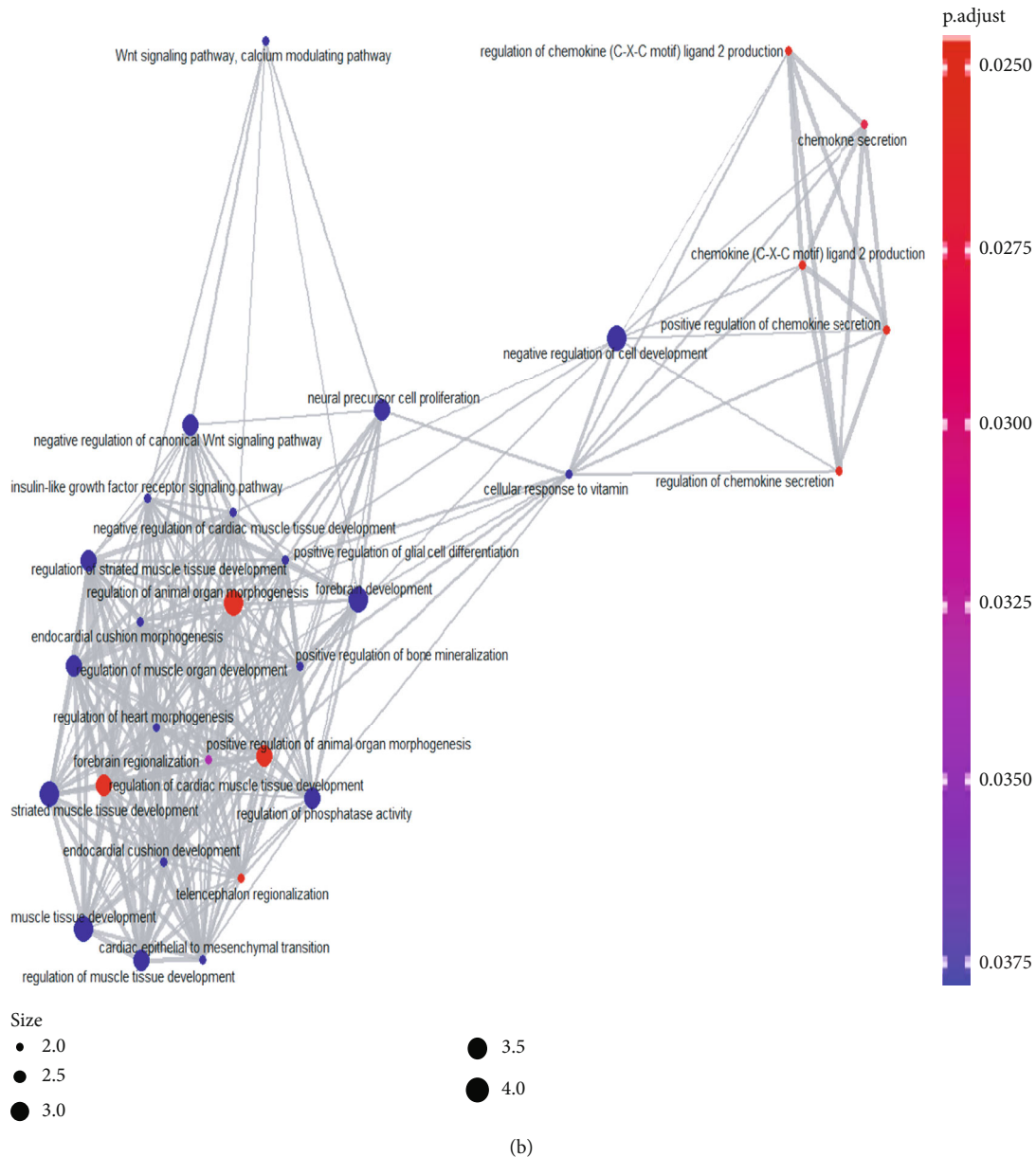
FIGURE 3: GO and KEGG enrichment analysis results: (a) count number, gene ratio, and adjusted p value of common DEGs; (b) the interaction relationship of the GO and KEGG terms.

of the MAPK signaling pathway related to the DEGs was established (Figure 4). MAPKAPK3, HSPA2, TGFBR1, and p53 signaling pathways were involved.

3.4. Targeted Transcript Factor Prediction. The targeted transcript factors of MAPKAPK3, HSPA2, and TGFBR1 were obtained from http://amp.pharm.mssm.edu/Enrichr/, which indicated ETV4 and NPE2 were the potential ones. The relationship of transcript factors, DEGs, and other targeting genes is shown in Figure 5.

4. Discussion

High risk of wound infection and healing failure was found in diabetes, and the abnormal function of fibroblasts was

assumed as a major issue contributing to the delayed wound healing [9–11]. Noticeably, fibroblasts exert an important role in wound inflammatory response by release of various antibacterial regulators, providing a robust defense of skin against infections [12–14]. Diabetes patients are susceptible to infections due to the dysregulated function of the T cells, leading to the overactivated tissue inflammation. In this bioinformatic research, functional enrichment analysis was performed, and the systematic results suggested that the highest p value was the MAPK signaling pathway among DEGs in fibroblasts. And the regulatory roles for diabetic wound healing were identified in MAPKAPK3, HSPA2, and TGFBR1.

Phosphorylation of transcription is one of the modifications of MAPK-dependent regulation in cellular responses [15]. Three subfamilies were found in the MAPK signaling

TABLE 3: Information on KEGG pathways linked with diabetes type 2.

Code	KEGG
hsa00061	Fatty acid biosynthesis
hsa04910	Insulin signaling pathway
hsa01100	Metabolic pathways
hsa00640	Propanoate metabolism
hsa00620	Pyruvate metabolism
hsa04920	Adipocytokine signaling pathway
hsa03320	PPAR signaling pathway
hsa04930	Type II diabetes mellitus
hsa05332	Graft versus host disease
hsa04672	Intestinal immune network for IgA production
hsa05322	Systemic lupus erythematosus
hsa04660	T cell receptor signaling pathway
hsa04940	Type I diabetes mellitus
hsa05416	Viral myocarditis
hsa05330	Allograft rejection
hsa05320	Autoimmune thyroid disease
hsa04514	Cell adhesion molecules (CAMs)
hsa04920	Adipocytokine signaling pathway
hsa04512	ECM receptor interaction
hsa04640	Hematopoietic cell lineage
hsa03320	PPAR signaling pathway
hsa05320	Autoimmune thyroid disease
hsa04514	Cell adhesion molecules (CAMs)
hsa04660	T cell receptor signaling pathway
hsa04010	MAPK signaling pathway
hsa01100	Metabolic pathways
hsa00061	Fatty acid biosynthesis
hsa04910	Insulin signaling pathway
hsa04920	Adipocytokine signaling pathway
hsa04060	Cytokine-cytokine receptor interaction
hsa04630	Jak-STAT signaling pathway
hsa04080	Neuroactive ligand-receptor interaction
hsa00360	Phenylalanine metabolism
hsa00350	Tyrosine metabolism
hsa00760	Nicotinate and nicotinamide metabolism
hsa04920	Adipocytokine signaling pathway
hsa04610	Complement and coagulation cascades
hsa04920	Adipocytokine signaling pathway
hsa03320	PPAR signaling pathway
hsa04610	Complement and coagulation cascades
hsa04115	p53 signaling pathway
hsa04610	Complement and coagulation cascades
hsa04512	ECM receptor interaction
hsa04510	Focal adhesion
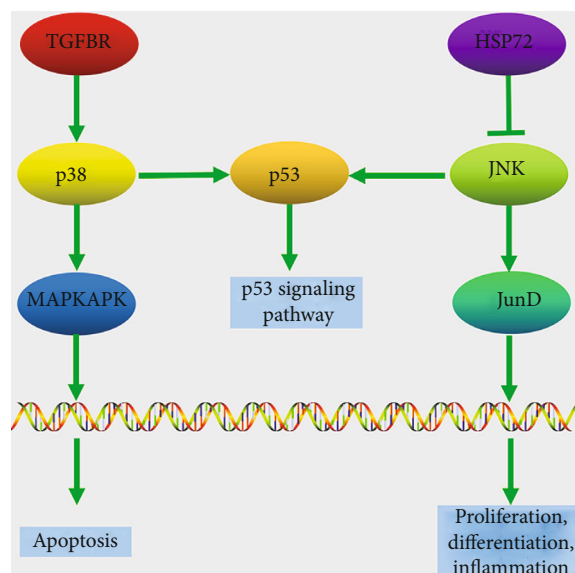
FIGURE 4: The part of the MAKP signaling pathway related to the common DEGs. MAPKAPK3, HSPA2, TGFBR1, and p53 signaling pathways were involved, resulting in apoptosis, proliferation, differentiation, and inflammation.

pathway, including the extracellular-signal-regulated kinases (ERK MAPK, Ras/Raf1/MEK/ERK), the c-Jun N-terminal or stress-activated protein kinases (JNK, SAPK), and p38 [16–18]. Once the pathway was activated, a number of downstream target kinases including MAPKAPK3 could be activated [19]. Recently, some researchers have fabricated an in situ injectable hydrogel which can markedly accelerate diabetic wound healing through activating the TGF-β/MEK/ MAPK signaling pathway [20]. Similarly, Qian et al. demonstrated that protein tyrosine phosphatase 1B was capable to enhance fibroblast proliferation and mitigation via activation of the MAPK/ERK pathway, thereby promoting diabetic wound healing [21]. In the current study, we found a consistent result that the MAPK signaling pathway plays a key role in the regulation of diabetic wound healing, and MAPKAPK3, HSPA2, and TGFBR1 are the potentially critical genes in this regulation process. Moreover, to uncover the potential targeted transcript factors of MAPKAPK3, HSPA2, and TGFBR1 genes, we used the online software (Enrichr, http://amp .pharm.mssm.edu/Enrichr/) and the results suggested that ETV4 and NPE2 were the potential transcript factors for these genes. Thus, it was assumed that ETV4 and NPE2 may exert a critical role in the regulation of diabetic wound healing.

Some limitations also existed in this bioinformatic research. First, the current results were based on a public database and only two datasets were included in our study; the sample size should be enlarged to minimize the possible confounding factors. Furthermore, this is a pure bioinformatic research; more experimental validation is needed to confirm the candidate pathways and their potential transcript factors. Moreover, clinical specimens of different degrees of DFUs should be collected to validate our current findings.

(a)

(b)
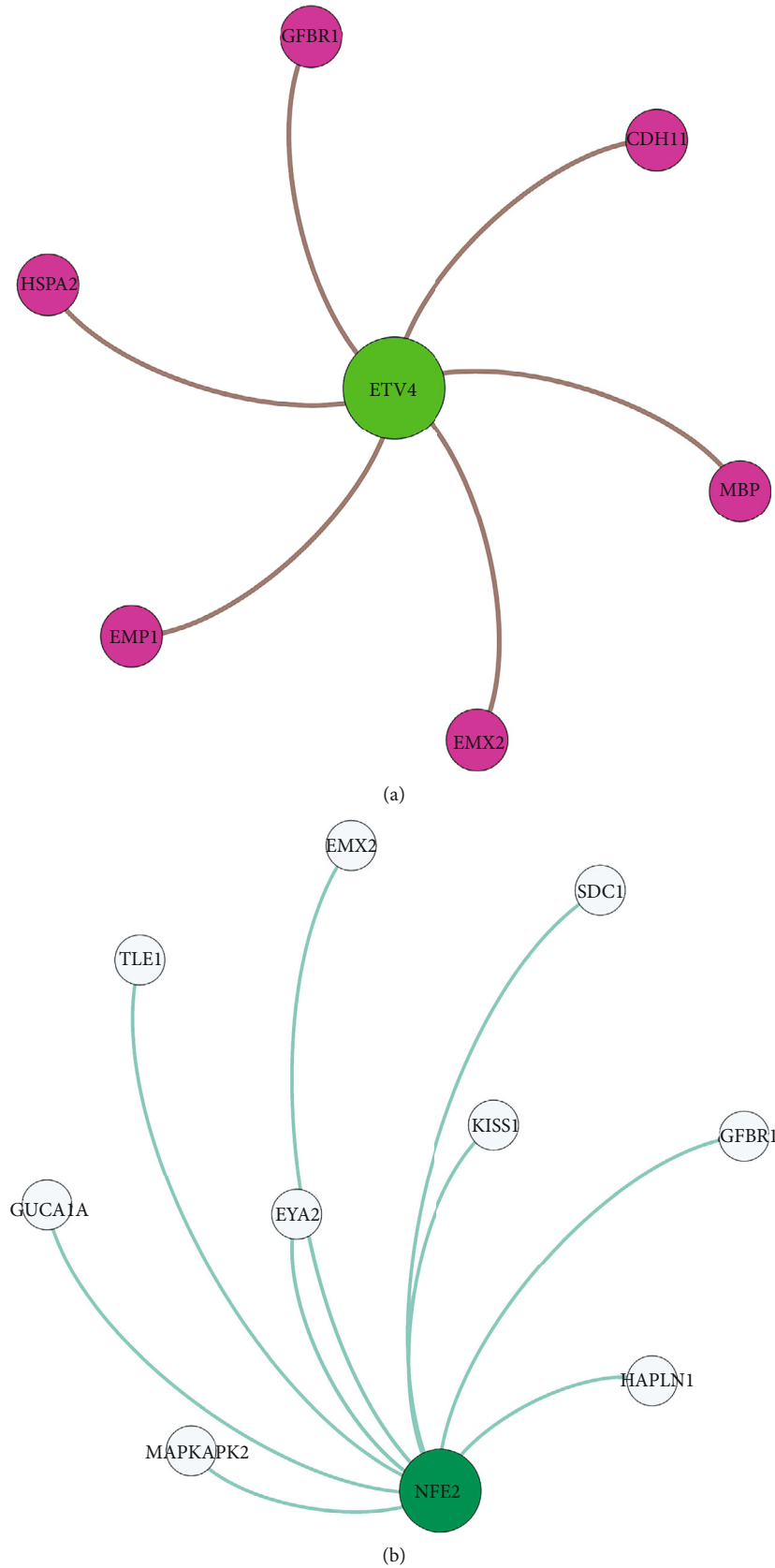
Figure 5: Targeted transcript factor prediction of the DEGs in the MAKP signaling pathway. They were ETV4 and NPE2. ETV4 may target TGFBR1, HSPA2, EMP1, EMX2, MBP, and CDH11. NPE2 may target MAPKAPK3, GUCA1A, TLE1, EYA2, EMX2, SDC1, KISS1, TGFBR1, and HAPLN1.

5. Conclusions

Our findings suggested a functionally enriched MAPK signaling pathway, with a focus on the potential role of ETV4 and NPE2 in the regulation of diabetic wound regeneration. The current study may provide novel therapeutic targets in diabetic wound treatment.

Data Availability

The data used to support the findings of this study are available from the corresponding author upon request.

Conflicts of Interest

The authors declare that there is no conflict of interest regarding the publication of this paper.

References

[1] Y. Xiong, L. Chen, T. Yu et al., "Inhibition of circulating exosomal microRNA-15a-3p accelerates diabetic wound repair," *Aging*, vol. 12, no. 10, pp. 8968–8986, 2020.

[2] Y. Hu, R. Tao, L. Chen et al., "Exosomes derived from pioglitazone-pretreated MSCs accelerate diabetic wound healing through enhancing angiogenesis," *Journal of Nanobiotechnology*, vol. 19, no. 1, p. 150, 2021.

[3] Y. Xiong, L. Chen, C. Yan et al., "Circulating exosomal miR-20b-5p inhibition restores Wnt9b signaling and reverses diabetes-associated impaired wound healing," *Small*, vol. 16, no. 3, article e1904044, 2020.

[4] B. Mi, L. Chen, Y. Xiong et al., "Saliva exosomes-derived UBE2O mRNA promotes angiogenesis in cutaneous wounds by targeting SMAD6," *Journal of Nanobiotechnology*, vol. 18, no. 1, pp. 68–82, 2020.

[5] W. Zhang, L. Chen, Y. Xiong et al., "Antioxidant therapy and antioxidant-related bionanomaterials in diabetic wound healing," *Frontiers in Bioengineering and Biotechnology*, vol. 9, p. 707479, 2021.

[6] K. Chen, T. Yu, and X. Wang, "Inhibition of circulating exosomal miRNA-20b-5p accelerates diabetic wound repair," *International Journal of Nanomedicine*, vol. 16, pp. 371–381, 2021.

[7] X. Chen, W. Zhou, K. Zha et al., "Treatment of chronic ulcer in diabetic rats with self assembling nanofiber gel encapsulated-polydeoxyribonucleotide," *American Journal of Translational Research*, vol. 8, no. 7, pp. 3067–3076, 2016.

[8] M. Khamaisi, S. Katagiri, H. Keenan et al., "PKCδ inhibition normalizes the wound-healing capacity of diabetic human fibroblasts," *The Journal of Clinical Investigation*, vol. 126, no. 3, pp. 837–853, 2016.

[9] N. C. Nowak, D. M. Menichella, R. Miller, and A. S. Paller, "Cutaneous innervation in impaired diabetic wound healing," *Translational Research*, vol. 236, pp. 87–108, 2021.

[10] R. An, Y. Zhang, Y. Qiao, L. Song, H. Wang, and X. Dong, "Adipose stem cells isolated from diabetic mice improve cutaneous wound healing in streptozotocin-induced diabetic mice," *Stem Cell Research & Therapy*, vol. 11, no. 1, pp. 120–131, 2020.

[11] S. D. Burr and M. B. Harmon Jr., "The impact of diabetic conditions and AGE/RAGE signaling on cardiac fibroblast migration," *Frontiers in Cell and Development Biology*, vol. 8, p. 112, 2020.

[12] P. A. Borges, I. Waclawiak, J. L. Georgii et al., "Adenosine diphosphate improves wound healing in diabetic mice through P2Y12 receptor activation," *Frontiers in Immunology*, vol. 12, p. 651740, 2021.

[13] J. Chen, Y. Wu, C. Li et al., "PPARγ activation improves the microenvironment of perivascular adipose tissue and attenuates aortic stiffening in obesity," *Journal of Biomedical Science*, vol. 28, no. 1, pp. 22–35, 2021.

[14] A. Shaikh-Kader, N. N. Houreld, N. K. Rajendran, and H. Abrahamse, "Levels of Cyclooxygenase 2, Interleukin-6, and Tumour Necrosis Factor-α in Fibroblast Cell Culture Models after Photobiomodulation at 660 nm," *Oxidative Medicine and Cellular Longevity*, vol. 2021, Article ID 6667812, 13 pages, 2021.

[15] Y. Liu, W. Liu, Z. Yu et al., "A novel BRD4 inhibitor suppresses osteoclastogenesis and ovariectomized osteoporosis by blocking RANKL-mediated MAPK and NF- _κ_ B pathways," *Cell Death & Disease*, vol. 12, no. 7, pp. 654–669, 2021.

[16] Q. Ling, F. Li, X. Zhang et al., "MAP4K1 functions as a tumor promotor and drug mediator for AML via modulation of DNA damage/repair system and MAPK pathway," *eBioMedicine*, vol. 69, p. 103441, 2021.

[17] A. Cordido, L. Nuñez-Gonzalez, J. M. Martinez-Moreno et al., "TWEAK signaling pathway blockade slows cyst growth and disease progression in autosomal dominant polycystic kidney disease," *Journal of the American Society of Nephrology*, vol. 32, no. 8, pp. 1913–1932, 2021.

[18] T. Shi, D. M. K. van Soest, P. E. Polderman, B. M. T. Burgering, and T. B. Dansen, "DNA damage and oxidant stress activate p53 through differential upstream signaling pathways," *Free Radical Biology & Medicine*, vol. 172, pp. 298–311, 2021.

[19] S. Kataoka, P. Manandhar, J. Lee et al., "The costimulatory activity of Tim-3 requires Akt and MAPK signaling and its recruitment to the immune synapse," *Science Signaling*, vol. 14, no. 687, 2021.

[20] P. Lou, S. Liu, Y. Wang et al., "Injectable self-assembling peptide nanofiber hydrogel as a bioactive 3D platform to promote chronic wound tissue regeneration," *Acta Biomaterialia*, vol. 135, pp. 100–112, 2021.

[21] L. Qian, Q. Wang, C. Wei et al., "Protein tyrosine phosphatase 1B regulates fibroblasts proliferation, motility and extracellular matrix synthesis via the MAPK/ERK signalling pathway in keloid," *Experimental Dermatology*, 2021.

Research Article

KLF4 Promotes Diabetic Chronic Wound Healing by Suppressing Th17 Cell Differentiation in an MDSC-Dependent Manner

Xiong Yang [ID],[1] **Bryan J. Mathis** [ID],[2] **Yu Huang** [ID],[1] **Wencheng Li** [ID],[1] and **Ying Shi** [ID][1]

[1]*Department of Urology, Wuhan Union Hospital, Tongji Medical College, Huazhong University of Science & Technology, China*
[2]*International Medical Center, University of Tsukuba Affiliated Hospital, Japan*

Correspondence should be addressed to Ying Shi; 82625338@qq.com

Objectives. Diabetic wound inflammation deficiencies lead to ulcer development and eventual amputation and disability. Our previous research demonstrates that myeloid-derived suppressor cells (MDSCs) accumulate during inflammation and promote chronic wound healing via the regulation of Kruppel-like factor 4 (KLF4). In this study, we aimed to investigate the potential roles of MDSCs and KLF4 in diabetic wound healing. *Methods*. An ob/ob mouse pressure ulcer (PU) model was used to evaluate the process of wound healing. The expression levels of KLF4 and IL-17A were measured by real-time PCR, and the population of MDSCs and Th17 cells was measured by flow cytometry. The levels of cytokines were determined by an immunosuppression assay. *Results*. KLF4 deficiency in the diabetic PU model resulted in decreased accumulation of MDSCs, increased expansion of Th17 cells, and significantly delayed wound healing. Conversely, KLF4 activation by APTO-253 accelerated wound healing accompanied by increased MDSC populations and decreased numbers of Th17 cells. MDSCs have been proven to mediate Th17 differentiation via cytokines, and our *in vitro* data showed that elevated KLF4 expression in MDSCs resulted in reduced Th17 cell numbers and, thus, decreased levels of cytokines indispensable for Th17 differentiation. *Conclusions*. Our study revealed a previously unreported function of KLF4-regulated MDSCs in diabetic wound healing and identified APTO-253 as a potential agent to improve the healing of pressure ulcers.

1. Introduction

Wound healing is a multifactorial, pathophysiologic process characterized by four discrete temporal phases that overlap: hemostasis, inflammation, proliferation, and remodeling [1]. Acute inflammation following dermal injury activates diverse growth factors and cytokines that facilitate the subsequent proliferation stage. However, wounds in diabetics will usually stall in a sustained inflammatory state resulting in nonhealing ulcers. The amputation and disability caused by these wounds are among the most common complications of type 2 diabetes, and, due to the estimated 10.9% prevalence of diabetes within the Chinese adult population [2], the number of potential victims is tremendous. Management of inflammation in nonhealing wounds, therefore, will open the way for the development of therapies that improve both prognosis and quality of life for such patients.

Kruppel-like factor 4 (KLF4) is a transcription factor critical in maintaining the epidermal permeability barrier [3], and it has been found to mediate cutaneous wound healing in murine hair follicle stem cells [4]. Myeloid-derived suppressor cells (MDSCs) are a heterogeneous population of bone marrow-derived cells possessing phenotypic plasticity, carrying monocyte markers [5], and contributing to wound healing [6]. Our previous study showed that KLF4 facilitates the healing of wounds via the mediation of both monocytic MDSC recruitment and differentiation of these cells into fibrocytes [7], but the effects of KLF4-mediated MDSCs on diabetic wounds still remain unknown.

Numerous literature reports that inflammatory mediators are highly associated with immune alterations in the initiation and development of chronic inflammatory diseases [8, 9]. Interleukin- (IL-) 17A mediates the early inflammatory stages of wound repair and may hinder normal healing

[10] as evidenced by the application of IL-17 suppressive antibody that reverses delayed wound closure in leptin-deficient ob/ob mice [11]. Th17 cells are a major IL-17-producing cell type, and both cell type and cytokine are highly associated with the pathogenesis of diverse human autoimmune diseases, including inflammatory bowel disease, psoriasis, and rheumatoid arthritis [12, 13]. Recently, several studies have identified a link between MDSCs and Th17 cell differentiation in different disease contexts, such as experimental autoimmune encephalomyelitis and autoimmune arthritis [14, 15], while direct evidence of Th17 mediation of *H. pylori*-induced peptic ulcers links IL-17 to impaired mucosal barrier function through suppression of regulatory T cells [16]. Therefore, we postulate that KLF4 might improve the repair of diabetic wounds by mediating Th17 cell differentiation in an MDSC-dependent manner.

In this report, we used a pressure ulcer (PU) model in ob/ob mice to show that compromised diabetic wound repair correlates with decreased expression of KLF4 and upregulation of IL-17A. The application of a KLF4 inducer can significantly accelerate wound healing as evidenced by the expansion of CD11b$^+$Gr-1$^+$ MDSCs and concomitant decreases of Th17 cells and IL-17A expression. We also observed efficient MDSC suppression of Th17 differentiation and IL-17A production *in vitro*, and KLF4 expression is critical for this process. Our data highlights the importance of KLF4-mediated MDSCs in facilitating diabetic wound repair during chronic inflammation and suggests that targeting KLF4 has potential to treat diabetic patients with chronic wounds.

2. Materials and Methods

2.1. Mice. C57BL/6 (wild type, WT) and ob/ob mice were obtained from Beijing Vital River Laboratory Animal Technology Company (Beijing, China). All mice were 8-12 weeks of age with an equal ratio of males to females. All experiments and procedures involving mice were approved by the Institutional Animal Care and Use Committee of the Huazhong University of Science and Technology.

2.2. Wound Healing Mouse Model and APTO-253 Treatment. Our murine PU model was created as described previously [17], and wound evaluation was also performed as previously described [7]. Briefly, KLF4 was induced by an APTO-253 (MCE Chemicals & Equipment) treatment via intraperitoneal injection every other day at a concentration of 1 mg/kg in DMSO (Sigma-Aldrich) while vehicle injections served as controls. Injections commenced two days before the first I/R cycle (day 0), and mice were sacrificed for further examination on day 3. For those mice marked for wound evaluation, the APTO-253 treatment continued to day 8.

2.3. RNA Extraction and Real-Time PCR Analysis. The TRIzol reagent (Invitrogen) was used to prepare total RNA according to the manufacturer's instructions. First-strand cDNA synthesis and real-time PCR were carried out as

described previously [7]. Table S1 contains primer sequences utilized in real-time PCR experiments.

2.4. Flow Cytometry Analysis. Splenocytes and peripheral blood monocytes (PBMCs) were prepared as described previously [7]. Briefly, single-cell suspensions were created from wound site tissue that was minced and digested with 1.0 mg/ml collagenase (Sigma) before purification by Percoll gradient (Sigma). Next, such dissociated single cells were treated with fluorochrome-conjugated antibodies specific for mouse CD11b, Ly6G, and CD4 (eBioscience). For intracellular staining, fluorochrome-conjugated mouse IL-17 antibody (eBioscience) was used. A FACSAria III (BD) and FlowJo (BD) were used to image cells and analyze data.

2.5. Coculture of CD4$^+$ T Cells and MDSCs. Spleen-derived MDSCs were isolated using FACS. Naïve CD4$^+$ T cells were sorted from single-cell lymph node suspensions of WT mice and activated with Dynabeads™ Mouse T-Activator CD3/CD28 (Thermo). Triplicate batches of cells were cultured in RPMI 1640 media supplemented with 10% FBS, 50 μM 2-mercaptoethanol, and 2 mM L-glutamine/1% penicillin/streptomycin (Gibco) at a ratio of 1 : 2 (MDSC/T cells). For APTO-253 treatment, MDSCs were incubated with APTO-253 (50 nM) for 72 h and washed with PBS before coculturing. DMSO served as a control.

2.6. Immunosuppression Assays. The supernatant was collected 48 h after coculturing, and samples of blood and skin tissues were prepared for ELISA (MDL) according to the manufacturer's instructions. The levels of cytokines IL-1β, IL-6, TGF-β, IL-17A, and IFN-γ were determined.

2.7. In Vitro Th17 Cell Differentiation. T cells were collected and washed 120 h after coculturing, and intracellular staining of IL-17 was performed as described previously. The ratio of Th17 cells to undifferentiated T cells was assessed by flow cytometry.

2.8. Statistical Analysis. Statistical analysis was performed with SPSS 16.0 software. Data were represented as the mean $\pm$ SEM and analyzed using t-testing (two-group comparison) and one-way ANOVA (multigroup comparison). A p value < 0.05 was considered to indicate statistical significance.

3. Results

3.1. Compromised Wound Healing of PU in ob/ob Mice Associated with Decreased Expression of KLF4 and Upregulation of IL-17A. We first identified possible roles for KLF4 and IL-17A in diabetic wound healing. As expected, wound closure kinetics were significantly delayed from day 3 to day 9 in ob/ob mice compared to wild-type (WT) mice (Figure 1(a)). We examined the expression of KLF4 and IL-17A in ob/ob mice on day 3 by qRT-PCR, and a substantial decrease of KLF4 expression in the peripheral blood and granule tissue of the skin was detected while IL-17A expression was significantly elevated in both blood and skin (Figure 1(b)). We further confirmed IL-17

(a)

(b)
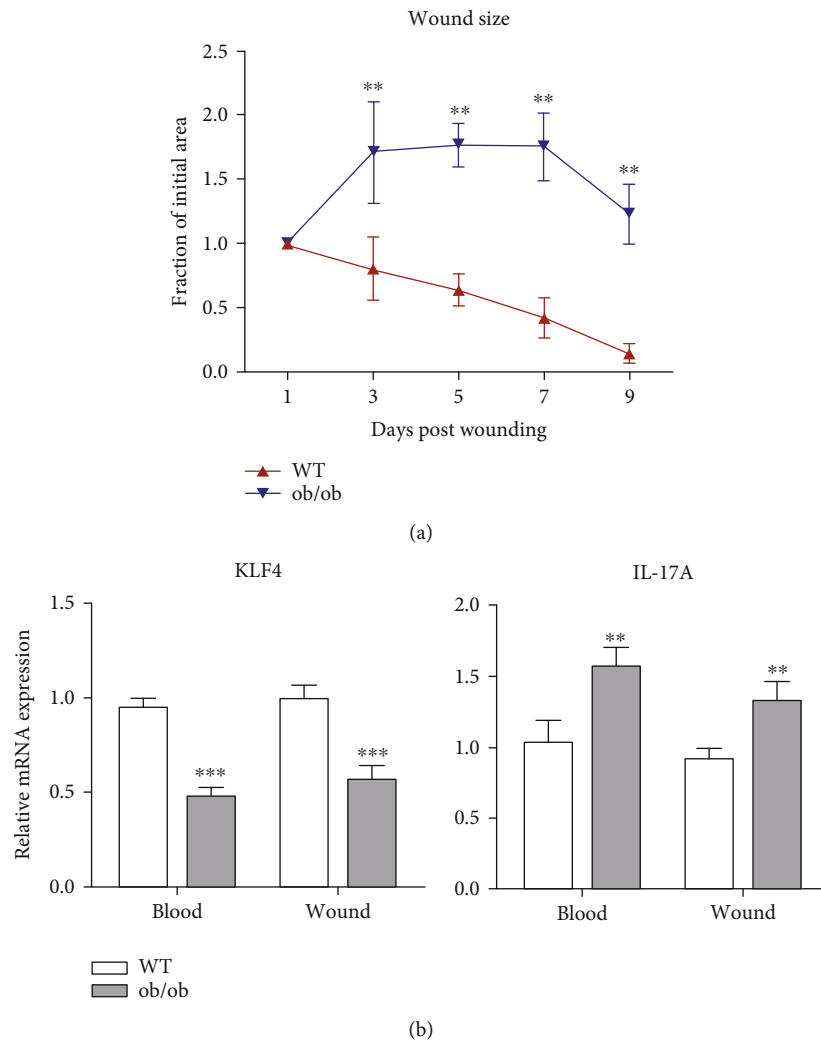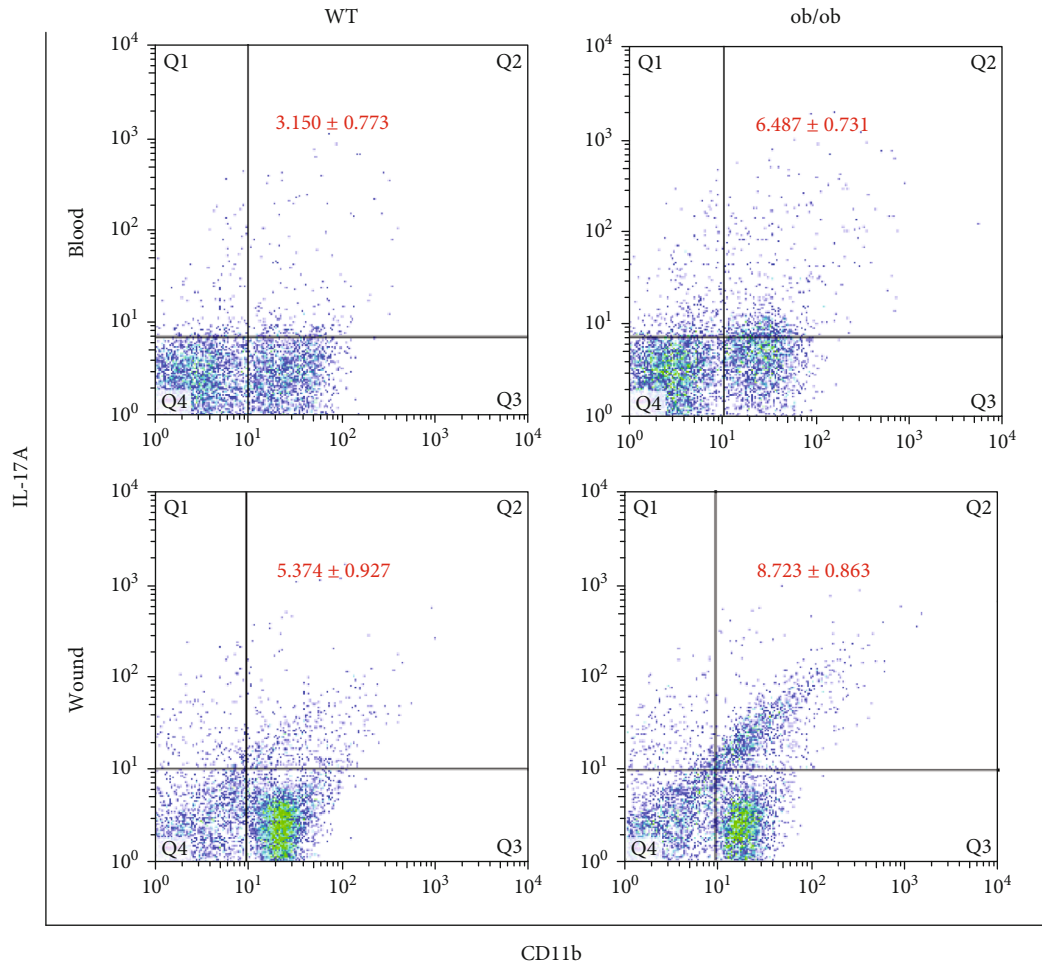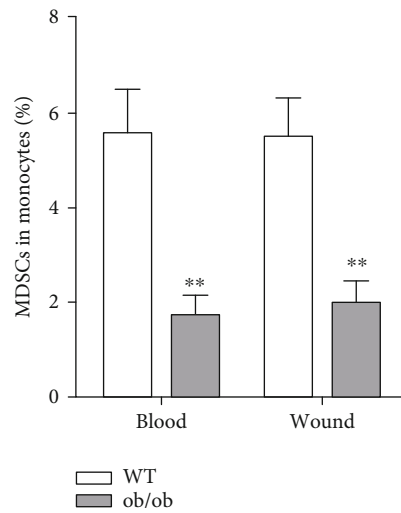
FIGURE 1: Continued.

FIGURE 1: Compromised wound healing of pressure ulcer (PU) in ob/ob mice associated with decreased expression of Kruppel-like factor 4 (KLF4) and upregulation of IL-17A.

expression using flow cytometry. On day 3 after wounding, increased IL-17 expression in ob/ob mice was observed compared with WT (ob/ob $6.487 \pm 0.731\%$ $vs.$ WT $3.150 \pm$ 0.773% in blood, $p < 0.01$; ob/ob $8.723 \pm 0.863\%$ $vs.$ WT $5.374 \pm 0.927\%$ in skin, $p < 0.05$) (Figure 1(c)), which was consistent with a previous report [11].

(a)　　　　　　　　　　　　　(b)
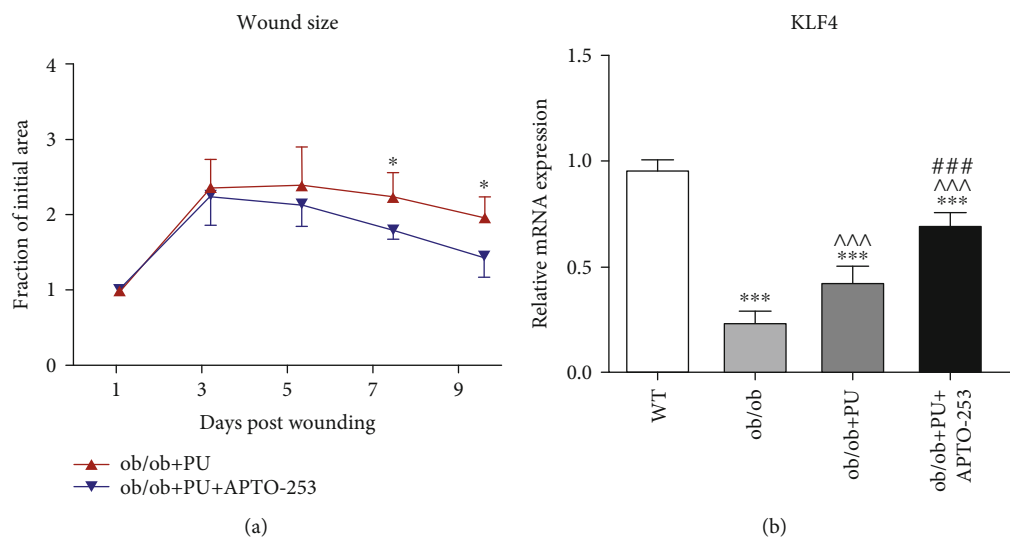
FIGURE 2: Kruppel-like factor 4 (KLF4) activation by APTO-253 accelerated pressure ulcer (PU) in ob/ob mice accompanied by increased CD11b$^+$Gr-1$^+$ myeloid-derived suppressor cells (MDSCs) and decreased Th17 cells.

To determine if KLF4 deficiency reduced the population of MDSCs in blood and wounds on day 3, we performed flow cytometry, and the results demonstrated a concomitant decrease in MDSCs in both sites ($p < 0.01$ in blood and $p < 0.01$ in skin, Figure 1(d)). These preliminary data indicated that KLF4, MDSCs, and IL-17A were all involved in the inflammation stage of diabetic wound healing.

3.2. Activation of KLF4 by APTO-253 Improved Diabetic Wound Healing Accompanied by Elevated MDSC Expansion and Decreased Th17 Population. APTO-253 is a small molecule that inhibits c-Myc expression and mediates anticancer activity through induction of KLF4-mediated tumor suppression [18]. As shown in Figure 2(a), the application of APTO-253 significantly improved the progression of wound healing from day 7 to day 9 in our ob/ob PU model. Subsequent qRT-PCR analysis revealed that the baseline KLF4 expression in ob/ob mice was significantly lower than WT ($p < 0.001$), but APTO-253 rescued KLF4 expression in these mice ($p < 0.001$, vs. ob/ob) (Figure 2(b)), consistent with the kinetic shifts presented in Figure 2(a). In parallel with increased KLF4 expression in the APTO-253-treated group, the populations of CD11b$^+$Gr-1$^+$ MDSCs in blood and skin wounds were also increased compared to ob/ob PU mice without APTO-253 treatment ($p < 0.01$ in blood and $p < 0.05$ in skin, Figure 2(c)).

Th17 cells are a newly identified, distinct subset of T helper cells that generate IL-17 [10]. Reports have demonstrated the key role of MDSCs in the differentiation of Th17 cells [14, 15, 19–21]. Thus, we were able to observe populations of Th17 cells in blood and skin wounds and found that APTO-253 treatment suppressed the expansion of Th17 cells in both sites ($p < 0.01$ in blood and $p < 0.05$ in skin, Figure 2(d)). APTO-253 consistently reduced the expression of IL-17A and IFN-γ in blood and wounds, indicating that the inflammatory status was improved (Figure 2(e)). These findings suggest that KLF4 regulation

of MDSCs might downregulate Th17 cell differentiation and inflammation in the context of diabetic wound healing.

It was reported that KLF4 could promote Th17 cell differentiation and IL-17 expression by directly binding to the il-17a promoter [22, 23], an effect opposite to what we observed. We postulate that KLF4-regulated Th17 cell differentiation in an MDSC-dependent manner is much stronger than the direct effect of KLF4 on T cells. Since cytokines IL-1β, IL-6, and TGF-β play important roles in MDSC-driven Th17 differentiation [14], we assessed these factors using ELISA. The concentrations of IL-1β, IL-6, and TGF-β in blood and wounds were all significantly elevated in response to pressure ulcers while the activation of KLF4 significantly suppressed the expression of these cytokines (Figure 2(e)).

3.3. MDSCs Regulate Th17 Cell Differentiation in an ob/ob Pressure Ulcer Model. The in vivo data suggested that MDSC regulation of Th17 cell differentiation depended on the cytokine milieu within the inflamed sites. To further determine the way that MDSCs modulated Th17 differentiation, we cultured sorted WT naïve CD4$^+$ T cells with spleen-derived MDSCs from different groups in vitro. At 48 h after coculture, the supernatant was collected and analyzed using ELISA. Similar to the results in vivo, MDSCs from the ob/ob PU group efficiently enhanced not only IL-17A and IFN-γ expression from T cells but also endogenous expression of IL-1β, IL-6, and TGF-β secreted by MDSCs themselves. This was reversed when the mice underwent APTO-253 treatment (Figure 3(a)). The qRT-PCR analysis also demonstrated that APTO-253 intervention significantly raised KLF4 expression in MDSCs from ob/ob mice ($p < 0.001$, Figure 3(b)). At 120 h after coculture, T cells were collected for flow cytometric analysis. A substantial increase in the percentage of Th17 cells was found in CD4$^+$ cells cultured with MDSCs from the ob/ob+PU group, and a reduced population of Th17 cells was observed upon upregulation of

(a)

(b)

(c)
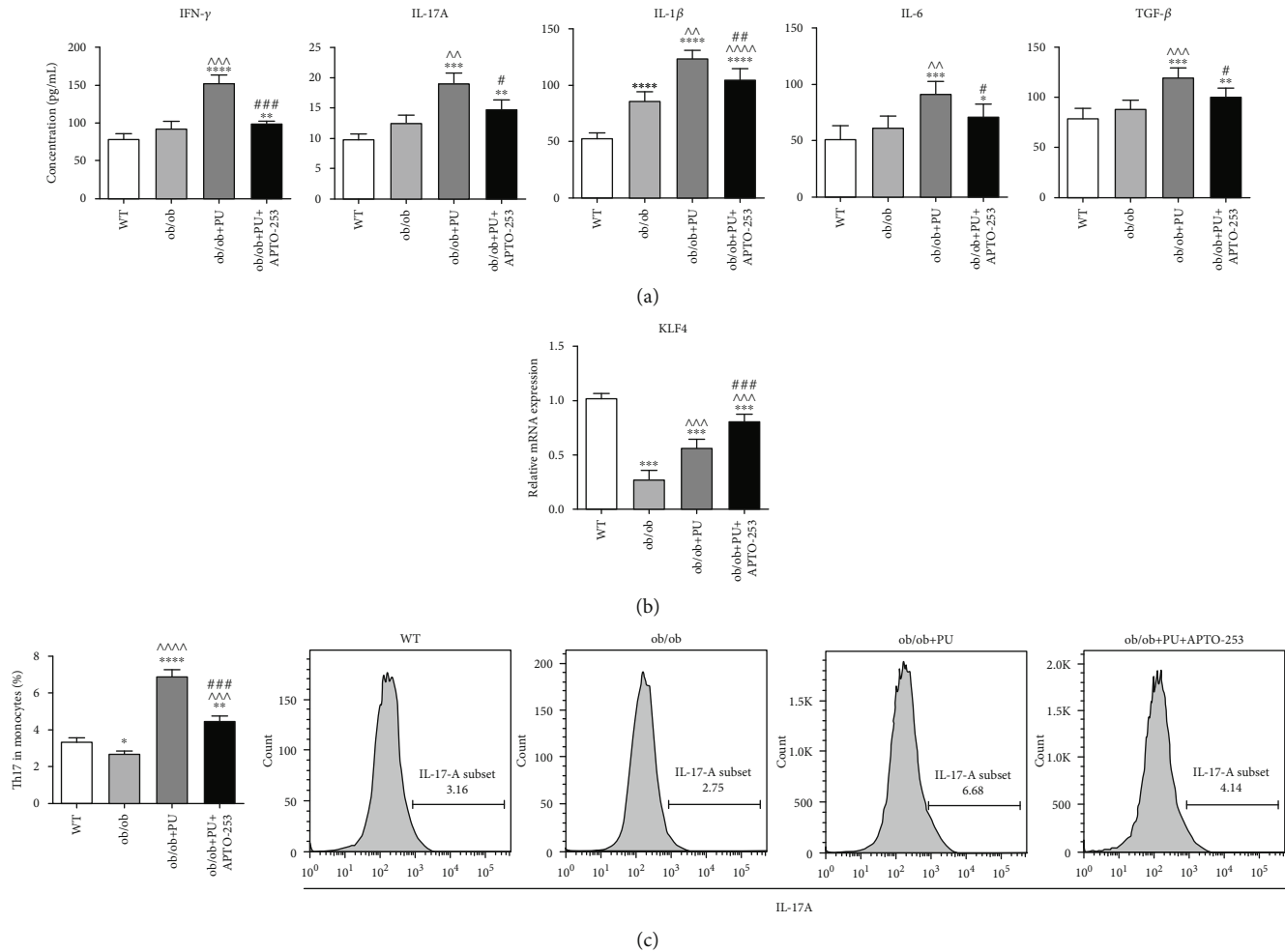
Figure 3: CD11b$^+$Gr-1$^+$ myeloid-derived suppressor cells (MDSCs) regulate the differentiation of Th17 cells.

KLF4 as well (Figure 3(c)). These observations were in line with the changes in cytokine expression shown in Figure 3(a).

3.4. MDSC-Regulated Th17 Cell Differentiation Is Mediated by KLF4 in ob/ob Mice. We next investigated whether MDSC regulation of Th17 differentiation relied on KLF4 expression in MDSCs. MDSCs were sorted from ob/ob mice and cultured with naïve WT CD4$^+$ cells, and, in the experimental group, MDSCs were treated with APTO-253 for 72 h before coculture. After 48 h of coculture, we examined the supernatant and MDSCs using ELISA and qRT-PCR, respectively. As expected, the expression of IL-17A and IFN-γ and the main cytokines required for Th17 differentiation (IL-1β, IL-6, and TGF-β) were all inhibited in the experimental group (Figure 4(a)) with a concomitant increase in KLF4 expression ($p < 0.05$, Figure 4(b)). Flow cytometry was then performed to detect the percentage of Th17 cells at 120 h after coculture. The results revealed that MDSCs from ob/ob mice efficiently enhanced the differentiation of Th17 cells ($p < 0.001$), but this was significantly reduced when KLF4 expression was upregulated by APTO-253 ($p < 0.05$, Figure 4(c)), indicating that KLF4 expression in MDSCs is the key to Th17 differentiation.

4. Discussion

Our previous research showed that KLF4 mediates cutaneous wound healing via MDSCs [7], but no current studies delineate the effects of KLF4 on diabetic wound repair. In this report, using an ob/ob mouse pressure ulcer model, we demonstrated that KLF4-regulated MDSCs promoted diabetic wound healing by suppressing Th17 differentiation and subsequent IL-17A expression. Emerging evidence indicates that agents targeting inflammatory cytokines/receptors can significantly ameliorate the pathogenesis and progression of autoimmune diseases [24, 25]. Indeed, IL-17 inhibitors such as secukinumab and ixekizumab have been tested and shown safe for use in both ankylosing spondylitis and psoriasis [26, 27]. However, extensive clinical trials of such inhibitors in wound healing have not been conducted. Meanwhile, the current study reveals that APTO-253, a commercialized KLF4 activator, is also able to accelerate the healing of pressure ulcers, making KLF4 upregulation a promising alternative candidate for wound healing applications.

Basal levels of KLF4 in ob/ob mice are lower than WT mice, and, even with the stimulus of a pressure ulcer, KLF4 expression in ob/ob mice is still reduced in comparison

(a)

(b)

(c)
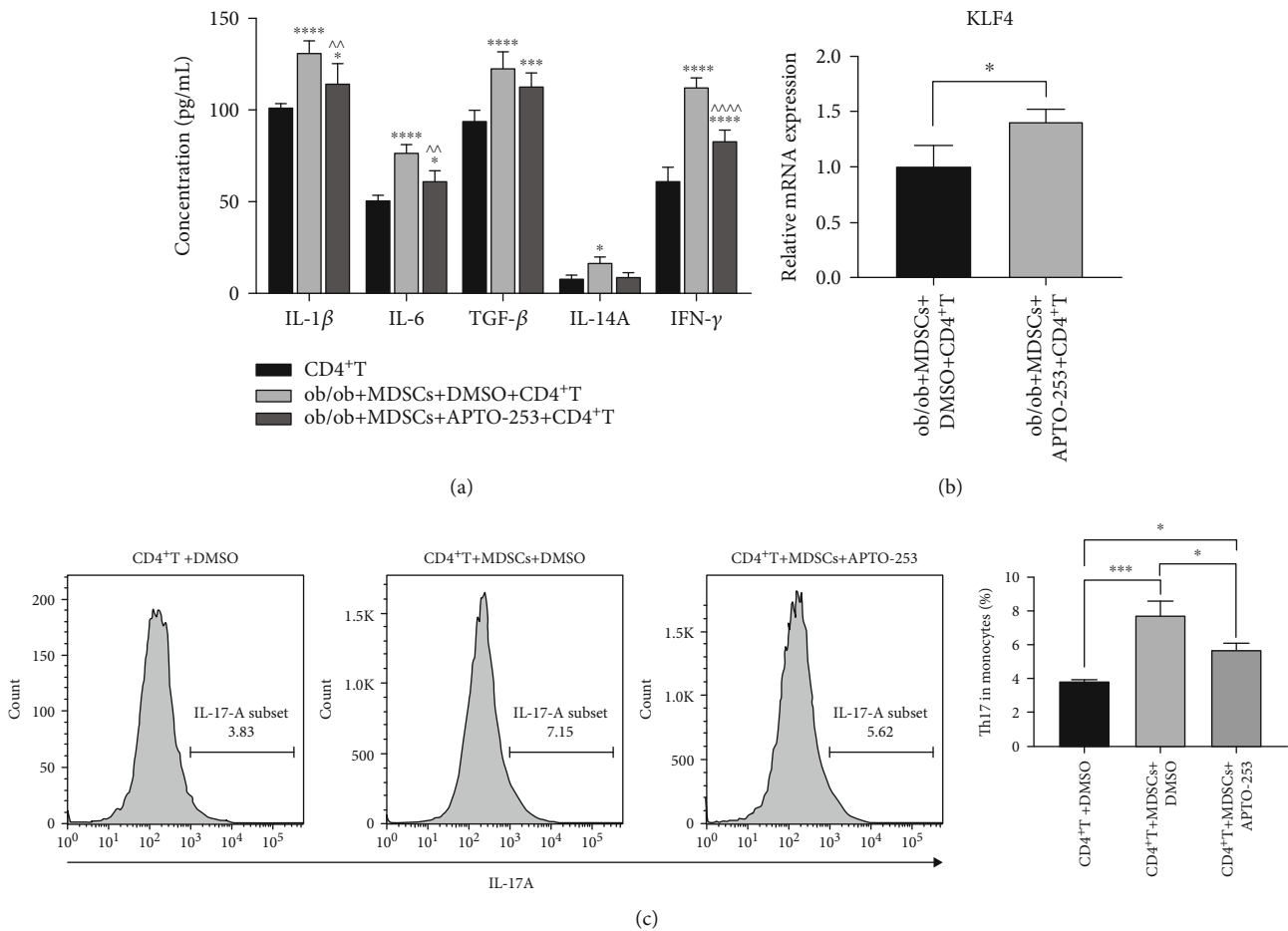
FIGURE 4: Kruppel-like factor 4 (KLF4) regulates the differentiation of Th17 cells by CD11b$^+$Gr-1$^+$ myeloid-derived suppressor cells (MDSCs).

(Figures 1(b) and 2(b)). However, wound closure was rescued by activation of KLF4 in ob/ob mice (Figure 2(a)), indicative of KLF4 playing a pivotal role in diabetic wound healing. Nonhealing wounds associated with diabetes are characterized by a prolonged inflammatory stage, and we found that IL-17A expression was significantly elevated in the ob/ob PU model (Figures 1(b) and 1(d)) but suppressed due to upregulation of KLF4 (Figure 2(d)). Although KLF4 was reported to be capable of directly binding to the promoter of *Il-17a* and positively regulating its expression [22, 23], we postulate that, in diabetic wound healing, KLF4 negatively regulates IL-17A in an *Il-17a*-independent fashion.

MDSC/Th17 cellular interaction varies by microenvironment and is mainly mediated by cytokines rather than direct cellular contact [21]. In wound healing, MDSCs are a major source of IL-6, IL-1β, and TGF-β, the indispensable cytokines for Th17 differentiation [14, 21]. Our ELISA results thus demonstrated that increased basal levels of these cytokines, together with IL-17A and IFN-γ, most likely orient ob/ob mice to increased T cell polarization and inflammation. Interestingly, APTO-253 rapidly reduced inflammatory cytokine levels and concomitantly decreased expansion of Th17 cells (Figures 2(d) and 2(e)), all of which contributed to the observed improvements in wound healing

(Figure 2(a)). However, increased recruitment of MDSCs into the blood and wounds of ob/ob mice after APTO-253 raises concerns that the inflammatory suppression attributed to KLF4 may have been mostly due to the immunosuppressive nature of MDSCs independent of Th17 population effects. To determine the relative importance of MDSC-regulated Th17 differentiation, we then performed coculturing of MDSCs and naïve T cells *in vitro*. MDSCs extracted from ob/ob PU mice with APTO-253 treatment displayed a substantial increase of KLF4 expression, and a concomitant reduction of Th17 population was also observed in CD4$^+$ T cells compared to cocultured vehicle controls (Figures 3(b) and 3(c)). Cytokine changes in the supernatant were similar to those data *in vivo*, supporting the opinion that KLF4 regulates Th17 differentiation in an MDSC-dependent manner (Figure 3(a)).

The keystone effect of KLF4 in MDSC-Th17 interactions in diabetic wound healing was further confirmed by culturing CD4$^+$ T cells with ob/ob MDSCs pretreated with APTO-253. The elevated KLF4 expression was clearly associated with the attenuated efficiency of Th17 differentiation, and the ELISA data showed that cytokines IL-1β, IL-6, and IFN-γ were also reduced (Figure 4). Notably, there were significant changes in TGF-β and IL-17A. Yi et al. [14]

reported that IL-1β is a major mediator of MDSC-facilitated Th17 differentiation while IL-6 and TGF-β mediate the efficiency. Therefore, any IL-1β deficiencies may be more likely to compromise Th17 differentiation. As for IL-17A, although its decrease upon APTO-253 treatment was not statistically significant, the levels in the pretreated group were close to blank control, indicating that upregulation of KLF4 still attenuated IL-17A expression by suppressing Th17 differentiation.

Collectively, the current study not only reveals the necessity of KLF4 in MDSC-regulated Th17 differentiation in the context of nonhealing diabetic wounds but also points to the need for KLF4-based interventions, such as KLF4 activation by APTO-253 to treat diabetic PU patients. Further investigations will determine the molecular mechanisms by which KLF4 in MDSCs mediates T cell differentiation using specific transgene mice while detailed pharmacological kinetics of APTO-253 will be detailed in diabetic wound healing.

Data Availability

The data used to support the findings of this study are included within the article.

Conflicts of Interest

The authors declare that they have no conflicts of interest.

Acknowledgments

Supplementary Materials

Primer sequences for RT-PCR are shown in Table S1. (Supplementary Materials)

References

[1] R. F. Diegelmann and M. C. Evans, "Wound healing: an overview of acute, fibrotic and delayed healing," *Frontiers in Bioscience*, vol. 9, no. 1-3, pp. 283–289, 2004.

[2] L. Wang, P. Gao, M. Zhang et al., "Prevalence and ethnic pattern of diabetes and prediabetes in China in 2013," *JAMA*, vol. 317, no. 24, pp. 2515–2523, 2017.

[3] J. Jaubert, J. Cheng, and J. A. Segre, "Ectopic expression of kruppel like factor 4 (Klf 4) accelerates formation of the epidermal permeability barrier," *Development*, vol. 130, no. 12, pp. 2767–2777, 2003.

[4] J. Li, H. Zheng, J. Wang et al., "Expression of Kruppel-like factor KLF4 in mouse hair follicle stem cells contributes to cutaneous wound healing," *PLoS One*, vol. 7, no. 6, article e39663, 2012.

[5] M. H. Manjili, "Phenotypic plasticity of MDSC in cancers," *Immunological Investigations*, vol. 41, no. 6-7, pp. 711–721, 2012.

[6] A. G. Cuenca, M. J. Delano, K. M. Kelly-Scumpia et al., "A paradoxical role for myeloid-derived suppressor cells in sepsis and trauma," *Molecular Medicine*, vol. 17, no. 3-4, pp. 281–292, 2011.

[7] L. Ou, Y. Shi, W. Dong et al., "Kruppel-like factor KLF4 facilitates cutaneous wound healing by promoting fibrocyte generation from myeloid-derived suppressor cells," *The Journal of Investigative Dermatology*, vol. 135, no. 5, pp. 1425–1434, 2015.

[8] S. A. Bakheet, B. S. Alrwashied, M. A. Ansari et al., "CXC chemokine receptor 3 antagonist AMG487 shows potent antiarthritic effects on collagen-induced arthritis by modifying B cell inflammatory profile," *Immunology Letters*, vol. 225, pp. 74–81, 2020.

[9] B. Xie and X. Y. Li, "Inflammatory mediators causing cutaneous chronic itch in some diseases via transient receptor potential channel subfamily V member 1 and subfamily A member 1," *The Journal of Dermatology*, vol. 46, no. 3, pp. 177–185, 2019.

[10] L. Brockmann, A. D. Giannou, N. Gagliani, and S. Huber, "Regulation of TH17 cells and associated cytokines in wound healing, tissue regeneration, and carcinogenesis," *Int J Mol Sci*, vol. 18, no. 5, p. 1033, 2017.

[11] M. P. Rodero, S. S. Hodgson, B. Hollier, C. Combadiere, and K. Khosrotehrani, "Reduced Il17a Expression Distinguishes a Ly6c^{lo}MHCII[hi] Macrophage Population Promoting Wound Healing," *The Journal of Investigative Dermatology*, vol. 133, no. 3, pp. 783–792, 2013.

[12] S. A. Bakheet, M. A. Ansari, A. Nadeem et al., "CXCR3 antagonist AMG487 suppresses rheumatoid arthritis pathogenesis and progression by shifting the Th17/Treg cell balance," *Cellular Signalling*, vol. 64, p. 109395, 2019.

[13] L. A. Tesmer, S. K. Lundy, S. Sarkar, and D. A. Fox, "Th17 cells in human disease," *Immunological Reviews*, vol. 223, no. 1, pp. 87–113, 2008.

[14] H. Yi, C. Guo, X. Yu, D. Zuo, and X. Y. Wang, "Mouse CD11b +Gr-1+ myeloid cells can promote Th17 cell differentiation and experimental autoimmune encephalomyelitis," *Journal of Immunology*, vol. 189, no. 9, pp. 4295–4304, 2012.

[15] L. Zhang, Z. Zhang, H. Zhang, M. Wu, and Y. Wang, "Myeloid-derived suppressor cells protect mouse models from autoimmune arthritis via controlling inflammatory response," *Inflammation*, vol. 37, no. 3, pp. 670–677, 2014.

[16] N. Bagheri, A. Razavi, B. Pourgheysari et al., "Up-regulated Th17 cell function is associated with increased peptic ulcer disease in _Helicobacter pylori_ -infection," *Infection, Genetics and Evolution*, vol. 60, pp. 117–125, 2018.

[17] I. Stadler, R. Y. Zhang, P. Oskoui, M. S. Whittaker, and R. J. Lanzafame, "Development of a simple, noninvasive, clinically relevant model of pressure ulcers in the mouse," *Journal of Investigative Surgery*, vol. 17, no. 4, pp. 221–227, 2004.

[18] A. Local, H. Zhang, K. D. Benbatoul et al., "APTO-253 stabilizes G-quadruplex DNA, inhibits MYC expression, and induces DNA damage in acute myeloid leukemia cells," *Molecular Cancer Therapeutics*, vol. 17, no. 6, pp. 1177–1186, 2018.

[19] S. Chatterjee, S. Das, P. Chakraborty, A. Manna, M. Chatterjee, and S. K. Choudhuri, "Myeloid derived suppressor cells (MDSCs) can induce the generation of Th17 response from naive CD4$^+$ T cells," *Immunobiology*, vol. 218, no. 5, pp. 718–724, 2013.

[20] B. Hoechst, J. Gamrekelashvili, M. P. Manns, T. F. Greten, and F. Korangy, "Plasticity of human Th17 cells and iTregs is orchestrated by different subsets of myeloid cells," *Blood*, vol. 117, no. 24, pp. 6532–6541, 2011.

[21] L. Wen, P. Gong, C. Liang et al., "Interplay between myeloid-derived suppressor cells (MDSCs) and Th17 cells: foe or friend?," *Oncotarget*, vol. 7, no. 23, pp. 35490–35496, 2016.

[22] L. Lebson, A. Gocke, J. Rosenzweig et al., "Cutting edge: the transcription factor Kruppel-like factor 4 regulates the differentiation of Th17 cells independently of RORγt," *Journal of Immunology*, vol. 185, no. 12, pp. 7161–7164, 2010.

[23] J. An, S. Golech, J. Klaewsongkram et al., "Krüppel-like factor 4 (KLF4) directly regulates proliferation in thymocyte development and IL-17 expression during Th17 differentiation," *The FASEB Journal*, vol. 25, no. 10, pp. 3634–3645, 2011.

[24] M. A. Ansari, A. Nadeem, S. A. Bakheet et al., "Chemokine receptor 5 antagonism causes reduction in joint inflammation in a collagen-induced arthritis mouse model," *Molecules*, vol. 26, no. 7, p. 1839, 2021.

[25] M. J. McGeachy, D. J. Cua, and S. L. Gaffen, "The IL-17 family of cytokines in health and disease," *Immunity*, vol. 50, no. 4, pp. 892–906, 2019.

[26] Y. Yin, M. Wang, M. Liu et al., "Efficacy and safety of IL-17 inhibitors for the treatment of ankylosing spondylitis: a systematic review and meta-analysis," *Arthritis Res Ther*, vol. 22, no. 1, p. 111, 2020.

[27] A. Armstrong, C. Paul, L. Puig et al., "Safety of ixekizumab treatment for up to 5 years in adult patients with moderate-to-severe psoriasis: results from greater than 17, 000 patient-years of exposure," *Dermatology and Therapy*, vol. 10, no. 1, pp. 133–150, 2020.

Research Article

Integrated Bioinformatics-Based Identification of Potential Diagnostic Biomarkers Associated with Diabetic Foot Ulcer Development

Long Qian,[1] Zhipeng Xia,[2] Ming Zhang,[1] Qiong Han,[1] Die Hu,[1] Sha Qi,[1] Danmou Xing,[1] Yan Chen,[1] and Xin Zhao [1]

[1]*Department of Hand Surgery, Wuhan Fourth Hospital; Puai Hospital, Tongji Medical College, Huazhong University of Science and Technology, Wuhan 430033, China*
[2]*Department of Intensive Care Unit, Tongji Hospital, Tongji Medical College, Huazhong University of Science and Technology, Wuhan 430073, China*

Correspondence should be addressed to Xin Zhao; zx18062700138@126.com

The present study was designed to detect possible biomarkers associated with diabetic foot ulcer (DFU) incidence in an effort to develop novel treatments for this condition. The GSE7014 and GSE29221 gene expression datasets were downloaded from the Gene Expression Omnibus (GEO) database, after which differentially expressed genes (DEGs) were identified between DFU and healthy samples. These DEGs were then arranged into a protein-protein interaction (PPI) network, and Kyoto Encyclopedia of Genes and Genomes (KEGG) pathway and Gene Ontology (GO) term enrichment analyses were performed to explore the functional roles of these genes. In total, 1192 DEGs were identified in the GSE7014 dataset (900 upregulated, 292 downregulated), while 1177 were identified in the GSE29221 dataset (257 upregulated, 919 downregulated). GO analyses revealed these DEGs to be significantly enriched in biological processes including sarcomere organization, muscle filament sliding, and the regulation of cardiac conduction, molecular functions including structural constituent of muscle, protein binding, and calcium ion binding, and cellular components including Z disc, myosin filament, and M band. These DEGs were also enriched in the adrenergic signaling in cardiomyoctes, dilated cardiomyopathy, and tight junction KEGG pathways. Together, the findings of these bioinformatics analyses thus identified key hub genes associated with DFU development.

1. Introduction

Diabetic foot ulcers (DFUs) are among the most common complications affecting the lower extremities in diabetes mellitus patients [1]. These ulcers and complications thereof can cause high rates of morbidity and mortality among affected patients owing to associated angiopathy, oxidative microenvironmental damage, and repeated bacterial infections [2]. While substantial progress has been made in the treatment of DFUs in recent years, a large proportion nonetheless develops into chronic wounds through processes that are ultimately irreversible [3]. It is thus essential that the molecular mechanisms governing DFU development be

clarified in order to aid in the prevention and treatment of these debilitating wounds [4].

Identifying genetic markers associated with DFU has the potential to guide the design of novel treatments while simultaneously elucidating the etiological basis for this condition [5]. Microarrays are commonly used to conduct large-scale bioinformatics studies aimed at simultaneously clarifying the relationship between multiple different genes and a given disease [6, 7]. One recent integrated bioinformatics analysis highlighted a role for the MAPK signaling pathway in DFU development [8]. Microarrays have also identified estrogen receptor 1, matrix metalloproteinase-2, and bone morphogenetic protein-4 as DFU-specific proteins
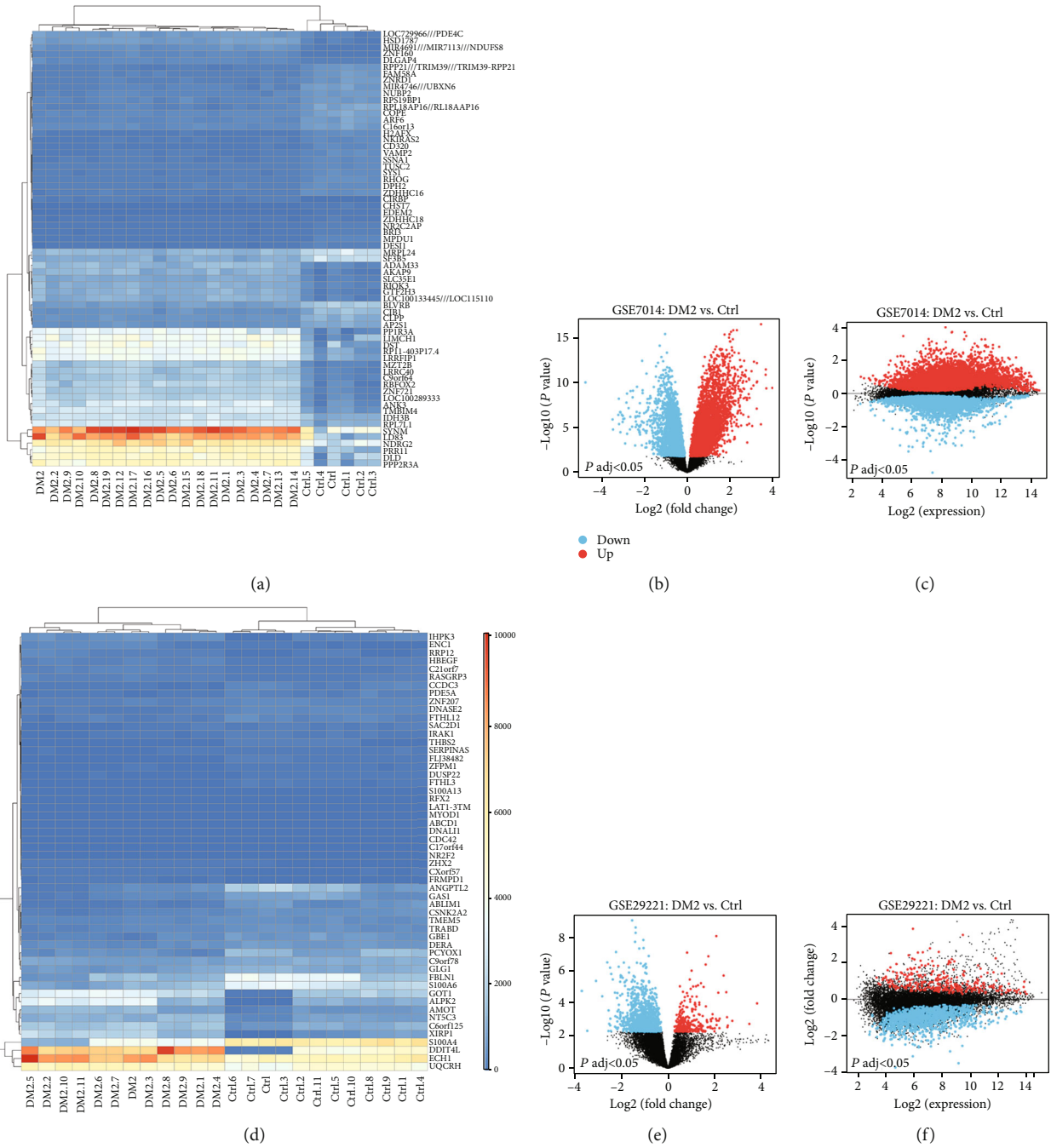
Figure 1: Detection of differentially expressed genes (DEGs) in the GSE7014 and GSE29221 datasets. (a) An expression heat map of the top 80 DEGs in the GSE7014 dataset, as determined based upon P values. (b) A volcano plot corresponding to the GSE7014 dataset. (c) A Meandiff plot for the GSE7014 dataset. (d) An expression heat map of the top 80 DEGs in the GSE29221 dataset, as determined based upon P values. (e) A volcano plot corresponding to the GSE29221 dataset. (f) A Meandiff plot for the GSE29221 dataset.

[9–11]. In previous reports, differentially expressed genes (DEGs) associated with DFU progression have been attributed to a range of molecular functions, biological processes, and cellular structures. [12, 13]

In the present report, DFU-related DEGs were identified by analyzing previously published datasets containing DFU and normal tissue samples. We then conducted functional enrichment and protein-protein interaction (PPI) network analyses aimed at elucidating the mechanisms whereby these

genes interact and cooperate to drive DFU development. Together, these results have the potential to clarify novel DFU-related biomarkers and to offer new insight regarding the molecular basis for this debilitating condition.

2. Materials and Methods

2.1. Dataset Selection. Microarray gene expression data of interest were downloaded from the Gene Expression Omnibus
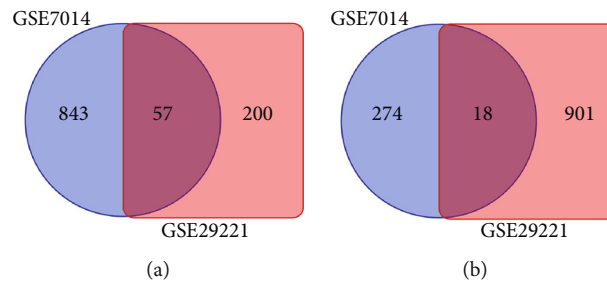
FIGURE 2: Identification of shared DEGs. (a) DEGs upregulated in both the GSE7014 and GSE29221 datasets. (b) DEGs downregulated in both the GSE7014 and GSE29221 datasets.

TABLE 1: Functional and pathway enrichment analyses for module genes. The top 3 terms were selected based upon p value rankings when >3 terms were enriched for a given category.

A, biological processes				
Term	Name	Count	P value	Genes
GO:0045214	Sarcomere organization	7	1.3E-9	FHOD3, MYH3, ACTN2, CASQ2, CAPN3, LDB3, CASQ1
GO:0030049	Muscle filament sliding	4	4.4E-4	MYH3, ACTN2, MYL3, DMD
GO:1903779	Regulation of cardiac conduction	4	1.4E-3	PLN, CASQ2, ATP2B2, CASQ1
B, molecular functions				
Term	Name	Count	P value	Genes
GO:0008307	Structural constituent of muscle	9	4.8E-12	MYOM1, PDLIM3, ACTN2, MYOT, MYL3, CAPN3, NEXN, DMD, MYOM2
GO:0005515	Protein binding	50	5.9E-4	FHOD3, MYOM1, BTG1, LGALSL, LDB3, SAT1, N4BP2L2, HK2, MYOM2, MED14, JPH2, XPO4, RASSF5, CAPN3, KIF1B, CTSC, ACTN2, IGFBP3, MYH1, PPP1R3C, MYOT, PRR16, CASQ2, TKT, FKBP3, CAMK2B, USP54, MGST1, THBS1, GTF2E2, PDLIM3, UGP2, PLN, CMYA5, KCNN2, DMD, PPARGC1A, S100A11, MPZL2, LGI1, MYH7B, DTNA, FAM46C, AGL, DDIT4L, ATP2B2, PPP2R3A, EFNA1, PKIA, CUTC
GO:0005509	Calcium ion binding	10	2.2E-3	ACTN2, MYL3, CASQ2, CAPN3, ATP2B2, PPP2R3A, CASQ1, THBS1, PLCD4, S100A11
C, cellular component				
Term	Name	Count	P value	Genes
GO:0030018	Z disc	11	2.5E-11	FHOD3, JPH2, PDLIM3, ACTN2, MYOT, CASQ2, CAPN3, NEXN, LDB3, KCNN2, DMD
GO:0032982	Myosin filament	4	2.9E-5	MYH1, MYH7B, MYH3, MYOM2
GO:0031430	M band	4	9.1E-5	MYOM1, CMYA5, MYOM2, MYOM3
D, KEGG pathway				
Term	Name	Count	P value	Genes
hsa04261	Adrenergic signaling in cardiomyocytes	5	4.5E-3	CAMK2B, PLN, MYL3, ATP2B2, PPP2R3A
Hsa05414	Dilated cardiomyopathy	4	8.0E-3	PLN, SGCD, MYL3, DMD
hsa04530	Tight junction	4	8.8E-3	MYH1, MYH7B, MYH3, ACTN2
KEGG: Kyoto Encyclopedia of Genes and Genomes.				

(GEO, http://www.ncbi.nlm.nih.gov/geo) database, which compiles a range of different high-throughput sequencing and microarray-based datasets. We searched this database for studies comparing DM2 and normal tissue samples and then downloaded the resultant files for analysis.

2.2. DEG Identification. Genes that were differentially expressed in DFU samples were identified using the default settings of the GEO2R tool (https://www.ncbi.nlm.nih.gov/geo/geo2r/), with DEGs being those genes with a $P < 0.05$ and a $|logFC| > 1$. GEO2R was additionally used to construct

(a)

(b)
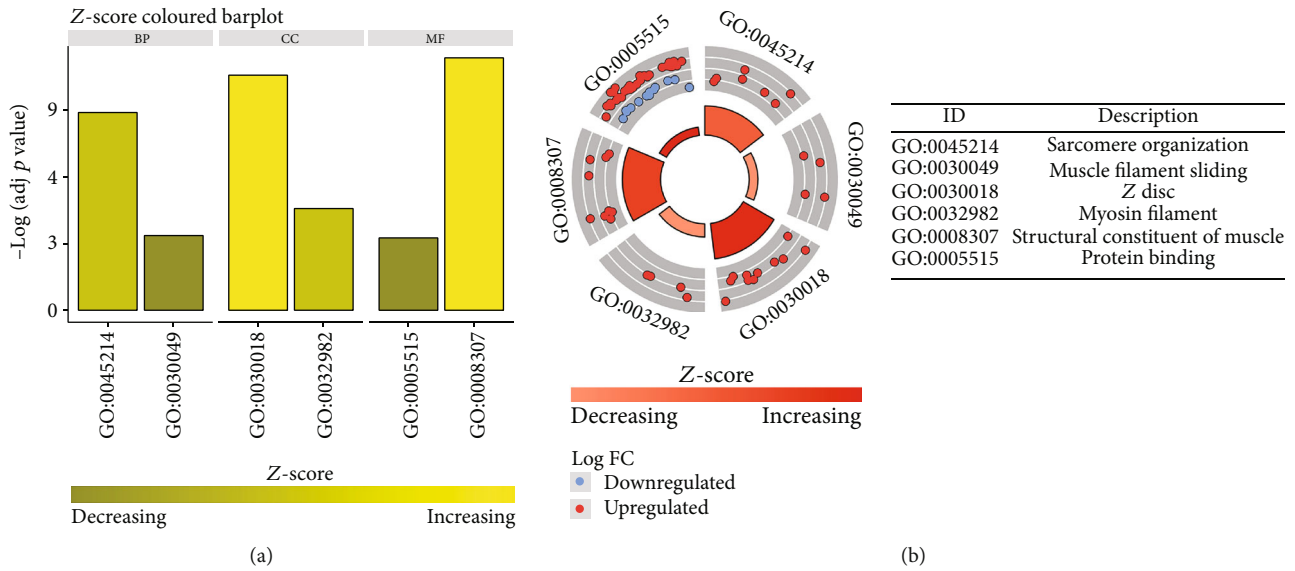
Figure 3: GO term enrichment analysis results. (a) Z-score results for the top 6 GO terms, including the top 2 BPs, CCs, and MFs. (b) Enrichment results for DEGs and the top 6 GO terms. Z-scores were defined as follows: (upregulated genes – downregulated genes)/total genes.

(a)

(b)
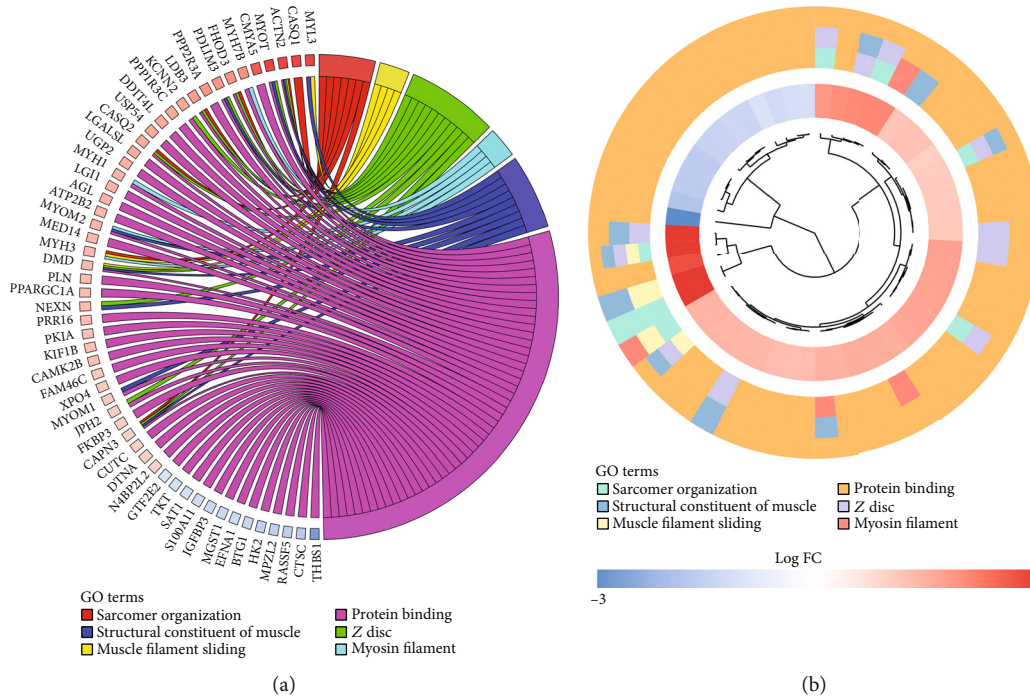
Figure 4: KEGG pathway enrichment results. (a) Relationships between DEGs and the top 5 enriched KEGG pathways. (b) Cluster plots corresponding to DEGs and the top 5 enriched KEGG pathways.

volcano and Meandiff plots. Additionally, log2-transformed mRNA expression data were arranged into heatmaps using the "pheatmap" R package, while DEGs that were shared among datasets were determined using the Venn online tool (http://bioinformatics.psb.ugent.be/webtools/Venn/).

2.3. Functional Enrichment Analyses. The biological functions of identified DEGs of interest were assessed using the Database for Annotation, Visualization, and Integrated Discovery version (DAVID) Bioinformatics Resources (v6.8). Briefly, shared DEGs were imported into DAVID, and GO and KEGG enrichment analyses were then conducted. For GO analyses, enriched biological processes (BPs), molecular functions (MFs), and cellular components (CCs) were assessed. The "GOplot" R package was used to visualize the results of these enrichment analyses.
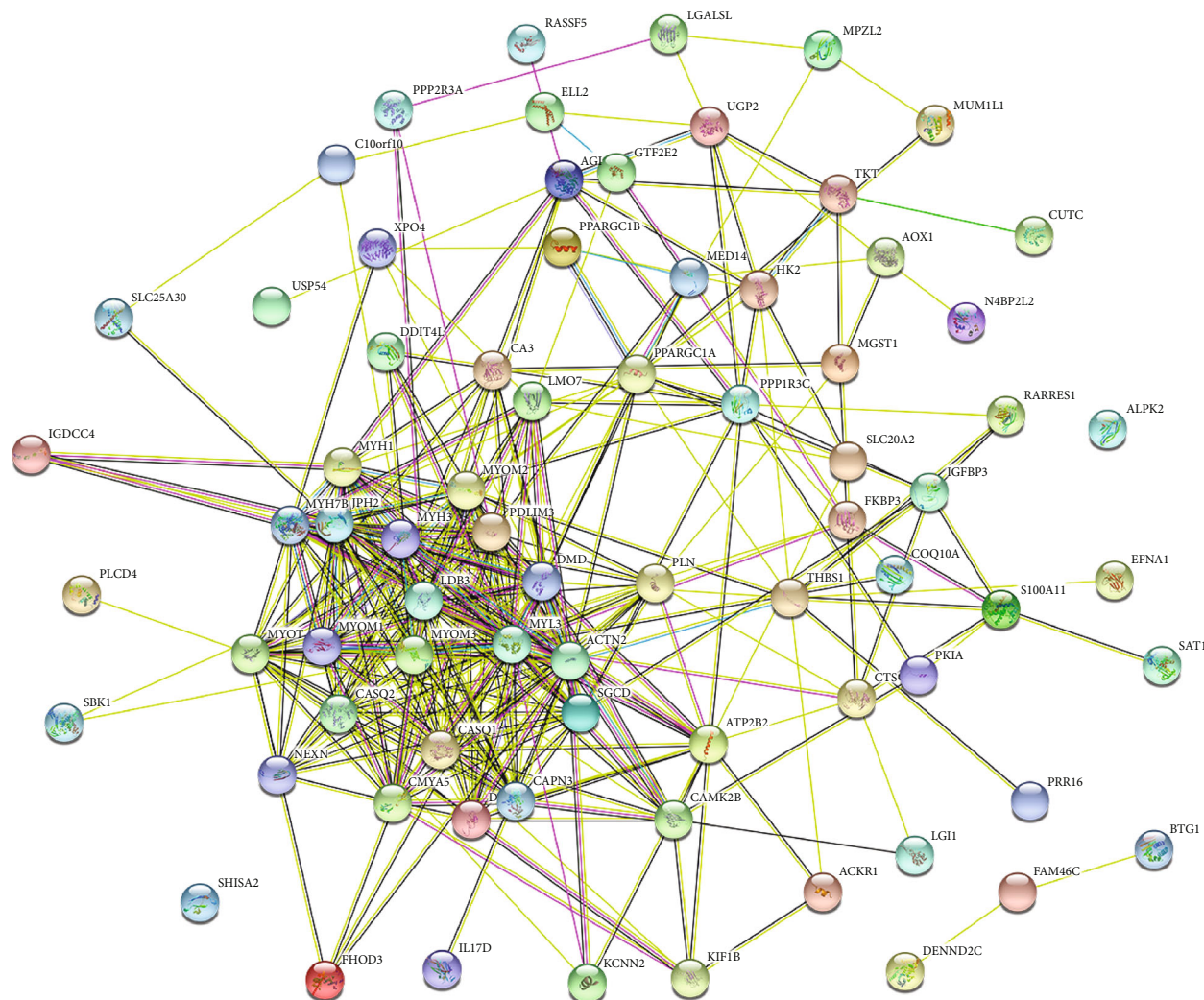
Figure 5: A DEG PPI network constructed using the STRING database.

2.4. Protein-Protein Interaction (PPI) Network Analyses. To understand interactions among DEGs, PPI networks were constructed by importing up- and downregulated DEGs into the Search Tool for the Retrieval of Interacting Genes (STRING), with those interactions with a combined score >0.5 being used for network construction. Cytoscape (v 3.7.2) was used to visualize the network, while the cyto-Hubba plugin was used to rank genes within this network based upon their degree centrality values. Hub genes were considered to be those with the top 10 highest degree values.

3. Results and Discussion

3.1. DEG Identification. The GSE7014 and GSE29221 gene expression datasets were downloaded from the GEO database obtained from the GEO database. The GSE7014 dataset included 20 DM2 biopsy samples and 6 biopsy samples from normal individuals, whereas the GSE29221 dataset included 12 DM2 biopsies and 12 biopsies from normal individuals. In total, 1192 DEGs were identified in the GSE7014 dataset (900 upregulated, 292 downregulated), while 1177 were

Table 2: Degree of top 10 genes in top module.

Gene ID	Gene name	Degree	
MYL3	Myosin Light Chain 3	31	Up
ACTN2	Actinin Alpha 2	30	Up
DMD	Dystrophin	26	Up
PDLIM3	PDZ And LIM Domain 3	24	Up
LDB3	LIM Domain Binding 3	24	Up
MYH1	Myosin Heavy Chain 1	22	Up
MYOM2	Myomesin 2	22	Up
MYOT	Myotilin	21	Up
CASQ2	Calsequestrin 2	21	Up
CAPN3	Calpain 3	21	Up

Up.

identified in the GSE29221 dataset (257 upregulated, 919 downregulated). The top 80 DEGs with the highest *P* values are presented in Figure 1. In total, 57 upregulated DEGs and 18 downregulated DEGs were shared between these two

(a)

(b)
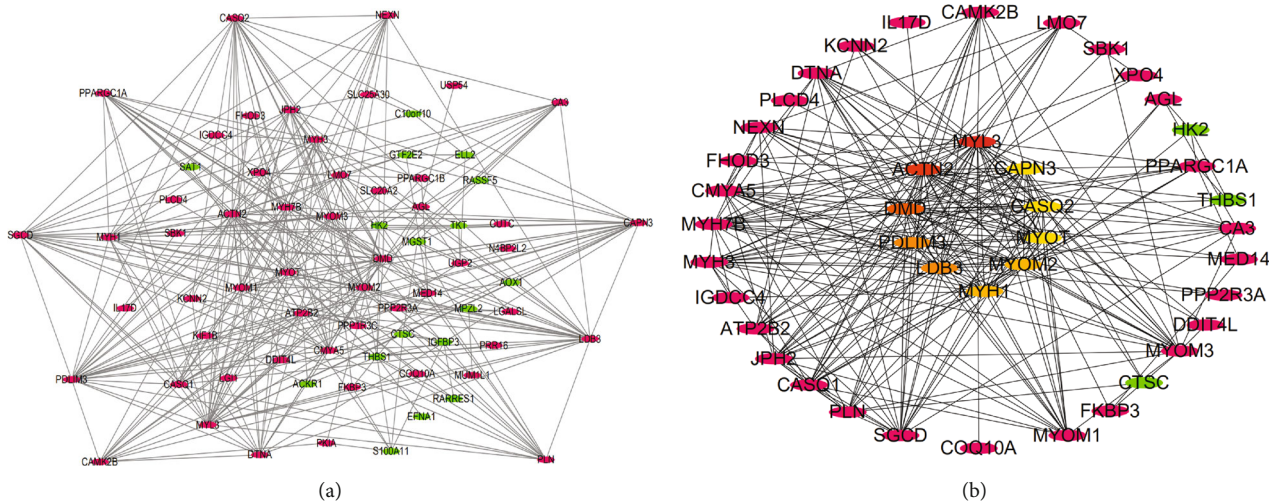
FIGURE 6: Hub gene identification. (a) A DEG PPI network constructed using Cytoscape, with upregulated and downregulated genes being shown in red and green, respectively. (b) The top 10 genes with the highest degree values were identified using CytoHubba. These genes were ranked in descending degree order from red to orange to yellow.

datasets, as identified through Venn diagram analyses (Figure 2).

3.2. Pathway Enrichment Analyses. GO analyses revealed these DEGs to be enriched in biological processes including sarcomere organization, muscle filament sliding, and the regulation of cardiac conduction, molecular functions including a structural constituent of muscle, protein binding, and calcium ion binding, and cellular components including Z disc, myosin filament, and M band. These DEGs were also enriched in KEGG pathways including the adrenergic signaling in cardiomyocytes, dilated cardiomyopathy, and tight junction pathways (Table 1 and Figure 3). Enrichment results pertaining to these analyses are compiled in Figure 4.

3.3. PPI Network Construction and Hub Gene Identification. The STRING database was next used to construct a DEG PPI network (Figure 5), and the top 10 hub genes therein with the highest degree values were determined using Cytoscape v. 3.7.2. These hub genes were MYL3, ACTN2, DMD, PDLIM3, LDB3, MYH1, MYOM2, MYOT, CASQ2, and CAPN3 (Table 2 and Figure 6).

4. Discussion

Aberrant gene expression is closely linked to a range of pathological conditions, including DFU. Key driver genes linked to the onset and progression of this condition, however, remain to be fully clarified. In this study, we identified 900 upregulated and 292 downregulated DFU-related DEGs in the GSE7014 dataset, as well as 257 upregulated and 919 downregulated DFU-related DEGs in the GSE29221 dataset. These genes were associated with the adrenergic signaling in cardiomyocytes, dilated cardiomyopathy, and tight junction pathways. We were further able to identify 10 hub genes associated with DFU, including MYL3, ACTN2, DMD, PDLIM3, LDB3, MYH1, MYOM2, MYOT, CASQ2, and CAPN3.

DFU and other chronic wounds are associated with well-characterized morphological changes, but the underlying cellular and molecular biomarkers that drive these tissue changes remain poorly understood [14]. Changes in mRNA expression are valuable biomarkers that are well known to play a role in the development of diabetes-related diseases [15, 16]. For example, one prior study identified Prenylcysteine oxidase 1 (PCYOX1), beta-ala-his dipeptidase (CNDP1), and extracellular matrix protein 1 (ECM1) as valuable diagnostic biomarkers associated with the incidence of gestational diabetes [17]. Saik et al. further found the JAK-STAT, MAPK, and protein kinase B signaling pathway to be closely linked to diabetes complications and hypoxia responses [18]. The GO and KEGG analyses conducted in this study suggested the top DEGs to be enriched in sarcomere organization, muscle filament sliding, and the regulation of cardiac conduction, potentially playing a role in regulating angiogenesis. These genes were also enriched in molecular functions including a structural constituent of muscle, protein binding, and calcium ion binding, and in the adrenergic signaling in cardiomyocytes, dilated cardiomyopathy, and tight junction pathways, suggesting a potential role for the activation of inflammatory responses in DFU.

DFU-related hub genes identified in this study included MYL3, ACTN2, DMD, PDLIM3, LDB3, MYH1, MYOM2, MYOT, CASQ2, and CAPN3, all of which were involved in the top 5 KEGG pathways with the smallest P values. Degree centrality corresponds to the relationship between a given node and all other nodes in the network, while closeness centrality denotes the degree of closeness between a node and all other nodes in the network, and betweenness centrality measures the frequency with which a given node serves as the shortest bridge between two other nodes.

As most of the genes identified in this study have not previously been reported to be related to DFUs, there is a clear need to verify the functional importance and mechanistic roles of these genes in this pathological context. In addition, in vitro studies of human skin fibroblasts and

human umbilical vein endothelial cells are warranted to explore the molecular mechanisms whereby these genes shape DFU development. The development of mice of other animal models in which these genes are conditionally knocked out may further aid in efforts to elucidate their functions as regulators of these debilitating chronic wounds.

5. Conclusions

In summary, the results of these bioinformatics analyses highlight novel mechanisms and important hub genes which may contribute to DFU development. However, further research is essential to better clarify the regulatory roles of these genes in order to firmly establish their value as clinical biomarkers and/or therapeutic targets.

Data Availability

The data used to support the findings of this study are available from the corresponding author upon request.

Conflicts of Interest

The authors declare that there is no conflict of interest regarding the publication of this paper.

Authors' Contributions

Long Qian and Zhipeng Xia contributed equally to this study.

References

[1] Y. Xiong, L. Chen, C. Yan et al., "Circulating exosomal miR-20b-5p inhibition restores Wnt9b signaling and reverses diabetes-associated impaired wound healing," *Small*, vol. 16, no. 3, article e1904044, 2020.

[2] Y. Xiong, L. Chen, T. Yu et al., "Inhibition of circulating exosomal microRNA-15a-3p accelerates diabetic wound repair," *Aging*, vol. 12, no. 10, pp. 8968–8986, 2020.

[3] X. Chen, W. Zhou, K. Zha et al., "Treatment of chronic ulcer in diabetic rats with self assembling nanofiber gel encapsulated-polydeoxyribonucleotide," *American Journal of Translational Research*, vol. 8, no. 7, pp. 3067–3076, 2016.

[4] Y. Hu, R. Tao, L. Chen et al., "Exosomes derived from pioglitazone-pretreated MSCs accelerate diabetic wound healing through enhancing angiogenesis," *Journal of Nanobiotechnology*, vol. 19, no. 1, p. 150, 2021.

[5] Y. Xiong, B. B. Mi, M. F. Liu, H. Xue, Q. P. Wu, and G. H. Liu, "Bioinformatics analysis and identification of genes and molecular pathways involved in synovial inflammation in rheumatoid arthritis," *Medical Science Monitor : international medical journal of experimental and clinical research*, vol. 25, pp. 2246–2256, 2019.

[6] T. Yu, Z. Wang, X. You et al., "Resveratrol promotes osteogenesis and alleviates osteoporosis by inhibiting p53," *Aging*, vol. 12, no. 11, pp. 10359–10369, 2020.

[7] T. Yu, X. You, H. Zhou et al., "p53 plays a central role in the development of osteoporosis," *Aging*, vol. 12, no. 11, pp. 10473–10487, 2020.

[8] M. Tian, J. Dong, B. Yuan, and H. Jia, "Identification of potential circRNAs and circRNA-miRNA-mRNA regulatory network in the development of diabetic foot ulcers by integrated bioinformatics analysis," *International Wound Journal*, vol. 18, no. 3, pp. 323–331, 2021.

[9] S. Qi, Q. Han, D. Xing et al., "Functional analysis of estrogen receptor 1 in diabetic wound healing: a knockdown cell-based and bioinformatic study," *Medical Science Monitor : international medical journal of experimental and clinical research*, vol. 26, article e928788, 2020.

[10] R. F. Chen, M. Y. Yang, C. J. Wang, C. T. Wang, and Y. R. Kuo, "Proteomic analysis of peri-wounding tissue expressions in extracorporeal shock wave enhanced diabetic wound healing in a streptozotocin-induced diabetes model," *International Journal of Molecular Sciences*, vol. 21, no. 15, 2020.

[11] C. Loretelli, M. Ben Nasr, G. Giatsidis et al., "Embryonic stem cell extracts improve wound healing in diabetic mice," *Acta Diabetologica*, vol. 57, no. 7, pp. 883–890, 2020.

[12] B. Mi, L. Chen, Y. Xiong et al., "Saliva exosomes-derived UBE2O mRNA promotes angiogenesis in cutaneous wounds by targeting SMAD6," *Journal of Nanobiotechnology*, vol. 18, no. 1, p. 68, 2020.

[13] E. Takematsu, A. Spencer, J. Auster et al., "Genome wide analysis of gene expression changes in skin from patients with type 2 diabetes," *PloS One*, vol. 15, no. 2, article e0225267, 2020.

[14] I. Oh, G. Muthukrishnan, M. J. Ninomiya et al., "Tracking anti-staphylococcus aureusAntibodies ProducedIn VivoandEx Vivoduring foot salvage therapy for diabetic foot infections reveals prognostic insights and evidence of diversified humoral immunity," *Infection and Immunity*, vol. 86, no. 12, 2018.

[15] J. A. D. van, J. W. Scholey, and A. Konvalinka, "Insights into diabetic kidney disease using urinary proteomics and bioinformatics," *Journal of the American Society of Nephrology : JASN*, vol. 28, no. 4, pp. 1050–1061, 2017.

[16] H. A. Ramirez, L. Liang, I. Pastar et al., "Comparative genomic, microRNA, and tissue analyses reveal subtle differences between non-diabetic and diabetic foot skin," *PloS One*, vol. 10, no. 8, article e0137133, 2015.

[17] D. Mavreli, N. Evangelinakis, N. Papantoniou, and A. Kolialexi, "Quantitative comparative proteomics reveals candidate biomarkers for the early prediction of gestational diabetes mellitus: a preliminary study," *In Vivo*, vol. 34, no. 2, pp. 517–525, 2020.

[18] O. V. Saik and V. V. Klimontov, "Bioinformatic reconstruction and analysis of gene networks related to glucose variability in diabetes and its complications," *International Journal of Molecular Sciences*, vol. 21, no. 22, p. 8691, 2020.